

UC Merced

UC Merced Electronic Theses and Dissertations

Title

Approaches To Integrating A High Penetration Of Solar PV and CPV Onto The Electrical Grid

Permalink

<https://escholarship.org/uc/item/6vq9z0mk>

Author

Hill, Steven Craig

Publication Date

2013

Peer reviewed|Thesis/dissertation

UNIVERSITY OF CALIFORNIA, MERCED

This is the Title of My Dissertation

A dissertation submitted in partial satisfaction of the requirements for the degree
Doctor of Philosophy

In

Approaches To Integrating A High Penetration Of Solar PV and CPV Onto The
Electrical Grid

By

Steven Craig Hill

Committee in charge:

Assistant Professor Elliott Campbell, Chair

Assistant Professor Yanbao Ma

Associate Professor Jay Sharping

Professor Roland Winston

2013

The Dissertation of Steven Craig Hill is approved, and it is acceptable in quality and form for publication on microfilm and electronically:

University of California, Merced

2013

Acknowledgement

First I would thank my parents Lloyd and Beverly Hill. My mother was a perfect homemaker who always gave kind words of encouragement and always could see the good and potential in us. Dad was a great engineering leader for the United States Steel Corporation who transferred his practical engineering skills to helping neighbors with their landscaping, sprinkling systems, building projects and even animal control problems. Dad has always been the best neighbor I have ever known.

Next I would like to thank my wife Lynn, the light of my life, and son Michael for their sacrifice in putting up with my absence the past six years. I appreciate their loyalty, patience and desire for me to finish the task. I express my love to the rest of the children Andy, Jenny, Rob and Craig and their wonderful spouses Cami, Mark, Amanda and Leanne. They have given me fourteen wonderful grandchildren: Drew, Brady, Addison, McKenna, Samantha, Abigail, Lidia, Molly, Charlotte, Jane, Max, McKenzie, Thomas and Evrett. I hope my effort will motivate them to seek a good education and serve the world well with their learning.

I would like to especially acknowledge and thank Professor Roland Winston, my advisor and mentor. Without him I would have never begun or continued this adventure of the past six years. He inspires me to keep thinking. I express my appreciation to Professor Elliott Campbell, Professor Yanbao Ma, and Professor Jay Sharping for their time in serving on my Committee. Their comments have been very constructive and helpful in focusing my efforts. I also express thanks to Professor Gavilan, Shannon Adamson and Carrie King who have helped me acquire teaching assignments as well as Professor Tom Harmon, Lei Yue and Bob Rice for allowing me to help them teach. I also appreciate the Research Team from UC Merced consisting of Paul Thompson, Hatem Elgaili, Guadalupe Martinez Chavez, Neekole Acorda, Brian Weikel, Luis Perez, Elizabeth Rivera, and Erika Marie Generoso for all their help in contacting staff of the Waste Water Treatment plant in California.

I would like to thank past working colleagues Joel Yoder and Walt Swain from Westinghouse and Northrup Grumman, Roger Vanhoy and Greg Salyer from Modesto Irrigation District, Larry Gilbertson from Turlock Irrigation District, Jim Pope, Hari Modi, Ron Yuen, Tom Lee and Scott Tomashefsky from Northern California Power Agency and John Carrier from CH2MHill for their comments, encouragement and support.

I express my thanks to Dr. Peter Reischl at San Jose State University who encouraged me to pursue this course twenty years ago and Kaye Larsen, my Provo High School math teacher, who took an interest and motivated me forty five years ago.

Abstract

The United States has ample potential renewable energy resources, especially in wind and solar having a combined 15,000 Gigawatts of potential capacity [1,2].

For the past 30 years, California has led the nation in promoting and using energy efficiency programs and has led the nation with the most aggressive Renewable Portfolio Standard (RPS) goals. Energy efficiency and demand response programs are key strategies for addressing climate change and meeting AB 32 (California 's 33% RPS law). RPS goals have been adopted by 43 states that require on average 20% of energy delivered to customers by 2020 by from renewable resources [140].

Solar cost reductions, increasing cost of traditional resources, and Renewable Portfolio Standards have created the possibility of significant levels of distributed solar generation being installed on the grid and specifically, the distribution system [127]. Federal law requires grid modernization to enable an increased dependency on variable and distributed energy resources [143]. This means that existing market and grid control systems, based on traditional centralized resources and one-way distributed power flows, require new operational paradigms, systems architectures and market structures. California's utility rate design and the NEM program for rooftop solar will also require future changes.

Land use challenges, both local and remote, may lead to new applications of installing solar PV on water. Studies performed by the California Transmission Planning Group (CTPG) have shown the proposed "high potential" transmission upgrades may be insufficient, by themselves, to allow California to meet its 33% RPS goal. Because integrating a high penetration of distributed resources on to the distribution network is evolving with its own unique challenges, a floating water-borne solar PV design is discussed to assist in bridging the gap to assist in meeting RPS goals, energy efficiency goals and the Governor's goal to achieve 12,000MW of distributed generation in California. The floating water-borne PV system is capable of installation on waste water treatment plant (WWT) settling ponds. California has more than 800 WWT plants and estimates predict floating water-borne PV on WWT ponds could potentially generate greater than 1000 MW without the need to build additional transmission.

Table of Contents

1.0	Introduction	1
2.0	Challenges and Opportunities for Integrating Solar PV into Resource Portfolios to meet California’s RPS goals	6
2.1	Regulation and Policy Challenges for solar PV	6
2.1.1	Utility Rate Design and NEM.....	7
2.1.2	Exclusion of Rooftop Solar PV from RPS Eligibility	9
2.1.3	Distribution Reliability Problems	10
2.2	High PV Penetration on Utility Distribution Systems	12
2.2.1	Limitations Due To Clouds	12
2.2.2	Voltage Regulation	15
2.3	The Land Challenge for Solar.....	15
2.4	A LOCAL PV DEVELOPMENT OPTION- A BRIDGE TO THE FUTURE.....	20
2.5	Specification for a Water-borne System.....	22
2.5.1	Design for Life Cycle Cost.....	23
2.5.2	Structure	23
2.5.3	Cabling.....	24
2.5.4	Tracking.....	24
2.5.5	Reliability and warranty	24
2.5.6	Electrical, Controls & Protection.....	25
2.5.7	Maintainability	26
2.5.8	Performance Tests	26
2.5.9	OTHER	26
3.0	Floating Water-Borne PV application Consideration for Utility Application in California	28
3.1	Waste Water Treatment Plants.....	28
3.1.1	Activated Sludge	28
3.1.2	Fixed-Growth Biological Systems	29
3.1.3	Oxidation Ponds	29
3.2	Floating Water-Borne CPV System	30
3.3	ALGAE IN WASTE WATER TREATMENT.....	31

3.4	Potential for CPV Water-Borne Systems.....	35
3.5	Validation of the Water-Borne System.....	37
4.0	Cost Benefit Validation for Water-Borne CPV System.....	39
4.1	Cost Benefit Analysis Background and Perspective	40
4.2	Cost Benefit Analysis Requirement	40
4.3	Cost Benefit Steps.....	41
4.4	Cost Benefit Application for a PV Water-Borne System	42
5.0	Power System Integration Studies for Larger Solar PV Installations Connected to Transmission Lines	44
5.1	Power Flow Analysis Methodology	46
5.1.1	Steady State Power Flow Analysis	46
5.1.2	Short Circuit Duty Analysis.....	47
5.1.3	System Protection Analysis.....	47
5.1.4	Reactive Power Deficiency Analysis.....	47
5.1.5	Dynamic Stability Analysis.....	49
5.1.5.1	Dynamic Modeling	50
5.1.6	Substation Evaluation	50
5.1.7	Transmission Line Evaluation.....	51
5.2	CTPG Study Results.....	51
5.3	Summary of Power Flow and Application White Slough WWT	53
6.0	High PV Penetration Impacts on Utility Distribution Systems	54
6.1	Managing Energy Flows to Improve System Value	54
6.2	Solar photovoltaic Distributed Energy Resources (DER) Integration Assessment	56
6.2.1	Interconnection Standards and Guides	56
6.2.2	Distribution System Modeling	56
6.2.3	Modeling Algorithms and Networks.....	58
6.3	Control of Photovoltaic generators in a Distribution Network.....	60
6.3.1	Control of Utility Interactive Inverters.....	60
6.3.1.1	Maximum Power Point Tracking.....	60
6.3.1.2	Grid Synchronization.....	60
6.3.1.3	Anti-Islanding	61

6.3.2	Current Regulation	62
6.3.3	PWM	63
6.3.4	Desired PV Inverter Features	63
6.4	Off-Grid (Stand-Alone) PV Power System Control	65
6.5	Future Power System Control	66
6.5.1	Control Framework	69
6.6	Transition in Control Strategy for increased Penetration.....	70
6.6.1	CASE Study optimization based on cooperative control	72
6.6.1.1	Communication Topology.....	72
6.6.1.2	Case Study Results	73
6.6.2	Other Future Distribution System Configurations and Characteristics	74
7.0	Summary and Future Work.....	75
7.1	Future Research.....	76
	References	82
	Appendix A Concentration and Efficiency in Solar Photovoltaic Applications	101
A.1	Background	101
A.2	Nonimaging Optics	104
A.3	FRESNEL LENS DESIGN	108
A.3.1	Minimum Deviation	109
A.3.2	Nonimaging Fresnel Lens Design	114
A.3.3	Flux Density.....	115
A.3.4	Solar Disk Size and Brightness.....	117
A.3.5	Refractive Indices	119
A.3.6	Spectral Color Dispersion.....	120
A.3.7	Summary of Fresnel Lens Concentrators For Photovoltaic Applications.....	121
A.4	Concentrator Cell Efficiency	122
A.5	Geometrical Losses	124
A.6	Multijunction Devices	124
A.5.1	Device Architectures	128
A.7	Metal Semiconductor Contacts	129
A.8	Principles of operation under concentrated Sunlight	131

A.9	Nonimaging Secondary Concentrators for Photovoltaic Applications	135
A.10	Environmental Testing and Reliability	136
Appendix B	Waste Water Treatment Plants in California.....	137
Appendix C	Grid Synchronization, PI Control and the DQ Transformation.....	150
Appendix D	PWM Techniques.....	157
Appendix E	Solar Storms and Effect on the Grid	165

List of Figures

List of Figures	x
Figure 2.1 Renewable Energy Zones in California.....	17
Figure 2.2 Potential Renewable Energy Zones in Southwestern U.S.....	18
Figure 3.1 Floating CPV Modules	31
Figure 3.2 DNI for the Lodi.....	34
Figure 3.3 Aerial view of the Lodi Energy Center and the Lodi White Slough Facilities.	35
Figure 3.4 Pyron Solar’s Water-Borne CPV Prototype at SDG&E Test Site	37
Figure 5.1 Transmission Map near LEC	45
Figure 5.2 Equivalent Circuit for modeling	49
Figure 6.1 Model of Inverter connections to grid.....	61
Figure 6.2 Market mechanisms in feedback control loop	69
Figure 6.3 Control Architectures.....	71
Figure A.1 Relationship between sun and earth.....	102
Figure A.2 Concept of <i>etendue</i> and maximum 2D concentration	105
Figure A.3 Conceptual illustration of Fresnel lens	108
Figure A.4 Fresnel lens details	109
Figure A.5 Maximum Deviation Prism	110
Figure A.6 Dispersion of a prism	111
Figure A.7 Demonstration of f-number	114
Figure A.8 Cosine loss	116
Figure A.9 Flux Density factor	117
Figure A.10 Brightness distribution of solar flux.....	118
Figure A.11 Flux density factors for non-imaging Fresnel lens.....	118
Figure A.12 Refractive indices BK 7 glass & PMMA	120
Figure A.13 I-V characteristic of solar cells	123
Figure A.14 Efficiency histograms of last 5 generations of terrestrial cells.....	125
Figure A.15 Planned improvement in economics of multijunction cells	126
Figure A.16 Contour map showing cost with improvements in cell efficiency.....	127
Figure A.17 Epitaxial structure improvements	129
Figure A.18 Curves for cell fill factor and efficiency as a function of concentration.....	132
Figure A.19 Maximum power efficiency vs. concentration	133
Figure A.20 Open Circuit voltage vs. temperature and concentration.....	133
Figure A.21 Open circuit temperature coefficients vs. concentration	134
Figure C-1a Clarke’s Transformation.....	151
Figure C-1b Park’s Transformation	152
Figure C-2a VSI Power Topology	153
Figure C-2b Equivalent Circuit for the VSI.....	153
Figure C-3 Cross-coupling of the d & q components	155

Figure C-4a Current control of VSI feed-forward decoupling method	156
Figure C-4b Feed-forward decoupling block.....	156
Figure C-5a Current Control of VSI Feedback decoupling method	156
Figure C-5b Feedback decoupling block	156
Figure D-1 Topology three-leg voltage source inverter	158
Figure D-2(a) Topology $V1(pnn)$ of voltage source inverter	158
Figure D-2b Zero output voltage topologies.....	158
Figure D-3 zero voltage vectors in the α, β plane.....	159
Figure D-4a Output voltage vector in the α, β plane.....	159
Figure D-4b Output line voltages in the time domain	160
Figure D-5 Synthesis of required output voltage in sector 1	160
Figure D-6 Phase gating signals for SVM2 Symmetric Sequence.....	161
Figure D-7 Space Vector Modulation Divisions and Positions	162
Figure D-8 3 phase NPC Circuit	164
Figure E.1 Salem N.J. Nuclear Plant GSU Transformer Damage	166

Tables

Table 2.1 Cost PacifiCorp's Gateway Central Line.....	19
Table 2.2 Target Budget.....	26
Table 4.1 NCPA Member Waste Water Treatment Plants.....	39
Table 4.2 Floating CPV Benefit to Cost Ratios	43
Table A.1 Work Function for metallic contacts.....	130

1.0 INTRODUCTION

The United States has ample potential renewable energy resources. Land-based wind, the most readily available for development, totals more than 8000 GW of potential capacity. The capacity of concentrating solar power is nearly 7,000 GW in seven southwestern states [1][2]. The generation potential of photovoltaic (PV) resources is limited only by the land area devoted to it, 100-250 GW/100 km² [1][2]. The challenge is how to utilize these potential resources in an economical and reliable manner.

According to a recent solar development project in the California's central valley it takes about 154 acres to produce 25 MW of solar PV (about 6 acres/MW). An idea presented in this dissertation describes how a water-borne solar application can decrease the area to 3 acres/MW and potentially generate greater than 1000 MW of power by floating PV on the ponds of Waste Water Treatment plants in California.

A challenge with solar PV is the amount of valuable land it requires for installation unless it is mounted on rooftops or unless it is remotely located in areas where the solar irradiance is high, but where the land is worth much less. Also when many PV generators are concerned, there is a relationship between the land occupation and energy yield; increasing land occupation reduces mutual shading and therefore increases energy yield, however it comes with an additional price because of the extra land required. Hence, the study of the relationship between land occupation and energy yield is a key point in the design of larger PV plants.

Chapter 2 will discuss the land use issues including: 1-an introduction to the problem with integrating a high penetration of rooftop solar PV onto the grid 2- the issues of connecting to remotely located renewable resources including permitting challenges and transmission construction costs 3- An introduction to a water-borne solar PV application that can effectively reduce or mitigate the issues of high local penetration and remote access to renewable resources. The water-borne application is presented to reduce the land use problem associated with PV, develop localized renewables, and improve energy efficiency all of which help reduce the amount of long distance transmission required to import renewable energy sources.

Solutions to these challenges and opportunities is largely motivated by how utilities are going to meet the aggressive state renewable portfolio standards (RPS) and energy efficiency goals in a cost effective and timely manner. For the past 30 years, California has led the nation in promoting and using energy efficiency programs. Energy efficiency and demand response programs are key strategies for addressing climate change and meeting AB 32 goals for greenhouse gas emissions as explained in the CEC 2011 Integrated Energy

Policy Report [10]. The Energy Commission has coupled energy efficiency with promotion of solar photovoltaic systems through its New Solar Homes Partnership. According to the Association, solar is the fastest-growing clean energy technology available today.

The electric utility industry has been transitioning for over 30 years in terms of increasing diversity and distribution of resources. To date, 43 states representing more than 80% of the US population have enacted renewable portfolio standards or goals that require on average 20% of energy delivered to customers by 2020 [140]. The positive results are environmentally cleaner resources, better utilization of the grid and more efficient use of electricity by customers. However, as a consequence the grid has become increasingly complex and stressed by the variability that has been introduced by intermittent wind and solar photovoltaic (solar PV) resources and this is expected to increase with millions of distributed energy resources (DER) [113].

Energy efficiency programs are a top priority of the CEC and new project permits must address energy efficiency as a project alternative as part of the approval process. The California Long-term Energy Efficiency Strategic Plan, published in 2008 and updated in 2011 by the California Public Utilities Commission (CPUC), sets ambitious efficiency goals for the state. A core focus of the Strategic Plan is continued engagement with the broader stakeholder community, including manufacturers, contractors, local governments and others. The Plan addresses several main sectors: Residential, Commercial, Industrial and Agricultural.

The industrial sector provides great opportunity for achieving energy efficiency savings and other benefits such as greenhouse gas (GHG) reductions through resource management. Playing major roles in both driving California's economy and consuming energy, industrial users account for 16 percent of electricity use, 22 percent of energy use (33 percent of natural gas use alone) and 20 percent of end-use CO₂ emissions in the state [12]. Chapters 2 and 3 will discuss a water-borne PV application for Waste Water Treatment (WWT) plants and its potential role in meeting California's RPS and energy efficiency goals. Chapter 4 will discuss cost benefit analysis and the application of such an analysis to a water-borne PV system. The water-borne application is presented to reduce the land use problem associated with PV, develop localized renewables, and improve energy efficiency all of which help reduce the amount of long distance transmission required to import renewable energy sources.

The California Transmission Planning Group (CTPG) consisted of a group of electric utility planning engineers from the major utilities throughout the state of California. A major purpose of the CTPG studies initiated in mid-2009 was to examine potential corridors for new transmission lines to transport renewable energy resources in order to meet RPS goals and achieve GHG reductions and to provide a foundation for a state-wide transmission plan to identify the

transmission infrastructure needed to reliably and efficiently meet the state's 33% Renewable Portfolio Standard (RPS) goal by the year 2020 [15][16][17][18].

The CTPG utilized the GE Positive Sequence Load Flow (PSLF) software and base cases established the Western Electric Coordinating Council (WECC), the National Renewable Energy Laboratory (NREL) and the California Transmission Planning Group (CTPG) to perform various studies in California and the Western United States. These studies were to analyze and determine the most probable sites where significant amounts of wind and some solar might be integrated and the effect it would have on the reliability and stability of the transmission grid in the region. Because of the complexity of the study effort, a phased approach was undertaken by the CTPG [15]. Some of the significant findings of these studies are summarized in Chapter 5. Chapter 5 will also discuss the methodology for conducting these transmission planning studies.

The CTPG study results indicate that building new transmission lines alone (assuming they can be permitted and built) will not solve California's mandatory RPS requirements [15][16][17][18].

In addition to the CTPG findings, a couple of other points should also be considered when thinking about integrating solar and other renewable resources onto the electrical grid:

1. The recent FERC Order 1000 regarding cost allocation has introduced some challenges for public utilities involved with transmission planning and construction. This may spur more local resource development [19].
2. Caltech research suggests that adoption of solar PV in California could reach between 15%-50% by 2020 [140].

Although small penetrations of renewable generation on the grid can generally be smoothly integrated, higher PV penetrations can be problematic and a one size fits all answer does not apply [112]. Chapter 6 will cover various examples and studies [21, 112] that specifically address this problem and potential solutions of integrating a high penetration of solar onto distribution networks.

A 21st century grid (transmission and/or distribution) will have to balance fluctuating power flows from wind and solar generation, small-scale distributed sources, and quite possibly plug-in electric vehicles. The increasing penetration of renewable resources brings new challenges including technical issues, power quality, reliability and security as well as other non-technical issues.

These challenges are compounded by utility industry structure and California regulatory structure [11] and problems that the renewable energy industry has in technically integrating and seamlessly operating renewable sources on the grid.

Much of the grid is at or approaching the end of its expected life. The Brattle Group estimated transmission and distribution infrastructure investment could reach nearly \$1 trillion through 2030 in the U.S. [140]. Federal law requires grid modernization to enable an increased dependency on variable and distributed energy resources [143]. This means that existing market and grid control systems, based on traditional centralized resources and one-way distributed power flows, require new operational paradigms, systems architectures and market structures.

The transformation of the grid is the most ambitious reconstitution since its inception more than a century ago and the change will pose serious challenges affecting all of society. This is happening worldwide due largely to legislation and regulatory mandates to increase renewable energy in response to concerns about global warming, air pollution and peak oil prices. Maintaining grid stability, reliable energy supplies and affordability will require solutions in technology, public policy, markets, data communications and public understanding.

It is worth a quick mention that solar storms also have an impact on the stability and reliability of the electrical grid. It is interesting the application and implications that Liouville's theorem, the same theorem that expresses the conservation of the generalized *étendue* along the ray path for an optical system, and an important principle in understanding solar concentration (reference Appendix A), has on the apparent brightness temperatures of solar radio bursts to the propagation of radio waves through the solar corona, [9] useful in understanding solar storms. Solar storms can and have caused damage to the electrical grid and its components. While not the subject of this Dissertation, this is mentioned for the sake completeness in understanding the potential reliability issues and impacts that solar phenomena can have on the grid. This issue is receiving considerable attention by the Federal Energy Regulatory Commission (FERC), the National of Electrical Reliability Corporation (NERC) and the utility industry as explained further in Appendix E.

Chapter 7 will provide a summary and future work and research that needs to be done.

In summary this Dissertation is to provide the following contributions:

1. Provide a background to motivate policy change and present a new and creative solution that provide increased distributed generation, improve energy efficiency, increase renewable energy reliably without the need for additional transmission and help meet AB32.
2. Provide an integrated source of information, or reference for engineers, managers, legislators, and regulators involved with integrating renewable energy, particularly photovoltaic systems, into the electrical system.
3. Describe the limitations in integrating a high penetration of solar PV onto the grid and addresses some potential solutions and further studies that are required.
4. Discuss the potential issues facing rooftop solar installations.
5. Discuss the flaw of omitting grid reliability from RPS policy. The separation of RPS and CSI legislation creates a reliability gap as well as RPS gap.
6. Provide a solution to land use issues for larger PV installations by proposing a water-borne installation. Appendix A describes the principles behind a concentrated PV system (CPV). Chapter 2 contains a high level specification for developing water-borne PV independent of technology and provides a cost target and budget to motivate more rapid development and deployment of such systems.
7. Provide a water-borne PV system application to Waste Water treatment (WWT) plants in California. Such an application will be relatively easy to permit, improve plant efficiency, and contribute to the Governor's distributed generation goal. Potential conflicts of harvesting algae in WWT facilities will be examined.
8. Motivate policy development for the development for water-borne PV systems and integration of PV onto distribution networks.

2.0 CHALLENGES AND OPPORTUNITIES FOR INTEGRATING SOLAR PV INTO RESOURCE PORTFOLIOS TO MEET CALIFORNIA'S RPS GOALS

2.1 REGULATION AND POLICY CHALLENGES FOR SOLAR PV

Four state-level entities are responsible for major aspects for California's electricity structure: the California Public Utilities Commission (CPUC), the California Air Resources Board (CARB), the California Energy Commission (CEC), and the California Independent System Operator (CAISO). The CPUC and CEC are the two primary state agencies responsible for implementing programs to encourage the development, installation and purchase of renewable electricity; however the CAISO has also expanded its activities with various initiatives relating to renewable and distributed resources. This creates some problems and challenges because California has no single agency, law, regulatory decision, or document that describes all policies and programs for the development of renewable power resources.

Data compiled by the CPUC shows total statewide expenditure on electricity costs will grow by nearly 50% between 2010 and 2020. Of these forecasted costs, the largest share is for new transmission and distribution (much of which is driven by renewable needs), the second largest is for renewables, and the third is for new fossil fuel-related costs [11].

In January 2006, the CPUC adopted a program- the California Solar Initiative (CSI) - to provide more than \$3 billion in incentives for solar projects with the objective of achieving participation levels accounting for 3,000 MW of solar capacity by 2017. Senate Bill 1 was signed by the Governor in August 2006, expanding the CSI to include publicly-owned utilities with a total ratepayer-funded budget of \$3.5 billion. As of May of this year 968 megawatts have been installed on existing homes, businesses and other buildings. This program's goal is achieve 1,940 megawatts by the end of 2016 [11].

The issues with rooftop solar PV in California are:

- 1) Utility rate design and NEM;
- 2) Exclusion of rooftop solar PV from renewable portfolio standard (RPS) eligibility; and
- 3) Distribution reliability problems due to future high penetration levels of solar PV and distributed generation.

2.1.1 UTILITY RATE DESIGN AND NEM

Net energy metering (NEM) has been a core public policy credited with California's leading market success in the installation of solar PV generation, and it has been adopted in 43 U.S. states. Net metering is a billing arrangement for customers who install on-site renewable distributed generation, typically solar PV that is interconnected to the grid systems. Simply stated, with NEM, the customer's meter runs both forward and backward, and at the end of the billing period the customer pays for the net energy used, or receives a credit at the retail rate if more energy is produced than consumed. If the customer did not export power to the grid and 100% of PV generation was consumed on-site, there would be no need for NEM. The California legislature restricted the CPUC's ability to set cost-based rates as a result of the failed deregulation attempt leading to California's electricity crisis. Low tier rate caps enacted during the crisis limit electricity rate increases, despite growing costs, for low-usage and low-income residential customers. Independent Owner Utilities' (IOUs-such as Pacific Gas & Electric (PG&E), Southern California Edison (SCE) and San Diego Gas & Electric (SDG&E)) customers who are economically able to install PV panels on their home rooftops can use the NEM program to effectively opt out of rate increases for higher electricity tiers, despite potential heavy consumption, and instead receive electric service at the protected low-tier rates net of their self-generation. California IOU residential rates have a four-or five tiered pricing structure that increases the per unit rate above certain monthly consumption thresholds. The current rate design means that heavy users effectively cross-subsidize low-usage customers. Though current policies are encouraging rapid PV deployment in the short term, the rate imbalances being created could be limiting the broader, market-driven scale-up of these key technologies by aligning utility and consumer interests against them. Regulators must ensure that customer rates are both "just and reasonable" and utilities are concerned about not only the rate impact from NEM but also the erosion of their revenue streams.

The California Investor Owned Utilities (PG&E, SCE and SDG&E) and others contend that NEM causes a significant cost shift from customers who install solar to other, non-participating ratepayers [21]. Severin Borenstein, the E.T. Grether Professor of Business and Public Policy at the Haas School of Business, U.C. Berkeley, and the Director of the U.C. Energy Institute, stated at a California Energy Commission hearing (May 2012) that the "fundamental

problem isn't net metering, but rather marginal prices that greatly exceed marginal cost".¹

The challenge in the Commercial and Industrial (C&I) markets is to reduce the use of rate design elements such as demand charges that solar customers cannot easily avoid, which undervalue the avoided-cost benefits of NEM exports to the grid. Removal of these rate design barriers in the C&I market would hasten the day when solar is cost-effective for participants in the C&I market without significant tax credits or other direct incentives. The California Public Utilities Commission (CPUC) interpreted California's statutory 5% cap on NEM systems to allow more than 5,000 MW of NEM systems allowing significant growth in the solar market beyond the 2,300 MW of PV systems that will be installed in the IOU service territories under the CSI. However, at the same time the CPUC also announced that it would suspend NEM as of the end of 2014 unless it has developed new rules for NEM prior to that date.²

Most legislation for net metering programs place caps on enrollment. In the absence of changes to inverter design or distribution system architecture, as the penetration of PV and distributed generation increases, future solar PV customers will likely face alternate metering strategies or limits on supply of power to the grid [88]:

1. Net meters may be replaced with dual meters, which allow the utility to apply one rate for power supplied to the customer and a lower rate for power provided by the customer. Alternatively, net meters may be replaced by meters that only turn one way, giving no credit for power supplied to the grid.
2. Time-of-use rates (TOU) may be imposed. TOU rates were briefly imposed on new, net-metered, residential solar system in California. The high rates for power from sunset to 9 pm greatly reduced the

¹ Severin Borenstein, "Rate Design and Renewables," presentation to the May 22, 2012 Lead Commissioner Workshop on Renewable Energy Costs for the 2012 Integrated Energy Policy Report Update (CEC Docket #12-IEP-01), at Slide 8. Available at http://www.energy.ca.gov/2012_energypolicy/documents/2012-05-22_workshop/presentations/05_Borenstein_UC_Berkeley_2012-05-22.pdf

² See CPUC Decision No. 12-05-036, issued May 24, 2012

value of PV systems, and demand for new systems declined rapidly. Interesting that study results shown in [21] suggest that encouraging more residential NEM customers to adopt TOU rates would increase NEM benefits to non-participating ratepayers.

3. As deployment of distributed PV systems increases, many customers are likely to be subject to time-of-use rates and demand charges, and will be paid less for energy delivered to the utility at a particular time of day than they will be charged for energy delivered by the utility at that same time [88].
4. VAR reactive power charges are likely to be imposed on users unless PV generation can supply the VARs (unit for reactive power) at the source.

2.1.2 EXCLUSION OF ROOFTOP SOLAR PV FROM RPS ELIGIBILITY

The second solar PV problem in California is that while many of California's renewable programs procure power that is "RPS eligible" – the power that counts towards the 33% RPS requirement – other programs are "RPS ineligible," either because the energy produced under the program is difficult to measure or because it is not purchased by a utility directly. One example of an ineligible program is the previously mentioned California's Solar Initiative program (also known as the "Million Solar Roofs" program), which subsidizes the cost of installing rooftop solar panels. While the renewable energy PV production that is on the customer side of the meter reduces the amount of energy that the customer purchases from the utility, and thus lowers the utility's overall RPS obligation (which is based on system-wide energy usage), utilities must still plan for the total amount of RPS renewable (intermittent) energy on their system. The CEC has estimated that as of 2011, there were 127,000 customer-side solar projects; totaling roughly 1,300 MW [11] (not counted towards RPS).

The intermittent nature of renewable energy sources presents both planning and operational challenges for a utility. It is essential for grid reliability

to account for all renewables regardless of what program they may fall under. This will become increasingly more important as penetration levels of these resources continue to increase. Current regulatory policy does not address this reliability impact caused by the high penetration levels of distributed generation including solar PV on to the electrical grid. It should also be pointed out that the NERC (North American Electric Reliability Corporation) Reliability Standards approved by the by Federal Energy Regulatory Commission (FERC) also do not currently address this potential problem.

2.1.3 DISTRIBUTION RELIABILITY PROBLEMS

Renewable Portfolio Standards have created the possibility of significant levels of distributed solar generation being installed on distribution systems contributing to instabilities and possibly unsafe operations due to one or several of the following design and operational characteristics [88].

The third solar PV problem (including other distributed generation) deals with the issue of high and maximum penetration of these resources on the grid before reliability and stability problems are encountered.

There are utility concerns that a high penetration of inverter-based solar energy systems along with other distributed generation sources on distribution lines will contribute to instabilities and possibly unsafe operations due to one or several of the following design and operational characteristics [88]:

1. Because PV energy production does not always coincide with the times when it is most economical for utilities to use it, it can negatively impact utility operating economics.
2. From the utility perspective, net-metered, flat rate customers, especially those whose net demand approaches zero, do not pay a fair share of their costs as discussed above.
3. Power production from an individual PV system may increase or decrease rapidly due to cloud passages. In most cases, the rate of change of the collective output from PV systems will be moderated by the geographic dispersal of the systems. However, in a case where

the service area is relatively small and where rapid weather changes can occur, PV output power can change dramatically. Measurements by Tucson Electric Power show that a rapidly-passing cloud bank can essentially eliminate all solar generation across Tucson in less than 5 minutes, thus increasing the increased need and control of spinning reserves.

4. The addition of a large numbers of inverters has shown to increase the probability of islanding, during which inverters continue to supply local loads after a utility fault [88, 114].
 - Inverters are limited in their ability to introduce high levels of short circuit current, but the addition of large systems or many small systems can sum to large short circuit currents.
 - Utility protection relays are designed to detect a fault. The relays briefly disconnect to allow the line to clear, and then reconnect to provide continuing service. If islanding detection fails and inverters remain on line then the inverters may 1- be damaged by the reconnect 2- continue to supply current to maintain the fault 3- cause safety issues because of power being supplied to the load side of disconnects of downed power lines.

5. Large power flow into distribution systems that were designed for one-way flow may impact regulation and protection. The following potential issues have been identified due to the effects of high penetration of PV and other distributed generation on distribution system operation:
 - Reverse power flow can interfere with voltage regulation. High PV penetration power downstream from the voltage regulation system on a radial line will make line loading appear to be low.
 - Power injected just downstream of voltage regulation will cause customers at the end of the line to experience low voltage
 - Power injected near the end of the line, will cause high voltage to occur at that point
 - Fuses protect the current carrying capability of a line, but injection of power downstream from the fuse will not be detected, leading to the potential for overload.
 - Power electronics of the inverters inject higher order harmonics that may interfere with distribution equipment without the additional cost of filtering.

- Phase to neutral overvoltage will be worsened with high penetration of PV distributed systems due to 1- no dispatchability or interactive control 2- disproportionate installation on single phase systems.

2.2 HIGH PV PENETRATION ON UTILITY DISTRIBUTION SYSTEMS

Maximum renewable penetration on the grid is effected by voltage stability, dynamic stability, economic stability, but each can cause a different level of penetration. Stability effects due to clouds and voltage regulation and their effects on network stability and reliability will be discussed in this section.

2.2.1 LIMITATIONS DUE TO CLOUDS

PV cloud effects on voltage stability have been investigated mainly in either a large scale transmission level or an individual unit control with a simple network. Yun Tiam and Kirschen [122] implemented a PV reactive power control method for voltage regulation to deal with voltage fluctuations during large irradiation changes, but it is still at a transmission level. Low voltage distribution networks have their special characteristics namely: unbalanced nature, line drop compensation, dynamic loads (small induction motors and thermostats), high R/X ratio, etc. Steady and reliable performance in a large-scale transmission system does not necessarily mean the same performance can be achieved in a geographically small distribution system [87, 110, 123]. The following scenarios listed below show the effect of clouds on several different distribution networks.

One of the first issues studied was the impact on power system operation caused by PV system output fluctuations due to cloud transients at a central-station plant. A 1985 study [103, 164] in Arizona examined cloud transient effects where PV was deployed at a central station plant and found that the maximum tolerable system level penetration of PV was approximately 5%. The limit was imposed by the transient following capabilities (ramp rates) of the conventional generators. Another paper published in that same year [124] about the operating experience of the Southern California Edison central station PV plant at Hesperia, California, reported no such problems, but suggested the plant had a very stiff connection to the grid and represented a very low PV penetration level at its point of interconnection.

Cloud cover or shading levels are the main reasons for solar ramping and produce the fastest ramp rate output power fluctuation. One needs to know how

many types of cloud patterns exist, the shadowing coverage area, the cloud height, and optical transmission rates, in addition to the speed at which the clouds are moving [125, 20]. Studies have shown that squall line clouds and cumulus clouds produce the worst problems for PV. The squall line type, described as a solid line of dark clouds, produces almost a complete loss of PV generation. Conversely, cumulus types, which are faster moving and more well-defined with clear skies between them, in turn producing less ground shading area, produce a smaller percentage loss of PV output but at a much more random rate of change. This may be worst case since voltage regulation devices may not have time to operate. The intermittency caused by cumulus clouds is much less predictable than the squall line clouds. Sources available that will predict cloud coverage over a defined area are found in references [125, 20].

In 1988, a study dealt with voltage regulation issues with the Public Service Company of Oklahoma system when clouds passed over an area with high PV penetration levels, when the PV was distributed over a wide area (south Tulsa, Oklahoma) [103, 105]. At penetration levels of 15% cloud transients caused significant but solvable power swing issues at the system level, and thus 15% was deemed the maximum system-level penetration.

Another cloud transient study was released in March 1990 [106]. A Kansas utility quantified the impact of geographic distribution of PV on allowable PV penetration level at the system level. Most of the utility's generation was slow-responding coal-fired units. It was concluded the utility's load-following capability limited PV penetration to only 1.3% if the PV were in central station mode; the limitation was caused by unscheduled tie-line flows that unacceptably harmed the utility's economics. However the allowable penetration rose to 18% if the PV were spread over a 100 km² and to 36% if the PV were scattered over a 1000 km² area.

The impact of high penetrations of PV on grid frequency regulation appeared in a 1996 paper from Japan [163]. This study used modeled PV systems that respond to synthetically generated short-term irradiance transients caused by clouds. The study looked at system frequency regulation and the break even cost, which accounts for fuel savings when PV is substituted for peaking or base load generation and PV cost. The paper reaches three interesting conclusions: (1) the break-even cost of PV is unacceptably high unless PV penetration reaches 10% or so; (2) the thermal generation capacity used for frequency control increases more rapidly than first thought; and (3) a 2.5% increase in frequency control capacity over the no-PV case is required

when PV penetration reaches 10%. For penetration of 30%, the authors found that a 10% increase in frequency regulation capacity was required, and that the cost of doing this exceeds any benefit. Based on these two competing considerations, the authors conclude that the upper limit on PV penetration is 10%.

Distribution networks were designed for heavy loading conditions without any PV integration, but they still can operate well with low PV penetration levels. A simulation study by Saha and Yan [123], produced some interesting results:

- PV penetration is proportionate to its load. For example for 10% PV penetration, PV installation at each bus is 0.1 times the load of that bus. This result correlates with a series of reports produced by an International Energy Agency Working Group on Task V of the Photovoltaic Power Systems Implementing Agreement dealt with voltage rise [118].
- Cloud effects on voltage stability became a serious concern for the studied system when 40% power (penetration level) was contributed from PV systems in a geographically small area. The study concedes that the 40% level may not be identified properly because the loads are modeled as static loads. Detailed dynamic load models are therefore recommended for PV integration studies.
- With 20% storage units, which are controlled to smooth PV power fluctuations, voltage stability can be maintained. However, storage locations should be carefully chosen for maintaining voltage stability.
- The PV inverter reactive power control scheme was extremely effective for fast voltage support

A primary result of a series of reports produced by an International Energy Agency Working Group on Task V of the Photovoltaic Power Systems Implementing Agreement dealt with voltage rise [106]. Three configurations of high-penetration PV in the low-voltage distribution network were discussed: (all PV on one feeder, PV distributed among all feeders on a medium-voltage distribution/low voltage (MV/LV) transformer, and PV distributed on all MV/LV transformers on an MV ring). The study concludes that the maximum PV penetration will be equal to whatever the minimum load is on that specific feeder. That minimum load was assumed to be 25% of the maximum load on the feeder [106], and if the PV penetration were 25% of the maximum load, only insignificant overvoltage occurred (study assumed no automatic load tap transformers).

As can be seen from the studies listed above maximum penetration due to cloud effects, voltage regulation, frequency regulation and load can vary from 5-40%. The minimum load criteria and geographic diversity are important guidelines and rules of thumb to follow in determining maximum penetration for initial planning purposes.

2.2.2 VOLTAGE REGULATION

In August 2003 two major distributed generation studies were conducted by GE [106]. Only the first study will be summarized here because the distributed generators (DGs) interfaced to utilities through inverters. Key results of the first study [106] include:

- For DG penetration levels of 40% such that the system is heavily dependent on DGs to satisfy loads, voltage regulation can become a serious problem. The sudden loss of DGs, particularly as a result of false tripping during voltage or frequency events, can lead to unacceptably low voltages in parts of the system.
- The simulated distribution system was assumed to employ step voltage regulators (SVRs), which are essentially autotransformers with an automatically adjustable tap on the series winding. During periods of low load but high generation and with certain distribution circuit configurations, the reverse power flow condition could cause the SVRs to malfunction. Again, voltage regulation becomes a problem.

A voltage regulation function, implemented, through reactive power control, would significantly increase the benefits of inverter-based DGs to the grid. Unfortunately, this function would interfere with most anti-islanding.

2.3 THE LAND CHALLENGE FOR SOLAR

Prime farmland in California is protected from development by the Williamson Act and by the California Environmental Quality Act. Even when land is available, because of the amount of land required to develop utility-scale projects, special-status species (plant and animal) are often impacted. Urban

land is expensive and so most renewable energy zones tend to be located in more remote areas. Figures 2.1 and 2.2 show the renewable energy zones for California and the Southwestern United States.

These energy zones require transmission lines to transfer the power to the load centers. The cost of transmission lines is expensive. The recently completed Sunrise Transmission Powerlink Project completed by San Diego Gas & Electric (SDG&E) and PacifiCorp Gateway Central Line Project provide a good overview and reference point.

The Sunrise Powerlink project runs 150 miles between the Imperial Valley to San Diego. The Imperial County region has significant solar, geothermal and wind resources (see Figure 2.1) [156].

According to SG&E, the transmission line would have the capacity to ensure up to 1,000 megawatts to meet its obligations to purchase certain amounts of energy from renewable generation sources. SDG&E estimates the cost of the project to be \$1.9 billion [156,157]. The costs include a 500 kV line, several 220kV lines, the Suncrest substation and updates to seven other substations.

A few key dates are presented to show the length of time it takes to construct a project [156].

- Applications for the project submitted to the CPUC on December 14, 2005 and August 4, 2006
- Project approved CAISO on August 3, 2006
- The CPUC voted on December 18,2008 to approve the Final Environmentally Superior Southern Route and the Bureau of Land Management (BLM) issued a Record of Decision approving the same route on January 20, 2009.
- Construction to occur in 25 segments. Construction of these segments was authorized the fourth quarter of 2010 and the first quarter of 2011.
- Sunrise Powerlink Transmission Line, including the 500 kV and 230 kV links energized on June 15-17, 2012.



Figure 2.2 Potential Renewable Energy Zones in Southwestern U.S. (Courtesy of USE)

A study titled "Capital Costs For Transmission And Substations Recommendations For WECC Transmission Expansion Planning" [155] shows that baseline transmission costs range from \$1-3 million/mile based on the following assumptions:

- Aluminum Conductor Steel Reinforced (ACSR) conductors
- Tubular (230kV)/Lattice (345kV and 500 kV) pole/tower structure
- Lines longer than 10 miles

If high tensile low sag conductors were used, a multiplier of 3.6 would need to be applied. A Terrain multiplier for forested land would also add a multiplier of 2.25. In addition to the capital costs for transmission line equipment and difficulty of construction based on terrain, there are costs associated with acquiring land for the transmission line. In some cases, right of way costs can come to 10% of total project costs. This proportion varies between projects and is dependent on right of way widths for each voltage class and right of way costs per acre. Substation costs also vary with size. These costs are given as "overnight" costs, i.e. the cost if the project could be engineered, procured and constructed overnight without financing or overhead costs. A category called Allowance for Funds Used During Construction (AFUDC) and overhead is added to the transmission and substation costs to produce a realistic project cost.

Table 2.1 shows the actual cost breakdown of PacifiCorp's Gateway central Line (Populus-Terminal Segment). This 345-kV double circuit line segment is centered in Utah, and extends from the new Populus substation in southeastern Idaho to the existing Terminal substation in the Salt Lake City area.

It was completed in 2010. The most notable characteristic of this line is that it crosses a significant amount of mountainous terrain and urban and suburban terrain around Salt Lake City [155]. The examples provided are meant to show that transmission lines are costly and take from 7-10 years to build.

Table 2.1 Cost PacifiCorp's Gateway Central Line

Cost Component	Actual Cost
Line Cost (Including wires, Poles, etc.)	\$ 498,439,614
Right of Way Cost	\$ 70,183,253
Substation Cost	\$ 126,054,613
AFUDC/Overhead Cost	\$ 122,152,660
Total Cost	\$ 816,830,140

The ultimate structure of the electricity industry, as envisioned by the Federal Energy Regulatory Commission, includes large regional transmission organizations (RTOs) that will be responsible for planning and expanding transmission systems on a broad regional scale. This shift from planning conducted by individual utilities for their system to meet the needs of their customers to planning conducted by RTOs to meet the needs of regional electricity markets raises important issues. These issues include the objectives of planning (reliability vs. commerce), the role of congestion costs in deciding which projects to build, the consideration of generation and load alternatives to new transmission projects, the economic and land-use benefits of building larger facilities, the role of new solid-state technologies that permit operation of transmission systems closer to their thermal limits, and the growing difficulty in obtaining data on new generation and load growth caused by the separation of generation and retail service from transmission [11].

New transmission costs are paid for by tariffs or transmission access charges imposed at the load and paid by users. Transmission access charges (TAC) can amount to 33% of the cost of the electricity for low load conditions. Behind the Meter installations are good for the end use customer as can be seen in the cost benefit analysis shown in Table 4.2 of Chapter 4.

Another problem affecting the time it takes to develop remote renewable resources and new transmission line systems is the permitting process. It often takes as much time to permit as project as it does to construct it. There are reforms being reviewed by the Obama Administration to streamline environmental permitting and take climate change into account when granting permits by any federal agencies or in granting leases on public lands. The Bureau of Land Management, part of the Interior Department, is the nation's

biggest landlord, controlling 20 million acres of ideal solar potential, mostly west of the Rockies [13]. California has the largest renewable market in the US outside of Colorado [14].

While reform has been underway in California for some time, the process for permitting large scale solar is extremely rigorous and thorough, according to SolarReserve, which spent a significant amount of money permitting their Rice Solar Energy Project, in Riverside, California with the California Energy Commission [13].

Peter Weiner, chair of the environmental and energy regulatory practice at Paul Hastings has handled a number of the recent utility-scale solar energy permitting, with over 6 GW in projects. He said, “Large scale solar and wind are so much better for the planet when it comes to greenhouse gases. On the other hand they (large scale solar and wind) have very large footprints and a lot of the siting of these larger facilities has been in areas which have not had a lot of development, such as the desert. As a result the wildlife agencies-which are not very much involved in fossil fuel production became very involved” [13].

2.4 A LOCAL PV DEVELOPMENT OPTION- A BRIDGE TO THE FUTURE

Governor Brown’s goal is to develop 12,000 MW of distributed generation by 2020 [20]. The question is, what is an effective way to meet the governor’s goal to increase distributed generation as well as meet RPS goals. It has already been mentioned that the CSI and NEM are not applicable to RPS.

A logical option to avoid installing solar PV on land, avoid the rate structure issues of the CSI and avoid reliability and stability issues due to high penetration on distribution networks is to install solar PV on water. This can also help achieve Goal 1 of the Strategic Plan i.e. focusing on integration with other water, air quality and GHA resource management and energy efficiency strategies [12].

The water-borne application can effectively assist in the development of localized renewable distributed generation, and improve energy efficiency thus reducing the amount of long-distance transmission required to import renewable energy sources and minimize the land use issue. It can decrease the area required for solar PV installations by 50%, from 6 acres/MW to 3 acres/MW, and potentially generate greater than 1000 MW of power by floating PV on the ponds of wastewater treatment plants in California. Because of the geographic

diversity, the high penetration issues with rooftop solar on distribution networks can be avoided.

What was claimed to be the world's first floating photovoltaic system was installed in 2007 by SPG Solar on a pond at Far Niente Winery in NAPA California [165].

The idea of a floating water-borne Concentrated PV (CPV) system was conceived nearly a decade ago. However, the first large scale, tracking and floating CPV prototype was built and deployed by Pyron Solar in collaboration with San Diego Gas & Electric at the Mission Hills Training Center in San Diego in early 2011 [75].

K-water has installed a 100kW floating PV system on the water surface of Hapcheon dam reservoir in October 2011 for operation, K-water followed up this project with an additionally installed 500kW floating PV system on another location nearby in July 2012 [164]. This begs the question of why was such a system can be built in South Korea and not in the U.S. or California.

Several different design methods for floating water-borne PV systems have been proposed (including both flat panel photovoltaic and concentrated photovoltaic (CPV) systems) using various configurations and components. Some designs resemble land ground based systems installed on floating docks or specially designed floaters, others differentiate themselves by their collection system including tracking system and profile above the water surface, but all require some type of mooring system and marine cabling systems. A number of companies including Pyron Solar, Topsun Co. Ltd., Ciel & Terre, Phoenix Solar, GEITIS, Apex Energy Teterow GmbH, SPG, Novaton [149], K-water and Sunengy are developing systems to install on water; however while some have developed impressive proposals, commissioned capacity is still insignificant.

Wastewater treatment plant settling ponds can provide opportunistic sites for floating PV installations. These are relatively protected sites with calm water

near distribution/transmission lines. Based on a survey conducted for the energy baseline study for municipal wastewater treatment plants sponsored by Pacific Gas and Electric (PG&E), there are approximately 480 wastewater treatment (WWT) facilities in the PG&E service territory [74]. There are more than 800 plants in California and more than 21,600 in the United States.

2.5 SPECIFICATION FOR A WATER-BORNE SYSTEM

The intent of this section is not to favor a specific technology or design, but present some ideas and principles that could be included in a specification.

Concentrated solar PV (CPV) only makes sense if it can increase performance and economics. CPV with dual axis tracking are designed to yield the highest efficiency, but that may also come with a higher cost. Pyron Solar developed a CPV system that floats on water [75] that embodies the principles and technology discussed in Appendix A.

The current cost projections for a 10 MW size CPV plant is scaled to approximately \$3.30/watt. This design utilizes dual axis tracking and a concentration greater than 1000x on multijunction cells with an overall efficiency of 29%. The Pyron concept has some very innovative design features; however the low cost of flat panels and their increasing efficiency has really dampened the concentrated solar PV market.

The proven flat panel designs have an efficiency of 19% (although new designs: Sun Power's X22 and X24 series, are reported to be 22% and 24% efficient respectively).

The efficiency of both flat panel and CPV designs are increasing, so the important question in selecting a system is which system has the best life cycle costs for an equivalent amount of capacity and energy.

Life Cycle Assessment (LCA) is a structured, comprehensive method of quantifying material and energy flows and their associated impacts in the life cycles of products. The intent is for a product to be able to transform more energy as an output than what was required to produce it. Ref [161] includes detailed inputs and outputs of four technologies (mono- and multi-crystalline Si, DcTe and high concentration PV (HCPV) using III/V multijunction cells) for which there are well-established Life Cycle Inventories (LCI). These include detailed inputs and outputs during manufacturing of cell, wafer, module, and balance-of-system (i.e., structural and electrical-components) that were estimated from actual production and operation facilities. The LCA indicators in ref [161] are: Energy Payback Times (EPBT), Greenhouse Gas (GHG) emissions, SO₂, NO_x,

and heavy metals. The life –cycle of photovoltaics starts from the extraction of raw materials and ends with the disposal or recycling and recovery of the PV components.

When a PV plant or installation is proposed it should include an LCA. This includes the LCA for the modules and panels as well as the Balance of System

Balance of System (BOS) becomes more important in evaluating cost and environmental analysis or LCA as module and panel costs and environmental impacts decrease. For instance, a recent analysis of a large PV installation at the Springerville Generating Station in Arizona affords a detailed materials and energy balance for a ground-mounted BOS. Tucson Electric Power prepared the BOS bill of materials and energy consumption data for their mc-Si PV installations. The life expectancy of the PV metal support structures is assumed to be 60 years. Inverters and transformers are considered to last for 30 years, but parts must be replaced every 10 years, amounting to 10% of their total mass. The inverters are utility-scale, Xantrex PV-150 models with a wide-open frame, allowing failed parts to be easily replaced [162].

2.5.1 DESIGN FOR LIFE CYCLE COST

The system shall be designed for 25 years and shall be designed to minimize life cycle cost, including the ability to incorporate future technological upgrades. Product documentation shall include engineering structural, electrical and mechanical drawings, maintenance manuals, operating and commissioning manuals, and recommended spare parts lists. The system design shall provide an availability of 0.9. All components shall be off the shelf and shall be hardened or packaged as necessary for a marine environment.

2.5.2 STRUCTURE

The supporting structure shall be modular for easy field assembly designed for transport on a flat- bed truck no longer than 50 ft. long. Support structure can be circular or rectangular, must be capable of supporting 20-30 kW and weigh no more than 3,000 kg with all equipment installed. All structures must be corrosion resistant and electrical enclosures must be moisture proof. The design shall be low profile so that it does not extend more than 2 meters above the surface of the water. Test reports must show the design can withstand winds of 140 km/hr. The structure must be designed to support single axis azimuthal tracking; provide space, support and protection for 30 minutes of battery backup for all control functions; provide space, support and protection for the MPPT and DC/DC conversion; provide space, support and protection for all protective

devices (relays, fuses, breakers; raceways for cable management. Field assembly time from truck offload to crane hookup for pond placement shall not exceed 16 manhours per 25 kW module assembly. A suitable tethering mechanism must be provided. While the structure shall be designed for adjustable fix tilt placement of panels (flat panel design), it shall also be provided with a manual reset switch and appropriate mechanisms and linkages so that all panels can be directed to the horizontal position for cloudy and overcast days.

2.5.3 CABLING

All cabling shall be marine grade, be able to withstand 1000 vdc minimum and be supplied with waterproof connectors and splice kits. Cables and raceway design shall be coordinated and properly labeled for neat and reliable cable management. Cabling shall be designed so that all field cabling can be connected from the module to the inverter once placed in the pond up to 1000 meters distance. Cable and wire connection and termination, system checkout and commissioning shall be specified as a separate line item of the proposal. Ground faults management is of great concern especially in a water-borne environment; therefore cable management is critical. PV source-circuit conductors must be secured in a safe and serviceable manner; away from sharp edges, mounting hardware etc. Cable ties are not allowed for cable positioning, only hardware that ensures good positioning over the service life of the PV system is acceptable. Provide insulated bushings or smooth rounded entries at raceway and cable terminations to reduce insulation failure that may cause ground faults.

2.5.4 TRACKING

For flat panel design single axis is required (azimuthal tracking is preferred [148, 150, 151, 152]). Panels shall be able to be fixed at an angle from 0-25 degrees. If concentrated solar PV is provided dual axis tracking is required.

2.5.5 RELIABILITY AND WARRANTY

A 25 year warranty shall be provided for trackers, cables and protection devices. Inverters and batteries shall be warranted to 10 years. The warranty on PV panels and modules is negotiable depending on the price and efficiency of the module or panel. The goal is to design and install a system for the least life cycle cost.

2.5.6 ELECTRICAL, CONTROLS & PROTECTION

Controls for vertical or azimuthal tracking shall be included. Even though an adjustable fixed tilt position mechanism is to be provided for panel placement; a manual and remote manual switch shall be provided to move the panels to the horizontal position on cloudy days.

Electrical System design and installation shall comply with NEC (2008 or later). The following sections of the NEC shall apply: Article 110: Requirements for Electrical Installations; Article 230: Disconnect Means; Article 240: Overcurrent Protection; Article 250: Grounding; Article 300: Wiring methods; Article 480: Storage Batteries; Article 690 Solar Photovoltaic Systems and chapters 2 & 3 on Wiring methods and materials and Protection. UL 1741 shall also apply to all water-borne installations in that all grid-tied as well as non-grid tied inverters, regardless of size, should have full functionality for ground faults meaning that they will detect the ground fault, interrupt the fault current, indicate that a ground fault has occurred and disconnect the faulted part of the array. Photovoltaic source circuits and photovoltaic output circuits shall not be contained in the same raceway, cable, junction box or similar fitting as feeders or branch circuits of other systems.

Inverters shall be identified for use in solar PV systems (inverters listed to UL 1741) and be suitably packaged for marine application. AC modules shall have appropriate markings, overcurrent protection, disconnect means and Ground fault protection.

The dc circuit ground connection shall be made at a single point on the photovoltaic output circuit as close as possible to the power source to better protect the system from voltage surges due to lightning.

PV fuse links shall be fully tested to meet or exceed the requirements of IEC 60269-6 and also meet the requirements of UL 2579, thus being suitable for protecting PV modules in reverse current situations. Where three or more strings are connected in parallel, a fuse link on each string shall be included on each string to protect the conductors and modules from overcurrent faults and help minimize any safety hazards and also isolate the faulted string so that the rest of the PV system can continue to generate electricity. A fuse link on each sub-array will protect the conductors from fault current and help minimize any safety hazards. It will also isolate the faulted sub-array so that the rest of the PV system can continue to generate electricity. A fuse link positioned in the cable that carries the combined output of a number of strings should be protected by sub-array fuse links. If a number of sub-arrays are subsequently combined then a further fuse link should be incorporated. This would be termed the array fuse link.

For WWT facilities that are stand alone and not tied to the grid a plaque or directory shall indicate the location of system disconnecting means and that it is stand alone.

2.5.7 MAINTAINABILITY

Vendor shall provide daily, weekly, monthly and annual maintenance procedures and checklists for each pod (30KW assembly). A datalink shall be established to a plant control room that will monitor both key operating parameters, but also key equipment parameters. The system shall be designed for easy subassembly and major component removal (i.e. inverter, PV panel etc.) since maintenance is geared to this level of equipment replacement.

2.5.8 PERFORMANCE TESTS

All components shall be UL or CSA tested or equivalent. Any system connected to a transmission system shall be coordinated with the CAISO and WECC.

2.5.9 OTHER

The target budget value of \$2.70/watt shown in Table 2.2 is for illustrative purposes only. The \$2.70/watt corresponds to a cost of \$80/MWHR, a current fairly attractive market rate for renewable resources.

Table 2.2 Target Budget

Component	\$/Watt	Percentage
Support Structure &Tracking	0.40	15.0%
Modules & Cabling	1.70	63.0%
Inverters & converters	0.30	11.0%
Protection, Testing, Installation Project Management, Other	0.30	11.0%
Total	2.70	100%

This may seem an aggressive target since reference [160] shows that labor alone for a utility scale single axis tracking system was about the same cost. However, reference [160] also shows the evolutionary pathway for ground-mount, utility-scale, one-axis tracking PV system prices from the benchmark of

\$4.40/ $W_{p,DC}$ in 2010 to \$1.91/ $W_{p,DC}$ in 2020. It also shows the DOW SunShot utility-scale target of \$1.20/ $W_{p,DC}$ for comparison so while the target of \$2.70 is aggressive it is within reason. Crystalline silicon modules (panels) mounted on one axis trackers may experience a capacity factor benefit of between 25-30% (Campbell 2010b) in high solar resource locations, although the capital (system) penalty may be between 10-20%. In the future, (2020), as prices of (one-axis) trackers come down, the net-benefit of tracking c-Si modules in high resource areas may approach 20%. Because capacity factor and module efficiency are linearly correlated, the modified SunShot target for one-axis c-Si modules is estimated to be approximately \$1.20/ $W_{p,DC}$ [160].

3.0 FLOATING WATER-BORNE PV APPLICATION CONSIDERATION FOR UTILITY APPLICATION IN CALIFORNIA

The Northern California Power Agency (NCPA) is a Joint Power Agency that supplies power to its thirteen members and several other participants. One of the Power Plants NCPA operates is the Lodi Energy Center. The plant is contiguous to the City of Lodi's White Slough Water Pollution Control Facility and utilizes the treated water from the facility for its cooling tower operations.

Eight of NCPA's thirteen members are municipalities that own and operate waste water treatment facilities (Refer to Table 4.1). The City of Lodi (an NCPA member) operates the White Slough Water Pollution Control Facility that has approximately 50 acres of settling ponds (Figure 3.3). Figure 3.2 shows the location and the DNI of the Lodi Facility in relation to the surrounding area. This could be a good test site for installing a floating solar PV system as it could potentially float up to 15 MW of solar PV and is in close proximity to both electrical transmission and distribution.

3.1 WASTE WATER TREATMENT PLANTS

Based on a survey conducted for the Energy Baseline Study For Municipal Wastewater Treatment Plants sponsored by Pacific Gas and Electric (PG&E) there are approximately 480 wastewater treatment (WWT) facilities in the PG&E service territory [73]. Water and wastewater plants represent large electric and gas loads. Overall, wastewater treatment consumes approximately 1.5% of the total US electric power [74]. Other data suggest that waste water treatment facilities consume 4% of the country's total electricity [63]. After labor, electricity is the largest operating cost at wastewater treatment plants, typically 25 to 40% of total operating costs. The California Energy Commission reported that wastewater treatment plants are usually the single largest electricity user in local governments [74].

The following common methods for WWT are presented [74]:

- Aerobic activated sludge systems
- Trickling filter (fixed media or fixed film reactor) systems
- Oxidation pond systems

3.1.1 ACTIVATED SLUDGE

Aerobic activated sludge is the most commonly used wastewater treatment process consisting of primary treatment, secondary treatment, optional tertiary treatment, disinfection and sludge processing. Details of the processes for activated sludge WWT could be found in Hammer and Hammer (2004) and Metcalf and Eddy (2003). Major energy users in these processes include:

electric drives, various types of pumps, blowers, mixers, mechanical aerators, UV lamps and presses [74].

3.1.2 FIXED-GROWTH BIOLOGICAL SYSTEMS

Fixed growth biological systems are systems that cause contact of wastewater with microbial growth attached to the surface of supporting media. In these systems wastewater is distributed over a bed of rock, slag or synthetic media. Alternatively the media can move through the wastewater. Based on Hammer and Hammer (2004) these systems are categorized as:

- Tricking filter, where water is distributed over a bed of crushed rock or slag
- Biological tower, where synthetic media is used in place of rock with a greater depth
- Biological tower, where a series of circular plates on a common shaft are slowly rotated while partly submerged in wastewater.

Major energy users in these processes include: pumps for transport of wastewater, electrical drives for rotating the rotary wastewater distributors and hydraulic (water) drives for rotating the rotary wastewater distributors [74].

3.1.3 OXIDATION PONDS

Oxidation ponds, also called stabilization ponds or lagoons are utilized for smaller communities. According to Hammer and Hammer (2004), oxidation ponds are classified as facultative, tertiary, aerated and anaerobic according to the type of biological activity that takes place in them [74].

Facultative ponds are the most common type of ponds employed for municipal wastewater treatment. The bacterial reactions include both aerobic and anaerobic decomposition. Waste organics are decomposed by bacteria releasing carbon dioxide, nitrogen and phosphorous. Algae use these compounds, along with energy from sunlight for growth, releasing oxygen to the solution, which is in turn used by bacteria. These are shallow pools with 2-5 feet of depth [74].

Tertiary ponds also referred to as maturation ponds serve as third-stage processing of effluent from activated sludge or trickling filter secondary treatment. Stabilization by retention and surface aeration reduces suspended solids, BOD (Biochemical Oxygen Demand), microorganisms and ammonia. The water depth is generally limited to 2-3 feet for mixing and sunlight penetration.

Aerated ponds are completely mixed units, usually followed by facultative ponds. These are used for first stage treatment of high-strength municipal

wastewaters and for pretreatment of industrial wastewater. The basins are 10-12 feet deep and are aerated with pier-mounted floating mechanical units. The biological process does not include algae. BOD removal is a function of aeration period, temperature and nature of wastewater.

Major energy users in oxidation ponds include: pumps for transport of wastewater and electrical drives for surface aeration.

As previously stated, Waste Water Treatment plants can consume large amounts of power. This also means that many have transmission and distribution in close proximity. The high cost of power is a motivating factor for these facilities to implement the latest energy efficiency techniques some of which are described in the above mentioned studies commissioned by PG&E [73, 74].

3.2 FLOATING WATER-BORNE CPV SYSTEM

As mentioned in section 2.4, the idea of a floating water-borne CPV system was conceived nearly a decade ago. However, the first scale, tracking, floating CPV prototype was built and deployed by Pyron Solar in collaboration with San Diego Gas & Electric at the Mission Hills Training Center in San Diego in early 2011 as shown in Figure 3.4. The twelve month demonstration of the floating CPV solution provided proof-of principle validation of the technology [75]. All modules were connected to a neutrally buoyant substructure that floats just below the water's surface. The substructure was made of composite plastic material and connects all modules to a 50 foot diameter tracking ring and support structure as shown in Figure 3.1. The tracking ring was equipped with an azimuth and an elevation drive motor controlled by a microprocessor. The purpose in showing the design is not to promote a specific technology, but to show the low profile and basic structure that are attractive features regardless of the technology employed.

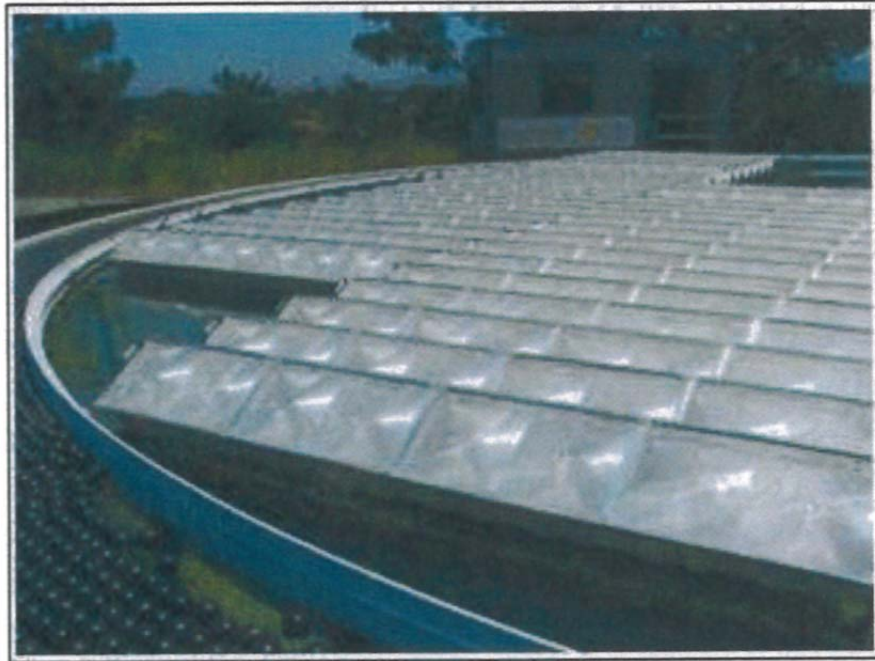


Figure 3.1 Floating CPV Modules

Since many WWT facilities have stabilization ponds and lagoons, the environmental permitting issues of land use and grid access could be simplified by installing floating PV systems on these ponds/ lagoons should it not interfere with the primary purpose of waste water treatment.

3.3 ALGAE IN WASTE WATER TREATMENT

This section will investigate the potential conflicts of floating solar PV on WWT ponds interfering with the primary purpose of the ponds for waste water management and the development of large-scale algal ponds for domestic and industrial liquid waste treatment.

Although originally used only to hold wastes, ponds were observed to substantially reduce pollution indicators-biochemical oxygen demand, odor, and settleable solids. The stabilization of organic matter in sewage wastes requires oxygen, which in secondary treatment plants is normally obtained from the atmosphere. The primary source of atmospheric oxygen is photosynthesis, for which the sun supplies the energy and water supplies the oxygen. Sewage contains the necessary nutrients for photosynthetic organisms to produce oxygen and at the same time to fix these valuable nutrient as well as solar energy in reclaimable material. This results because pond algae photosynthetically generates enough oxygen to allow bacterial oxidation of organic wastes. The

released nutrients (carbon dioxide, ammonia, phosphate, etc.) are converted into algal biomass [83]. Design equations have been developed to relate pond area requirements to sewage strength and flows, as well as local solar insolation and climatic conditions [84]. This engineering research has resulted in the widespread adoption of algal ponds (known as oxidation ponds) in many countries, including the United States, Australia, Israel, South Africa, and India.

Almost all presently used oxidation ponds are the “facultative” type- one to three meters in depth and arranged in cells of up to 50 hectares (hectare is 2.47 acres), and mixed only by wind action and perhaps recirculation of effluent. The bottom of these ponds are thus anaerobic (anoxic), resulting in fermentation of the settled sludge and algae, while the surface is kept aerobic by the algae, preventing odors from developing. The liquid detention time (days required to displace one pond volume) is long, from weeks to months (These are often referred to as Type 1 Oxidation ponds). This design may be optimal for waste treatment but not for algal growth.

If algal biomass production is to be maximized, the ponds must be shallow (30-50 cm), have short detention times (1-4 days in summer; up to 6 days in winter- these would be referred to as Type 2 Oxidation ponds), and be mechanically mixed (to minimize algal settling and prevent thermal stratification).

It should be pointed out that Type 1 ponds require about 18 acres of pond area for a flow of one million gallons of sewage per day while the acreage required to handle the same flow for a Type 2 pond would be about 9 acres or half that amount.

High rate ponds (1-6 days detention) produce well above 100 mg l^{-1} of algae (dry weight) and even facultative ponds normally have effluents of above 50 mg l^{-1} [83,84]. These levels of suspended solids are higher than those allowed by present US waste treatment plant discharge regulations; thus algae must now be removed from oxidation pond effluents. This step is also required for conversion of algal biomass into usable fuels.

Integrating floating PV onto waste water treatment ponds with Type 1 oxidation ponds or conventionally designed waste stabilization ponds would create little or minimal interference. Larger units of this type furnish oxygen by dilution and are comparable to natural lakes because their physical size is so great that they may receive wastes with little depletion of their oxygen reserves. Type 1 ponds would lend themselves well to floating PV application.

For Type 2 Oxidation ponds, Advanced Integrated Wastewater Pond Systems and systems designed to produce large amounts of algae for fuel harvesting, floating PV systems on ponds may be a competing system for light. Combined use systems for floating PV and algae harvesting would require further study. The photosynthetic oxygenation process requires consideration of influences of light, temperature, pond depth, heat content of the algal cell

material, and other limiting factors. Algal growth requires radiation in the visible range that will penetrate a smooth water surface. This represents only about 1/3 of the total radiation of the solar spectrum. According to Vannevar Bush, a plot of the influence of saturation intensity on light utilization by algae shows that as the incident light intensity increases, the fraction of available light utilized decreases regardless of the value of saturation light intensity [84]. It therefore appears possible that some combination of the two systems to coexist is feasible, but in what proportion would require further study.

Advanced Integrated Wastewater Pond Systems (AIWPS) have a series of four types of ponds [142]. The first series is the Advanced Facultative Ponds, followed Algal High rate ponds (HRP). The third series consists of Algae Settling Ponds followed lastly by Maturation Ponds. It may not be practical to install floating PV on HRP series of ponds for AIWPS, but it should be practical for the other pond series of AIWPS. Three such AIWPS plants have been so identified in California (Delhi, St. Helena and Hollister) [158] . These systems have great promise for waste water treatment plants because they do not require sludge management and use very little energy.

Another interesting project potentially involving Waste Water Treatment Plants is known as OMEGA- Offshore Membrane Enclosures For Growing Algae [25]. OMEGA is a system of photo-bioreactors (PBRs) filled with municipal wastewater, floating in seawater. It is constructed of flexible plastic with internal gas-permeable membranes diffusing CO₂ into cultures and external forward osmosis (FO) membranes concentrating nutrients in wastewater and dewatering the algae for harvesting. The FO membranes also clean the water released into seawater. The OMEGA modules float at the sea surface. The surrounding seawater provides structural support, temperature control and containment. Waves and bubbling provide mixing. OMEGA produces biomass for biofuel, food, and fertilizer, while treating wastewater and sequestering carbon [25].

It is generally agreed that microalgae are the most promising biofuels crop [25]. Photosynthesis for waste reclamation may have intrinsic values to the national economy when one considers that sewage is not truly a waste. Derived from the most nutritive photosynthate harvested from the land, sewage contains the low energy forms of every element critical to life. It has been stated that excreted, organic matter has undergone little more than a reduction in its chemical energy content, and it would be surprising if it were not an ideal medium for algal growth [84].

Several questions arise: 1- can the new algae cultivation methods be scaled up to meet the needs for biofuels 2- can they avoid competing with

agriculture 3- can they avoid competing with water-borne solar on waste water treatment plants.

In response to question 3 above, it should be noted that reference [25] indicates the laboratory testing of OMEGA components *chlorella vulgaris* was grown in lab-scale OMEGA modules. The growth conditions included using primary or secondary wastewater from the Sunnyvale wastewater treatment facility. The Sunnyvale wastewater treatment facility is a good example of a site that has potential for water-borne solar PV.

A key component of the OMEGA process is the mixing and temperature control benefit that occurs in the ocean. It would seem logical that the Omega process would need to be scalable for WWT plants near the ocean to simplify transportation issues. A review of Appendix B shows there are not many WWT facilities located so close to the ocean that would cause competing interest.

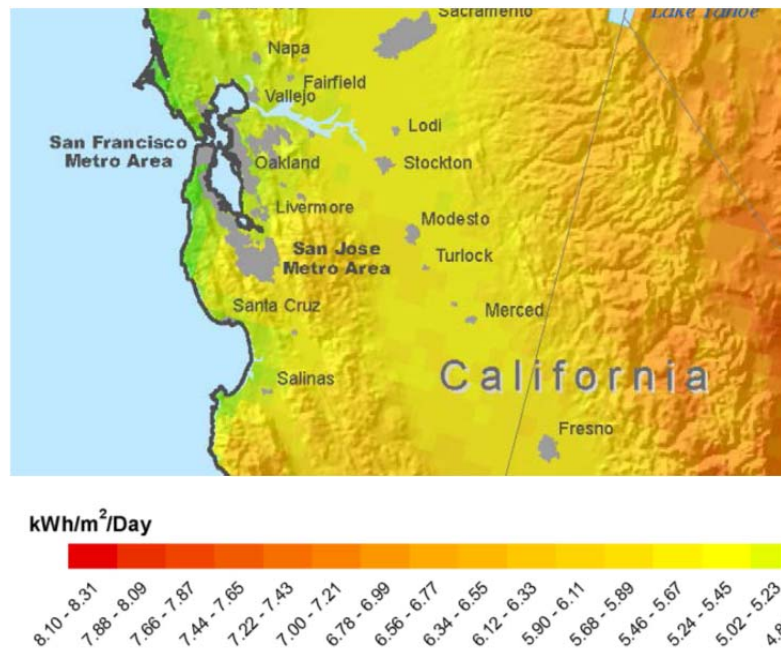


Figure 3.2 DNI for the Lodi



Figure 3.3 Aerial view of the Lodi Energy Center and the Lodi White Slough Facilities. (Photo courtesy of NCPA)

3.4 POTENTIAL FOR CPV WATER-BORNE SYSTEMS

Water-borne systems can provide the following advantages for large industrial or utility sized projects:

- Provide passive cooling for concentrated PV designs
- Simplify the structural components and associated control (tracking) systems (Figure 3.4)
- Provide water source for cleaning lenses or panels
- Provide denser pack layout
- Mitigate the land use issue. Prime land is not required
- Helps mitigate building new transmission and distribution because it is usually readily available at the site

The amount of support structure that is required is another huge advantage. A comparable 20kW ground-mounted PV arrays typically weighs 25,000-50,000 pounds. In contrast, the floating composite plastic prototype has a dry-weight of less than 5,000 pounds [75].

Since the system would be installed on WWT ponds there would be no land costs involved

If each facility in the Energy Baseline Study for Municipal Wastewater Treatment (WWT) Plants in the PG&E service territory had six acres of settling ponds, that could yield almost 3000 acres of space available for water-borne solar installation in Central California. There are over 800 publicly operated wastewater treatment plants in California. If one were to include the water treatment facilities in addition to WWT facilities, there would be more than 1200 located in PG&E's service territory [74].

The EPA estimates that water and wastewater capacity will need to grow by 5 to 8% annually over the next decade.

If the numbers are further extrapolated to gain 1 MW of peak solar capacity for every 3 acres this would represent approximately 1000 MW of peak capacity.

Extending the same reasoning to all 800 sites could yield 4800 MW peak capacity or 10,500 GWhs of energy assuming on average 6 hrs/day of sunlight. This represents 20% of the "net short" renewable energy projected in California for 2020. Of course not all waste water treatment plants are of the design with lagoons or oxidation ponds. Research is still ongoing to contact each of the 800 WWT in California to verify their design, pond acreage, grid access, energy requirements and feeder connection points.

3.5 VALIDATION OF THE WATER-BORNE SYSTEM



Figure 3.4 Pyron Solar's Water-Borne CPV Prototype at SDG&E Test Site
(Photo courtesy of Pyron Solar)

The following list includes some of the steps that need to be validated to assess the real potential of this application:

1. The settling pond/ basin size/acreage of the waste water treatment facilities.
2. Percentage of time the basins have at least two feet of water containment.
3. The proximity of transmission, distribution and substations to each facility.
4. Impact of adding from 15-30 MW to distribution/transmission at sites with more than 45 acres of ponds. This is determined by Power Flow Modeling
5. Field Testing of the system in an actual WWT facility
6. The installed costs plus system upgrade costs that might be incurred.

Eight of NCPA's thirteen member cities own and operate WWT facilities as shown in Table 4.1. The sites with a potential for generating at least 15 MW would be good candidates to tie into the PG&E transmission system. Transmission Studies (steady state and dynamic power flow analysis) and operating agreements with PG&E could then be considered. Lesser amounts (< 15 MW) would most likely be connected "behind the meter" for use at the WWT plant and connected to nearby distribution to serve local load. Power flow studies

would also need to be performed for connection to the distribution system. The power flow modeling studies are essential to investigate any upgrades to the transmission/distribution system. Any system upgrade costs would need to be included in the Cost Benefit Analysis; however for the cost benefit study discussed in chapter 4, system upgrades costs were not included.

Appendix B provides a list of many of the 480 WWT in the PG&E Service Territory as well as approximately 500 other sites located in California.

4.0 COST BENEFIT VALIDATION FOR WATER-BORNE CPV SYSTEM

It is a requirement for projects of public entities to conduct cost benefit analysis. Since most waste-water treatment (WWTs) are owned and operated by public entities, this becomes an essential requirement. The promising NCPA member WWT sites for floating PV application shown in Table 4.1 include: Biggs WWTP, Gridley WWTP, Healdsburg City WWTP, White Slough Water Pollution Control Facility in Lodi, and the San Jose/ Santa Clara Water Pollution Control Plant.

Table 4.1 NCPA Member Waste Water Treatment Plants

Facility Name	Facility Street	Facility City	Phone	Contact	Comments	Pond Acre	Grid connect
Biggs WWTP	3016 Sixth Street 95917	Biggs	(530)868 -5493	Hayden Wasser 530-693- 0568	Good Potential site	3 acres+ 70*	
Gridley WWTP	East Gridley Place 95948	Gridley	(530)846 -3631	Tim Hill 518-2989	Good Potential site	2 acres	0.5 MW
Healdsburg City WWTP	Felta Road 95448		(707)431 - 3346/336 9	Ryan Kirchner	Great Site Advanced plant	3 acres + 40 *acres	13 MW
Palo Alto Regional WQCP	250 Hamilton Ave 94301	Palo Alto	(650)329 -2598	James Allen/Phil Bobel	Maybe	No ponds; 2 acre marsh	0 MW
White Slough Water Pollution Control Facility	12751 North Thornton Road, 95242	Lodi	(209)333 -6749	Karen Owner	Excellent potential site	40+ acres	13 MW
Lompoc Regional WWTP	West 1801 Central Avenue, 93436	Lompoc	(805)736 -5083	Robert Archer 315- 7020	Must dredge each yr./ no fixed pumping system	2-3 Acres	1 MW
Dry Creek WWTP Pleasant Grove WWTP	316 Vernon Street 95678	Roseville	(916)746- 1800	Bob Lawrence 1902/1802	Not a Potential Site	Basins, but not filled;	0 MW
San Jose/Santa Clara Water Pollution Control Plant	700 Los Esteros Road, San Jose, 95134	Santa Clara	(408)635- 6600	Joanna DeSa/ Ron Nichols (electrical) Pam Good Potential site	Good Site		

The City of Biggs WWTF is undergoing some redesign that will include an additional 70 acres of storage ponds. These new ponds will be located within a quarter mile of a 60 KV Sub-transmission line so this site also has great potential. The City of Lompoc's Regional WWTP may have potential; however due to annual dredging that is required some special design and operating requirements would need to be implemented.

NCPA member sites with WWTs that would not qualify include : The City of Palo Alto since its process requires no ponds or lagoon's; likewise the City of Roseville's Dry Creek and Pleasant Grove plants have acres of lagoons, but they seldom contain water; hence they are not suitable. These later sites underscore the need to validate each facility for suitability.

4.1 COST BENEFIT ANALYSIS BACKGROUND AND PERSPECTIVE

Cost benefit analysis (CBA), sometimes called benefit–cost analysis (BCA), provides an economic evaluation of a potential product or technology. The idea of this economic accounting originated with Jules Dupuit, a French engineer in 1848. The formal concepts were formulated by the British economist, Alfred Marshall, but the practical development came as a result of the Federal Navigation Act of 1936. This act required that the U.S. Corps of Engineers carry out projects for the improvement of the waterway system when the total benefits of a project to whomsoever they accrue exceed the costs of that project. [82]. While the methods are still being resolved and refined even today, it is a requirement that public entities employ this type of analysis for project evaluation. The Benefit/cost (B/C) ratio is normally used for proposals to assess the potential of a project or new regulation.

An interesting CBA point to ponder is that for the past ten years federal agencies have issued approximately 4,000 new regulations per year. The Crane & Crane study conducted for the Small Business Administration estimates the total annual compliance cost for all Federal regulations at \$1.7 trillion (about 12% of the Gross Domestic Product). The interpretation is that we give up about 12% of the goods and services that we would otherwise have had available for consumption or investment in order to “buy” the “benefits” of regulation. The Crane study does not estimate the value of benefits of regulations [76, 77]. This underscores a couple of potential problems with applying a CBA; namely the categorization and honest accounting of all costs and benefits.

4.2 COST BENEFIT ANALYSIS REQUIREMENT

The U.S. Chamber of Commerce supports the use of cost-benefit analyses by federal agencies so the public can assess the likely impact of projects and of regulatory proposals, establish priorities, consider alternatives, and target resources to those activities that will most effectively use public

resources to achieve the maximum protection of human health and the environment. Executive Order 12866 requires federal agencies to prepare cost-benefit analyses for all significant regulatory actions. The U.S. Chamber of Commerce's Center for Capital Markets Competitiveness (CCMC) released a report written by Ohio State law professors Paul Rose and Christopher Walker entitled, "The Importance of Cost-Benefit Analysis in Financial Regulation," which finds that while regulators sometimes fail to use cost-benefit analyses appropriately, financial regulation grounded in rigorous, transparent, analytical standards is not only more efficient and effective, but is required by law [78, 79].

Benefit–cost analysis is a systematic process for calculating and comparing benefits and costs of a project, decision or government policy (hereafter, "project"). BCA has two purposes:

1. To determine if it is a sound investment/decision (justification/feasibility)
2. To provide a basis for comparing projects. It involves comparing the total expected cost of each option against the total expected benefits, to see whether the benefits outweigh the costs, and by how much.

In BCA, benefits and costs are expressed in monetary terms, and are adjusted for the time value of money, so that all flows of benefits and flows of project costs over time (which tend to occur at different points in time) are expressed on a common basis in terms of their "net present value."

4.3 COST BENEFIT STEPS

The US Army Cost Benefit Analysis Guide outlines eight steps of a CBA or BCA: 1- Define the problem / opportunity 2- Define the scope; formulate facts and assumptions 3- Define alternatives 4- Develop cost estimate for each alternative 5-Identify quantifiable and non-quantifiable benefits 6- Define alternative selection criteria 7- Compare alternatives 8-Report results and recommendations [80].

Typically a favorable benefit-cost (B/C) ratio would be greater than 1; however it is important to remember the following when performing or reviewing a cost benefit analysis. It can sometimes be a deficiency reviewing a benefit cost ratio to always hold the view that the higher the ratio the better the project and vice versa. While this may be the intent, the ratio can be misrepresented or manipulated by a decision maker on whether to classify an item as a cost or dis-benefit. Another common mistake is the fallacy of merely comparing proposals for change with a continuation of a present condition. Perhaps the most common failure of a cost benefit analysis is not including all the costs and mischaracterizing the benefits. [81]

4.4 COST BENEFIT APPLICATION FOR A PV WATER-BORNE SYSTEM

The results of a cost benefit analysis (CBA) show the Benefit Cost ratio (B/C) by comparing the cost of the water-borne PV systems to a market alternative similar to the renewable portfolio standard (“RPS”) PCC 1 or the bucket 1 category³.

The CBA analysis included a 4% discount rate, 10% financing charge and \$100K annual maintenance budget (increasing at 2.5%/year) for a 25 year operating period. The analysis was performed for two cases: 1- Installations connected to the grid and 2- installations connected “behind the meter”.

The installed costs reflected in the benefit cost ratios shown in Table 4.1 include all costs up to the inverter. Costs from the inverter to the substation, or metering panel are not included, but thought to minimal for “Behind the meter” installations. Any potential storage costs are also not included in the cost study.

“Behind-the-Meter Generation” means an electric generation unit that is interconnected on the load side of a load meter settlement location and which reduces net interchange at the load meter settlement location. Effectively, the generator is interconnected to the distribution system behind the Point of Interconnection where the load is interconnected to the transmission system, and at which point the amount of load consumed is metered.

As can be seen from the results in Table 4.1 below, the cost benefit ratio for the behind the meter installation is approximately 10% greater than for grid connections. This is because “behind the meter” installations do not need to pay transmission access and wheeling charges.

³ **Portfolio Content Category 1** (PCC1) also known as “Bucket 1” – energy from renewable resources connected to California distribution or California Balancing Authority transmission systems, or renewable energy scheduled directly (without substitution) into a California Balancing entity. This is generally the most expensive compliance product (up to \$100/MWh or more).

Table 4.2 Floating CPV Benefit to Cost Ratios

Installed Cost	B/C tied to grid	B/C Behind the meter
\$3.30/Watt	.94	1.05
\$2.70/Watt	1.14	1.27
\$2.00/Watt	1.51	1.68

At a price of \$2.70/Watt, the power from the system equates to an annualized cost of \$80/MWhr.

5.0 POWER SYSTEM INTEGRATION STUDIES FOR LARGER SOLAR PV INSTALLATIONS CONNECTED TO TRANSMISSION LINES

Large solar system installation (> 15 MW) might be examined for connection to a sub-transmission or transmission system. Smaller systems can be connected to a distribution network. This section will discuss the steps involved in integrating a system into the transmission network. Section 6 will focus on integrating systems into distribution networks. While power flow assessment studies are somewhat different for transmission systems and distribution systems, both are required to determine the impact of adding additional resources and load onto the system.

Mitigation measures may need to be applied if there is a significant change in reliability to the grid. The cost of mitigation needs to be reflected in the overall project cost in determining the suitability of a project for a given site location; hence the need for power flow system study is essential in project planning and evaluation.

Power System Studies can be classified as Steady-State, Dynamic and Transient. Steady-State studies can be further divided into the following: Production Cost Modeling, Load (Power) Flow, Voltage Regulation, Power Transfer and Short-Circuit Study. Dynamic studies can be divided into Voltage Stability and Power Angle Stability studies. Transient studies can be divided into Transient Stability and Harmonics. Steady State studies look at time spans ranging from years to minutes; Dynamic Studies look at time spans from minutes to seconds and Transient Studies look at time spans from seconds to milliseconds.

Transmission system studies are performed from a transmission system base case. The National Electricity Reliability Corporation (NERC) requires they be performed for selected demand levels over the range of forecast system demands. Hence to satisfy this requirement two system base cases are studied for each annual assessment.

The purpose of these studies is to [85]:

1. Identify transmission system impacts caused solely by the addition of the proposed Project.
2. Identify system reinforcements necessary to mitigate adverse impacts of the Project, if any, under various system conditions.
3. Identify the level of deliverability of the Project by means of a Deliverability Assessment, conducted by CAISO.

4. Provide cost estimates and work scope for the Interconnection Facilities necessary to interconnect the Project to the CAISO Controlled Grid.
5. Provide cost estimates and work scope for the Network Upgrades necessary to mitigate adverse impacts of the Project, if any, under various system conditions.
6. These studies form the basis of the Interconnection Facilities Study Agreement (IFASA); they define the scope, content, assumptions, and terms of reference.

If for example 15-20 MW of solar PV were to be added at the White Slough Water Pollution Control Facility, and the project's economics favored connection to the transmission over local distribution, the Project could either interconnect to Pacific Gas and Electric Company's (PG&E's) Gold Hill – Lodi Stig and Lodi Stig – Eight Mile Road 230 kV Lines via the existing NCPA Lodi switching station or alternately connect into the Gold Hill – Eight Mile Road 230 kV line.

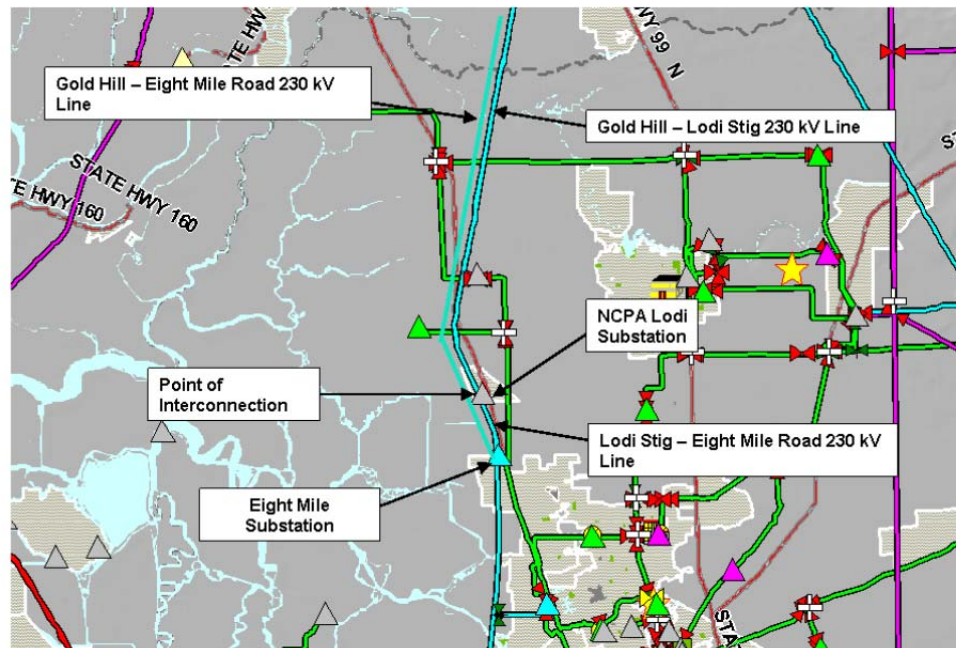


Figure 5.1 Transmission Map near LEC

5.1 POWER FLOW ANALYSIS METHODOLOGY

Power flow analysis is used to evaluate thermal and voltage performance of the system under NERC category A normal (all elements in-service) conditions and various NERC category B emergency (one element out of service), and Category C contingencies [86].

Usually a minimum of two power flow base cases are used to evaluate the feasibility of the proposed interconnection and the transmission system impacts on the CAISO Controlled Grid. While it is impractical to study all combinations of system load and generation levels during all seasons and at all times of the day, these two base cases represent extreme loading and generation conditions.

5.1.1 STEADY STATE POWER FLOW ANALYSIS

Power Flow analysis used to simulate the impact of the Project covers the transmission facilities within PG&E's Sacramento, Sierra, Stockton, and Stanislaus planning areas.

The single (CAISO Category "B") and selected multiple (CAISO Category "C") contingencies include the following outages [85]:

CAISO Category "B"

- All single generator outages within the study area.
- All single (60 - 230 kV for this case) transmission circuit outages within the study area.
- All single (60 - 230 kV for this case) transformer outages within the study area.
- Overlapping single generator and transmission circuit outages for the transmission lines and generators within the study area.

CAISO Category "C"

- Selected bus (60-230 kV for this case) outages within the study area.
- Selected outages caused by selected breaker failures (excluding bus tie and sectionalizing breakers) at the same above bus section.

- Selected combination of any two-generator/transmission line/transformer outages (except ones included above in Category “B”) within the study area.
- Selected outages of double circuit tower lines (60-230 kV for this case) within the study area.

Normal thermal loading is only reported when a transmission component is loaded above 90% of the appropriate MVA rating (as entered in the power flow database). Emergency thermal loading was only reported when a transmission component was loaded over 90% of its appropriate emergency MVA rating (as entered in the power flow database). In addition, both normal and emergency thermal loadings were only reported if the change in flow between the pre-disturbance case and the post-disturbance case exceeded 2 percent [86].

Reported normal voltage violations were limited to the conditions where per unit (p.u) voltages were less than 0.95 or greater than 1.05. Reported emergency voltage violations were limited to the conditions where per unit voltages were less than 0.90 or greater than 1.10. In addition, only voltage deviations greater than 5% between the pre and post-contingency states are reported [86].

5.1.2 SHORT CIRCUIT DUTY ANALYSIS

Short circuit studies are performed to determine the maximum fault currents on various buses in the vicinity of the Project. This will assess the impact of increased fault duty resulting from the added generation. Equipment that may become overstressed as a result of increased fault duty will be identified.

5.1.3 SYSTEM PROTECTION ANALYSIS

Preliminary system protection requirements are normally provided based on the scope and assumptions outlined in the study plan and technical information provided by the Interconnection Customer.

5.1.4 REACTIVE POWER DEFICIENCY ANALYSIS

With a proposed project included in the system model, CAISO Category “B” and “C” contingencies are analyzed to identify any reactive power deficiency:

- Whether the results show voltage drops of 5% or more from the pre-project levels
- Whether the results fail to meet applicable voltage criteria.

A post-transient power flow analysis will be performed, if deemed necessary, after considering the network topology or power transfer paths involved when a significant amount of power transfer occurs.

The power system study at an early stage of validation will most likely be limited to steady-state load flow studies. Dynamic modeling typically cannot be performed without specific vendor knowledge of the inverter system. The determination of the steady state power flow problem, also called load flow, generally aim at the following:

- Determine the state of the power system.
- Determine the system voltages, currents, the active and reactive powers and power factors.
- Determine the basic steady-state operating conditions
 - Generation supplies the load plus losses on the system
 - Maintain bus voltage near nominal or rated value
 - Generation operates within specified real and reactive power constraints
- Determine that Transmission and Distribution lines are not overloaded

It essentially involves finding the steady state voltages at each node, given a set of generation and load conditions.

There are two popular numerical methods for solving the power-flow equations. These are the Gauss-Siedel (G-S) and Newton-Raphson (N-R) Methods.

The N-R method exhibits faster convergence; however its “flat start” characteristic is not always possible since the solution at the beginning can oscillate without converging toward a solution. In order to avoid this problem, the load-flow solution is often started with a G-S algorithm followed by the N-R algorithm after a few iterations.

PV, Steady-State is typically modeled as a constant power source (P) with no reactive power component (Q). Figure 5.2 shows how a PV system is converted to an equivalent model for load flow simulation.

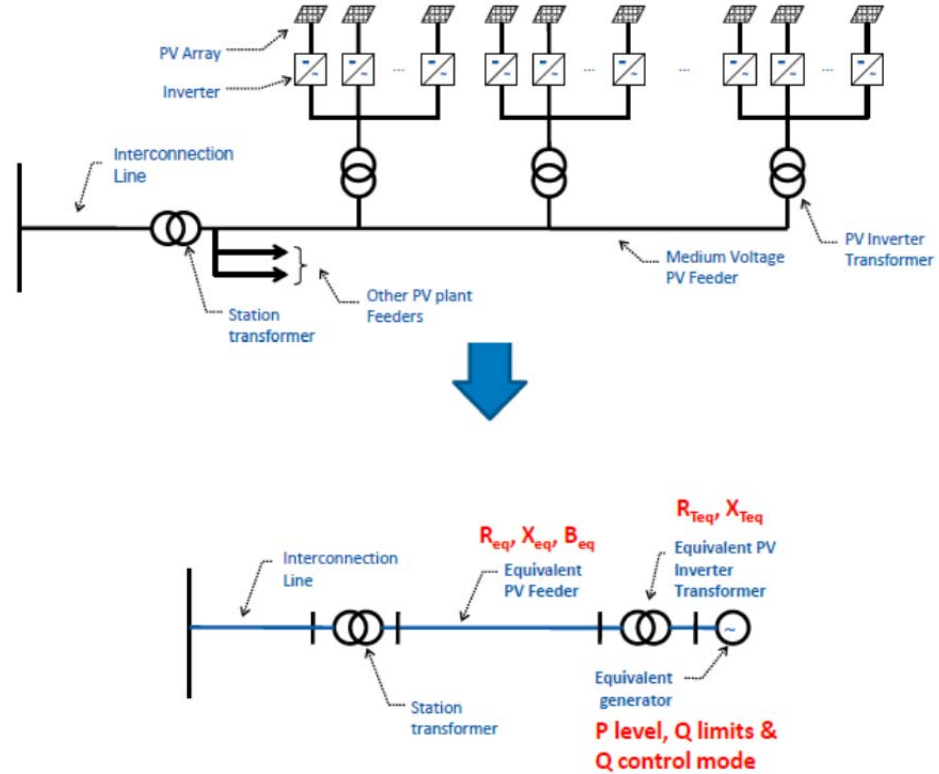


Figure 5.2 Equivalent Circuit for modeling

5.1.5 DYNAMIC STABILITY ANALYSIS

Dynamic stability studies are conducted using the appropriate Base Case to ensure that the transmission system remains in operating equilibrium through abnormal operating conditions after the new facility begins operation. Disturbance simulations will be performed for a study period of up to 20 seconds to determine whether the new facility will create any system instability during the following line and generator outages. Dynamic studies would include the following contingencies for generation added greater than 10MVA at the White Water Slough facility

CAISO Category “B”

- Full load rejection of the Project.
- Three phase fault with normal clearing time at Eight Mile Road 230 kV bus, Section E, followed by the loss of the Lodi Stig – Eight Mile Road 230 kV line.

- Three phase fault with normal clearing time at Gold Hill 230 kV Bus #1, followed by the loss of the Gold Hill – Lodi Stig 230 kV line.

CAISO Category “C”

- Three phase fault at Eight Mile Road Substation 230 kV bus, Section E, with normal clearing time
- Three phase fault at Gold Hill Substation 230 kV bus, with normal clearing time.
- Three phase fault at Eight Mile Road 230 kV bus, Section E, with normal clearing time followed by the loss of Eight Mile Road – Stagg 230 kV and Eight Mile Road – Tesla 230 kV Line.

5.1.5.1 DYNAMIC MODELING

Dynamic modeling typically includes modeling the exciter system, turbine governor and synchronous machine. The dynamic models for PV systems are still under development, but current models are based on IEEE-STD 1547 compliant inverters. Future updates may include Voltage Regulation (VR) and Low Voltage Ride through (LVRT).

Dynamic PV models typically include a constant power source with no reactive power, but include protective set points for voltage and frequency.

Dynamic Modeling for stability analysis is required prior to permitting a project and entering into an Interconnection Agreement. Dynamic modeling usually requires proprietary inverter information from vendors and is usually not available until contracts are finalized.

Transient studies are performed to determine if the system will remain in synchronism following major disturbances such as faults, sudden loss or gain of load, loss of generation, or line switching. Transient stability studies generally focus on 1 to 10 second period after a disturbance.

Transient PV models are dependent on control algorithms used in the inverter.

5.1.6 SUBSTATION EVALUATION

The substation evaluation identifies any existing equipment requiring upgrades to mitigate overstress or overload caused by the Project

5.1.7 TRANSMISSION LINE EVALUATION

Transmission line evaluation identifies any existing transmission lines or equipment requiring upgrades to mitigate overload or overstress caused by the Project.

5.2 CTPG STUDY RESULTS

The CTPG Study that was discussed in the Introduction also used the same Power Flow methodology described above for a statewide study. A few of the significant results of that study are included below.

The CTPG utilized the GE Positive Sequence Load Flow (PSLF) software and base cases established by the Western Electric Coordinating Council (WECC), the National Renewable Energy Laboratory (NREL) and the California Transmission Planning Group (CTPG) to perform various studies in California and the Western United States. These studies were to analyze and determine the most probable sites where significant amounts of wind and solar might be integrated and the effect it would have on the reliability and stability of the transmission grid in the region. Because of the complexity of the study effort, a phased approach was undertaken by the CTPG [15].

In Phase 1, CTPG used the 2020 energy forecast of the CEC's 2009 integrated Energy Policy Report (IEPR), which resulted in an estimated 289,697 GWh of retail load in the state of California subject to the state's renewable goal. Under that assumption, assuming a 33% RPS goal in year 2020, LSEs (Load Serving Entities i.e. Turlock Irrigation District, Modesto Irrigation District, Pacific Gas & Electric, Southern California Edison, Los Angeles Department Water Power, Sacramento Municipal Utility District etc.) would be required to obtain a total of 95,600 GWh of renewable energy in order to meet the target; or approximately 53,605 GWh would be acquired from resources over and above existing and new renewable resources and other miscellaneous additions. This is referred to as the Net Short [15].

This Phase 2 study modified the Net Short to 52,764 GWh. This number also reflects the CEC's projection of the impact of the California Solar Initiative (CSI), and other behind-the-meter distributed generation, on retail loads [16].

The Phase 3 study identified high commercial interest CREZs⁴. Those transmission line segments and transformers that were needed to connect the high ranking CREZs to the network, to facilitate the ability of the network to deliver the energy to the aggregate load, and/or were needed to reduce congestion that currently exists on the interconnected system but is exacerbated by the resources in a CREZ, were considered “high potential” transmission upgrades [17].

In Phase 4 the CTPG developed criteria for identifying “high potential” transmission corridors that may provide options going forward in response to the uncertainty of the eventual locations of the renewable resources that will be procured by the state’s LSEs [18].

It is not the purpose here to summarize all the results, but it is worth mentioning three significant findings:

1. The Phase 3 studies assumed that the output of fossil-fueled generation was decremented based on heat rate (as a proxy for relative operating costs) to achieve load-resource balance as the renewable resources were added to the resource dispatch. The results showed the proposed “high potential” transmission upgrades are insufficient, by themselves, to allow California to meet its 33% RPS goals without reliability criteria violations [17].
2. The Phase 4 analysis used to estimate the capability of the “high potential” transmission upgrades to accommodate renewable energy development indicated that the pattern of fossil generation re-dispatch significantly impacts the point at which increasing levels of renewable energy production will result in contingency-based reliability criteria violations [18].
3. Fossil generation decrementing patterns that are based only on eliminating reliability criteria violations may require the continued operation of coastal generation using Once Through Cooling (OTC) technologies and/or other relatively inefficient generation that could possibly be retired provided other infrastructure such as transmission and/or generation were constructed. Variables such as state policy, cost, and/or environmental concerns must be considered in determining the future disposition of older, fossil-fired

⁴ ‘CREZ’ is the acronym for ‘Competitive Renewable Energy Zones’, which are geographic areas in which renewable energy resources and suitable land areas are sufficient to develop generating capacity from renewable energy technologies.

generators. There is a cost to employing a fossil-fired generation decrementing strategy that deviates from strict merit-order. A different pattern of fossil fueled resource decrements might suggest a different set of high potential transmission upgrades than what the Phase 3 studies indicate [17].

The CTPG studies clearly point out the need for a multi-disciplined approach to solving complex systems and environmental problems. Engineering, regulatory, legal, industry and legislative organizations must work together to effectively implement renewable goals.

While integrating renewables onto transmission systems is important; it is also important to develop renewables at the local level so they can be cost effectively installed behind the meter on local distribution networks and integrated as energy efficiency programs for industrial applications.

5.3 SUMMARY OF POWER FLOW AND APPLICATION WHITE SLOUGH WWT

The above methodology is applied to all power flow studies and transmission line assessments. From previous studies conducted while permitting NCPA's Lodi Energy Center (LEC) adjacent to the City of Lodi's White Slough Water Treatment Facility, it was determined that additional power could not be added to the) Gold Hill – Lodi Stig and Lodi Stig – Eight Mile Road 230 kV line without suitable mitigation to the lines. For instance the LEC can supply 319 MW under proper weather conditions, but is only permitted to operate at 280 MW. Connecting to the Gold Hill – Eight Mile Road 230 kV line may be an option, but a separate power flow study would be required and an additional switchyard would need to be constructed so this option would not be the most economical at this time.

The best solution at this time for the White Slough Water WWT would be to install the system "behind the meter". The White Water Slough WWT would benefit from increased energy efficiency by direct connection the water borne solar plant and the City of Lodi could benefit from the clean power by connected to their distribution system.

6.0 HIGH PV PENETRATION IMPACTS ON UTILITY DISTRIBUTION SYSTEMS

The electric utility industry has been transitioning for over 30 years in terms of increasing diversity and distribution of resources. Solar cost reductions, increasing costs of traditional sources, and Renewable Portfolio Standards have created the possibility of significant levels of distributed solar generation being installed on distribution systems [90,93,99]. The positive results are environmentally cleaner resources, better utilization of the grid and more efficient use of electricity by customers. However, the grid has become increasingly complex and stressed by the variability that has been introduced due to the addition of intermittent wind and solar photovoltaic (solar PV) resources. This trend is expected to increase with more distributed energy resources (DER) coming on line in the future leading to high-penetration scenarios. To aid in the evaluation and help with this expansion of solar resources, there needs to be significant changes in the way that the electric power infrastructure is designed and operated [127].

In a distribution network that contains a high level of penetration of PV units, but has an insufficient number of storage devices, a sudden disturbance such as the change in sunlight due to a passing cloud/storm could trigger a rapid disconnection of these PV generators or the reduction of their operating capacity, resulting in a significant loss of active power support [89].

There are two main types of electrical distribution systems: radial and network. Most areas of the United States use simpler radial distribution systems to distribute electricity, but larger metropolitan areas like New York City typically use more complicated networks to increase reliability in large load centers. Unlike the radial distribution system, where each customer receives power through a single feeder and single transformer, a network delivers power to each customer through several parallel feeders and transformers [95] and requires different analysis.

6.1 MANAGING ENERGY FLOWS TO IMPROVE SYSTEM VALUE

This section lists some ideas to enable high penetration of PV into the current distribution infrastructure while improving PV system value and utility system reliability. If grid-connected PV power systems were negligibly cheap, the system operator would prefer to curtail power production (and waste available irradiant power) when demand drops [96]. However, all generating plants have some capital cost and their owners would prefer to operate them at full capacity to maximize revenue. The system operator must throttle back generation or increase the rate of storage (where available e.g. water pumping) when demand

drops, or the frequency will climb too high. This condition is currently managed by the system operator, who uses a combination of carrot (pricing) and stick (regulation) actions. As these types of actions that curtail power production are applied to grid-connected PV power systems; therefore designers have to choose between discarding available power and adding storage [96].

The following thoughts are under consideration that may give system operators some additional tools:

1. Improve communication capabilities to interactively control connection of the inverter/controller to the grid. One approach is to replace the current anti-islanding approach with interactive dispatch so the utility can command an inverter to ride through voltage sag, rather than having a large number of inverters go off-line while leaving the loads on-line [88]. An interesting and associated challenge is how to provide security to the cyber assets (i.e. networks, computers and controllers) that provide this control to prevent malicious hacking attempts to gain access and control of the bulk electric system. These attacks are on the rise.
2. Manage power flows to keep high power flows off the distribution system when they could interfere with system regulation and protection; therefore direct loads to operate when solar energy is available and not to operate during peak demand periods when solar is not available. Design and direct inverters to produce reactive power.

These ideas could be summarized to optimize value by dispatching loads to operate in concert with the availability of solar energy and/or cheap utility power. This is inclusive of energy efficiency strategies and storage. For buildings with demand charges, addition of storage has been shown to add value to the PV system [88]. Storage can enable the building to continue to operate critical loads during a utility outage.

3. Consider the rate structure when establishing the orientation (azimuth and tilt) of the PV modules. For example, for regions where utility demand peaks in the summer and time-of-use rate apply, having a portion of the array facing west may provide more value to the customer, even though total energy delivered may be lower.
4. Develop PV inverters to supply VARs at the source for businesses and industrial sites.

6.2 SOLAR PHOTOVOLTAIC DISTRIBUTED ENERGY RESOURCES (DER) INTEGRATION ASSESSMENT

6.2.1 INTERCONNECTION STANDARDS AND GUIDES

Impact studies for solar photovoltaic integration assessment are different than conventional induction or synchronous generators as a result of the different operational mode capabilities, with each one affecting the distribution system significantly different.

There are several standards available to provide information and assistance regarding DER interconnections with the distribution system. Most noteworthy is the IEEE 1547 series of interconnection standards. These include rules and interconnection policies for voltage limits, voltage regulation, flicker levels, harmonics, frequency, disconnection rules fault and protection considerations [87]. The Southern California Edison (SCE) Interconnection Handbook [130] and California Rule 21 [131] also provide general design, interconnection and operating requirements for connecting and operating DER generation facilities.

6.2.2 DISTRIBUTION SYSTEM MODELING

Distribution systems are complex to analyze because many are radial, with unbalanced impedances, unbalanced distributed loads, large number of nodes and branches, wide-ranging resistance, and high R/X ratio. Many programs of real-time applications in the area of distribution automation, such as network optimization planning, switching, state estimation, and so forth, require a robust power flow method. Most distribution analysis software packages use unbalanced phase impedance matrices and load flow solutions [87].

These features cause the traditional power flow methods used in transmission systems, such as the Gauss Siedel and Newton-Raphson techniques, to fail to meet the requirements in both performance and robustness aspects in the distribution system applications [111].

Some of the power flow algorithms specifically designed for distribution systems are: 1- Classical Newton-Raphson 2- Ratio-Flow 3-Forward Backward Substitution and 4- Ladder Network Theory.

Shirmohammadi et, al, [98, 12] have presented a compensation-based power flow method for radial distribution network and/or weakly meshed structure using a multi-port compensation technique and basic formulations of Kirchhoff's Laws. The radial part is solved by a straightforward two step procedure in which the branch currents are first computed (backward sweep) and then the bus

voltages are updated (forward sweep). In the improved version by Luo [98, 13], branch power flow was used instead of branch complex currents for weakly meshed transmission and distribution systems. In [98, 16], G. Renato Cespedes makes use of the bi-quadratic equation which, for every branch, relates the voltage magnitude at the receiving end to the voltage at the sending end and branch power flows. In [98,21] the authors proposed a Ratio- flow method which is based on forward-backward ladder equation for complex distribution systems by using voltage ratio for convergence control. Ladder network Theory is similar to the Forward-Backward Substitution method. In Ladder Network Theory, the currents in each branch are computed by KCL. In addition to the branch currents, the node voltages are also computed by KVL in each iteration. Thus magnitude of the swing bus voltage is also determined. The calculated value of the swing bus is compared with its specified value. If the error is within the limit, the procedure is stopped.

The convergence ability of distribution system load flow methods which are widely used for distribution system analysis is compared. The methods analyzed are: 1- Classical Newton-Raphson 2- Ratio-Flow 3-Forward Backward Substitution and 4- Ladder Network Theory [98]. The results were evaluated under different tolerance values, different voltage levels, different loading conditions and different R/X ratio, under a wide range of the exponents of the loads in a 30 buss radial distribution system. The results show that the Ratio-Flow method is simple and has fast convergence ability. It required less iterations and is less sensitive to distribution system parameters than Forward-Backwards substitution method and Ladder Network Theory, The Classical newton-Raphson method did not converge for the 30 bus system.

In [111] a direct approach for distribution power flow was proposed. The idea is that the LU decomposition and forward/backward substitution for the Y admittance matrix required in the traditional Newton Raphson and Gauss implicit Z matrix algorithms are not necessary. Two developed matrices, the bus-injection to branch current matrix (BIBC) and the branch-current to bus voltage matrix (BCBV), and a simple matrix multiplication are utilized to obtain power flow solutions. One of the major reasons, which make the power flow program diverge, is the ill-conditioned problem of the admittance (Y) matrix. It usually occurs when the system contains some very short lines or very long lines. Test results showed that the new direct approach had almost the same accuracy as the commonly used forward/backward method, and that for a 270-node systems was 24 times faster.

This above research on distribution engineering tools, however still does not really address the support for PV modeling. Until just recently, tools to model the behavior of multiple systems or PV fleets, has been lacking [127]. PV in the distribution system can be considered a “negative load” like other distributed generation sources, but its output is more complicated because it varies every hour. Its output is dependent upon several factors, such as hourly solar

irradiance, hourly ambient temperature, hourly sun angle, array azimuth and tilt, and PV module and inverter characteristics. In high penetration PV scenarios, the hours of maximum line loading do not necessarily correspond with maximum consumption. While conventional load flow studies are primarily concerned with the hour of greatest load (demand), this rule does not necessarily follow on circuits with high penetration of PV. For example, during lightly loaded hours with high solar production (such as weekends), there may be significant back-feed on some sections of the line. The highest loading may actually occur in these “off-peak” hours.

Incorporating PV and DER can also introduce bidirectional kW and kVAR power flows. The software needs to calculate voltage rise due to reverse kW flow and voltage drop due to forward kVAR flow on different phases. The voltage imbalance is also important since the interconnection standards list requirements pertaining to maximum or minimum voltage or flicker levels, and therefore violations may occur on only one phase rather than all three.

Traditional distribution planning makes use of a single point in time load flow analyses, which is adequate for peak power planning. Time series simulations using a batch process are required where both customer loads and PV outputs at various times of the day or in certain steps can be run in sequence to analyze the time-varying nature between them. Active and reactive power flow directions and levels can change every minute due to the intermittency of renewable generation such as PV DER [87].

PV cells rely on a clear sky with no haze, rain, or humidity to generate their rated power. Items such as inverter efficiency, AC and DC wiring losses, snow or ice buildup and transformer losses need to be applied to obtain a derating factor.

6.2.3 MODELING ALGORITHMS AND NETWORKS

A modern grid involves a shift in the operating paradigm on four dimensions: increased variability, shorter time cycles, resource diversity and resource dispersion. Large and small scale intermittent generation, like solar PV as well as wind and responsive demand from EVs and smart appliances, necessitate a change from traditional deterministic to stochastic methods for planning and controls [140].

Modeling needs to support high-penetration include (1) Utility distribution modeling and (2) Solar side modeling. The following general utility concerns are

broken into the need to quantify the impacts of distributed resources on protection, operation and planning and engineering studies.

From a protection standpoint software capabilities need to address: loadability- ability to serve load without tripping; selectivity- the system protective devices nearest the fault isolate the fault before more remote devices operate to isolate the fault; and sensitivity- the ability to sense faults. Some of the concerns include: improper coordination, nuisance few blowing, DR stability during faults, islanding, reclosing out of synchronism, transfer trip and equipment overvoltage [127].

From an operational standpoint software capabilities need to address the following concerns: voltage regulation malfunctions, substation load monitoring errors, switching impacts resulting from large levels of solar generation, protection and coordination with inverters, including sectionalizer miscounts, forecasting/planning for peak and light load, economic impacts on operations energy and capacity, financial impact on capital and O&M, cold load pickup with and without DERS, flicker, harmonics, stability during faults, and long feeder steady state stability [127].

From a planning and engineering standpoint software capabilities need to address the following concerns: distribution planning models that reflect actual system operation with high levels of DER generation, economic analysis of losses, generation planning and operation for both capacity and energy, including production profile throughout the year and type of production, the amount of generation (penetration level) that can be installed on a distribution feeder [127].

Modeling systems will need detailed PV inverter models in order to study impacts of high-penetration solar generation. These models need to be developed for power flow, short circuit and dynamic studies. Modeling should include programmable drag and drop solar inverter models that can accommodate solar input measurements to facilitate the study of high penetration of PV as part of the normal utility planning and operation process. Inverter models will also need to accept time sequence measurement data for load estimation and power flow. Load modeling studies will need to be made across time-varying load curves, such as 8,760 hourly time points. Modeling systems needs to be capable of stepping through an operational time sequence that is granular enough to capture the operational movement of all active elements within the circuit, such as time delays for voltage regulation, protective device operation, etc. [127]

Another categorization is to consider installations as PV clusters within minigrids. The PV cluster structure is commonly encountered in the sub-urban areas where many houses with rooftop PV installations are integrated into a local distribution network. In this configuration, the grid acts as an energy buffer to

firm up the variable output power of the PV. Typically about 100 to 300 PV houses would be connected to one lateral of a MV feeder that supplies thousands of houses. Current PV mini-grids are usually isolated power distribution networks that utilize PV in conjunction with other generation sources, mainly diesel generators, for rural and remote community electrification. These are isolated areas or geographical islands with no connection to the utility grid. Neither the PV cluster nor the remote community mini-grid completely represents the mini-grid of the future, which will operate in both autonomous and utility interconnected modes to supply multiple users [91]. Mini-grids of the future will need to be modeled in distribution networks.

6.3 CONTROL OF PHOTOVOLTAIC GENERATORS IN A DISTRIBUTION NETWORK

6.3.1 CONTROL OF UTILITY INTERACTIVE INVERTERS

It is important to understand several concepts in conjunction with inverter control: MPPT, Grid synchronization, anti-islanding, current regulation and PWM in order to understand potential future concepts of controlling the grid with high penetration of solar PV.

6.3.1.1 MAXIMUM POWER POINT TRACKING

The amount of solar energy available is subject to change with irradiance, temperature, and aging of PV panels or modules. Shading frequently occurs that also affects the performance of the array. The inverter, (that which converts the DC electric energy from the solar panels or modules into AC) needs to automatically adjust the power output to draw maximum available power at any time. The algorithm to draw maximum power available from the solar PV is called a maximum power point tracking (MPPT). The desired MPPT algorithm quickly adjusts the inverter to a maximum power condition during transients and without oscillating at steady state conditions [114].

6.3.1.2 GRID SYNCHRONIZATION

A phase tracking system is an important part of the control system. It affects synchronization to the grid, power factor control and harmonic content of the inverter output current. Many algorithms have been proposed. Ideally the phase tracking system algorithm should respond quickly to changes in the utility phasing, but should reject noise and higher harmonics in the utility voltage. The easiest implementation is based on zero crossing detection of the inverter output current being synchronized to the utility during zero crossings of the utility voltage. Phase-locked loop (PLL) techniques are used to estimate the phase of

a utility. PLL performs quite well in tracking the utility phase in the presence of higher order harmonics; however its performance may deteriorate in the presence of voltage unbalance. A couple of transformations of the time-varying, yet stationary, three phase utility voltage system (abc) to a rotating (synchronous) d, q reference frame have been implemented to develop various control algorithms. The advantage of the transformation is that the synchronous frame controller can eliminate steady state error and has fast transient response by de-coupling control. The disadvantage is that the stationary frame controller transforms the measured stationary frame ac current to rotating frame dc components, and transforming the result of control back to the stationary frame for implementation [114].

6.3.1.3 ANTI-ISLANDING

All utility interactive inverters are required to have over/under frequency (OFP/UFP) and over/under voltage (OVP/UVP) protection methods that prevent the inverter from supplying power to the utility if the utility voltage or frequency are outside of an acceptable range. Figure 6.1 shows a typical connection of an inverter to the utility grid. The inverter outputs power $P + jQ$ while local loads take $P_{ld} + jQ_{ld}$ the rest of the power supplied by the utility is $\Delta P + j\Delta Q$. The operation of the system after the utility disconnects depends on the amount of ΔP and ΔQ . If $\Delta P \neq 0$ the amplitude of the utility voltage will change and OVP/UVP can detect the change and prevent islanding. If $\Delta Q \neq 0$ the phase of the utility will suddenly shift and OFP/UFP will detect the change in frequency and detect the islanding condition.

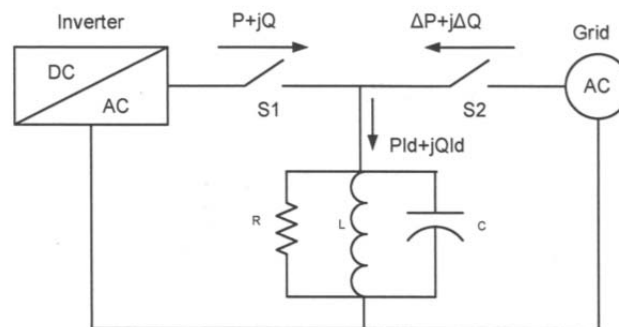


Figure 6.1 Model of Inverter connections to grid

If the real and reactive power of the inverter is not matched closely to the loads or the resonant frequency of the load network is not close to the resonant frequency of the inverter OVP/UVP, then the OFP and UFP would be adequate to detect the islanding condition. However, when the load requirements are

being satisfied by the inverter only, detection of an islanding condition becomes more challenging.

The non-detection zone (NDZ) concept [120] is developed to determine the effectiveness of the anti-islanding algorithm for a given ΔP and ΔQ .

There are many active and passive methods that have been developed to detect an islanding condition. The Sandia frequency and voltage shift algorithms are effective in detecting islanding if implemented at the same time [121]

The Sandia algorithm adds a small amount of positive feedback to both voltage and frequency regulation by the inverter, so the inverter is continuously trying to destabilize the utility. It can work well if the utility is stiff; however, it can be problematic with a deep penetration of renewable resources [114].

6.3.2 CURRENT REGULATION

The amount of desired output power delivered to the utility is controlled through the current regulation algorithm. The accuracy of the current regulation algorithm is important for effective maximum power processing [114]. While many control algorithms have been proposed to control inverter output current for utility interactive operations, three major classes of regulators have been developed over the last few decades: hysteresis regulators, linear PI regulators, and predictive dead-beat regulators [115]. Many control algorithms have been proposed to control inverter output current for utility interactive operations. An algorithm that works harmoniously with grid synchronization methods and is also applicable to multilevel inverters is shown Appendix C along with its mathematical development. The algorithm can be used for both three-phase and single-phase systems once the dynamics are transferred into the rotating d, q reference frame [114]. The PI controller has the transfer function:

$$D(s) = \frac{K_P s + K_I}{s} = K_I \frac{s^{\frac{K_P}{K_I} + 1}}{s} \quad (6.1)$$

Digital implementation of the PI Controller can be realized with a z transformation [126].

$$D(z) = K_P \frac{z - (1 - T \frac{K_I}{K_P})}{z - 1} \quad (6.2)$$

6.3.3 PWM

The Pulse Width Modulation (PWM) generation algorithm produces duty ratios for individual inverter switches. PWM generation is modeled such that it can produce the switching positions for inverters of 2, 3, 4 and 5 levels. The current controller produces a reference voltage (V_{ref}) between -1 and 1 that is scaled based on the number of levels in the topology; m denotes the number of levels. A multilevel comparator produces the switch position output between 0 to $m-1$ [114].

While PWM techniques provide independent control for each individual inverter phase leg, for three phase inverters it is possible to control all three inverter phase legs together to better use the available DC bus voltage.

Multilevel inverters generate their output voltage from three or more discrete voltage levels. For an m -level inverter the switching function for each phase takes on values between 0 to $m-1$. The phase leg voltage is:

$$V_{AnO} = \frac{S_{pos} * V_{dc}}{m - 1}$$

Each switching state produces uniquely defined three phase line voltages. If the switching positions for the three phases are i, j, k , respectively, then the inverter output voltages can be represented by the switching vector as:

$$\bar{V}(ijk) = V_{dc} \begin{bmatrix} i - j \\ j - k \\ k - i \end{bmatrix}$$

Switching vectors can be produced by the different switching positions of the inverter. For balanced output voltages, the sum of the line-to-line voltages must be zero; therefore the switching vectors can be represented in two dimensions. The reference voltage V_{ref} can be realized as an inverter output voltage by application of the three closest vectors consecutively during one cycle. The main objective of the modulator is to select the switching positions of the inverter and the duration of how long each switch position needs to be applied by the inverter in order to produce the reference voltage. Appendix D shows the switching position vectors in coordinates for a three level inverter and provides extra background on the space-vector modulation algorithm for multilevel three-phase converters [114].

6.3.4 DESIRED PV INVERTER FEATURES

The following advanced inverter features for PV control include voltage regulation, VAR control, power curtailment, ramp rate control as suggested in the Southern California Photovoltaic Project [127].

Voltage regulation should regulate the voltage at the point of common coupling during PV output fluctuations. The PV inverter can potentially act as an active filter to mitigate power quality issues caused by non-linear loads, such as flicker, voltage sag/swell, and voltage variations especially for installations as the end of the feeder. Several changes are anticipated to implement this change:

- Hardware may include changes to increase capacitor size and rating on the power electronic switches.
- Complexity of interconnection studies will increase due to higher degree of interaction with other voltage regulating devices, supervisory control and coordination requirements
- PV inverter control algorithms may change to droop control or output impedance synthesis.
- Communication among devices to enable status update of other voltage regulating devices and regulating voltage at a selected point of the feeder.

VAR control could be designed to control reactive power output of a PV inverter to sink or source reactive power as a function of PV active power output variations, changes in the system. Dynamic VAR control is to smooth out voltage fluctuations caused by power intermittency of PV inverters. Dynamic VAR control can also be utilized to compensate for voltage drop on part of a feeder to achieve a flat voltage profile or reduce feeder losses. Emergency VAR control is also being contemplated. In this control mode, upon distribution operator request, each PV inverter supplies the maximum available reactive power output without reducing the active power output or violating the voltage limits. Expected positive impacts include: eliminating the effect of PV inverters on feeder voltage increase, reducing the number of tap-changer operations for LTCs, voltage regulators, and capacitor banks. The potential adverse impacts include: complexity in system design and interconnection studies, potential for dynamic interactions among multiple PV inverters with different control modes and responses from varying manufacturers, complexity in calculating availability and reliability of reactive power capacity for emergency use.

Power Curtailment is a feature to provide some degree of dispatchability in PV inverters in terms of active power output reduction. The primary application is aimed at enabling utility operators to control the aggregated effect of total generation on distribution feeders during contingency conditions. A distribution operator could throttle back fast-acting generation to an aggregated reduced level rather than shutting down PV inverters or transmission connected systems. Expected benefits include: additional degree of flexibility for utility operators, reducing the voltage rise effect, managing unexpectedly large reverse power flow due

to sudden loss of load, and loss reduction. The potential adverse impacts include: potential voltage drop and under-voltage issues on part of a feeder, and loss of a large amount of renewable energy generation if there is no provision for energy storage resulting in uncaptured revenue for the PV system owner.

Ramp rate control can be used during fast power fluctuations caused by cloud effects for start-up and shut-down of large PV inverters to balance the level of generation and load in the entire system. The maximum ramp rate of a system is typically determined by available spinning reserve and has to be oversized if there is no provision for power and load balancing by addition of PV systems. Expected benefits include:

- Reducing the overall spinning reserve capacity requirements
- Minimizing downtime of renewable energy sources
- Contribution to frequency regulation of a system
- Low voltage and fault ride-through
- Islanding and microgrid operation capability

The principal objective of low voltage and fault ride-through is to prevent frequent disconnection of PV inverters during system transients that may cause significant voltage and frequency variations. Characteristics of low voltage and fault ride-through for distribution application are not well defined yet.

Incorporating intentional islanding and microgrid operation in a PV inverter requires a means of frequency regulation and load following capability. Although the control feature already exist in stand-alone PV inverters with battery storage, it is not typically implemented on large scale PV inverters due to the cost of energy storage and the additional components to perform simultaneous voltage/frequency regulation. The inverter and microgrid protection methodology and fast/accurate islanding detection schemes are some barriers that are not well established.

6.4 OFF-GRID (STAND-ALONE) PV POWER SYSTEM CONTROL

In the absence of the utility grid (standalone operation), it must be assured the inverter has an adequate supply of energy to draw upon. Unless there is battery backup in the system, the system cannot work on the principle of maximum power extraction from the source since this would lead to a sustained power imbalance. In standalone operation, power transfer is dictated primarily by the needs of the local loads and the losses within the inverter. If there is enough energy available at the source the local loads are fully supported by the inverter. If the demand from the loads is higher than the available energy at the source

then lower priority loads are needed to be shed to make energy available for supporting the higher priority loads [96,114].

There are parallels between the surge and demand variability characteristics of off-grid PV power systems and demand variation concerns faced by an electric power grid's system operator; however a couple of significant differences are important to mention. One difference is that the off-grid PV power system has a relatively small number of loads, many of which are significant by comparison with the generating capacity, so variations in load tend to be relatively large and abrupt. The grid has millions of loads many of which are tiny by comparison with the generation capacity, so variation tends to be smooth. The other difference is that the grid can store energy by reducing consumption of generating plant fuel. Solar power cannot be conserved this way for later use for off-grid systems hence the need for a storage subsystem to keep some power for low-light conditions. When the storage is full the PV power conversion is throttled back and available energy is discarded.

6.5 FUTURE POWER SYSTEM CONTROL

Over the past decade considerable research and architectural development has resulted in a set of architectural principals and reference architectures to address the needs of a modern grid. The convergence of information technology (ICT) and energy technology (ET) to the power grid is the basis for a smart grid and the Ultra Large-Scale (ULS) power System Control Architecture [113].

Much of this architectural foundation was conceived in the early 2000s before social networks and smart phones were launched. Also, with much of the early focus on customer information interactions and relatively modest adoption of distributed energy resources until relatively recently, many of the physical variable distributed energy resources (DER), such as wind, integration issues were focused at the transmission level and most of the customer responsive demand was not tightly linked into real-time control of the grid. Now it has become imperative to address the practical architectural and engineering issues related to modernizing a grid to support the scale and scope of the resources envisioned in existing legislative and regulatory mandates in many parts of the developed world. In essence, the modern grid design brief has changed. It has become clear that we must address the integration of the following four principles [116]:

1. Information and communication networks
2. Markets, especially participation of prosumers (prosumer refers to an electric customer that consumes energy from the grid as well as produces

power from onsite generation i.e. solar PV, fuel cell, etc. that feeds back into the grid) and merchant-provided DER services

3. Social networks as grids become interactive with customers and their smart devices.
4. Power grid (ET) with its inviolable set of physical rules

U.S. policy allows owners of distributed resources to effectively and reliably provide their services at scale, and operate harmoniously on an interconnected distribution and transmission grid [116]. At scale, DER markets and pricing mechanisms can have a material effect on grid stability and reliability as visible or hidden elements that are tightly coupled within a closed loop of a distribution control system managing reliability and power quality. Market design is an essential element in grid control architectures for a future with significant distributed resources. NERC Reliability Standard Development most likely will also need to contemplate market interaction in the future.

As such, the convergence of the electric grid with ICT, markets and social networks requires this modern grid [117] to have the following attributes:

- Observable – able to determine extended grid state from a set of measurements
- Controllable – able to reach any desired status in response to demands of consumers and other allowable control inputs
- Automated – intelligent autonomous control functions with human supervision
- Transactive – customer and merchant DER devices and systems (non-utility assets) participate in markets and grid operations
- Secure – integrated multi-faceted security supporting the first four attributes

Three of these five terms (observable, controllable and automated) are technical terms from control engineering.

Earlier efforts to create new grid control architectures based largely on enterprise IT principles rather than control systems paradigms do not provide the necessary framework to meet the four principles described above [113].

The following three issues highlight changes on current control and operational systems [113]:

1. The consequence of the retirement of older fossil fueled generating resources and increase of DER resources as part of the portfolio may result in a net decrease of rotational inertia and therefore grid stability. This reinforces the need for algorithms for fast dynamical control to ensure grid stabilization at both transmission and distribution levels. While stated somewhat differently, this was also one of the findings highlighted in the CTPG studies mentioned earlier in section 5.2 of this Dissertation.

2. The concept of transactive control where customer premises may interact with energy and power markets on a programmed basis puts those markets into the control loops. This raises two issues: one is that price responsive loads may cause price and grid instability and the second is that they may cause “flash crashes” in the energy and power markets, in a fashion similar to what can happen in the stock markets with programmed trading.

3. If we consider the grid control problem then we are concerned with the following functions:
 - Unit commitment, dispatch, and balance
 - Power flow control
 - Regulation of voltage, reactive power, and system frequency
 - Stabilization and synchronization
 - Variable and distributed energy resources integration, distributed generation and storage
 - Market integration as a control loop function, including price responsive loads
 - Responsive load management, including demand response and EEV charging
 - Market participant behavior

It is becoming necessary to provide a means for coordinating controls at various levels of the power delivery chain spanning dispatch/balancing, bulk and distributed generation, transmission, distribution and responsive load (customer premises or assets) levels. This does not mean that there should be one giant central control system; this is not feasible for many reasons. It does mean that macro control architecture should begin to embody certain architectural principles across these tiers, and to avoid ad hoc control architectures [113].

Traditionally, distribution was allowed to “float” based on tightly managing the transmission system since power flowed in one direction. In a future with perhaps 30% of power being provided by solar PV at customer sites these models break down quickly. It is becoming clearer that new distributed market

mechanisms are needed. The California Independent System Operator (CAISO) in a recent paper on DER pricing acknowledged that distribution level factors need to be considered. However, the CAISO paper doesn't recognize the control loop issues and actually suggests a pricing model that is inconsistent with control architecture principles described above [113]. New pricing mechanisms are needed to create effective closed loop systems that are tightly coupled with distribution control systems to ensure reliability and power quality [140].

Current market and pricing policy for most DER generally applies wholesale models to distributed resources that do not reflect distribution level information related to location, reliability or power quality considerations. While this simplifies aspects of wholesale market operations, at scale this approach may create power quality issues at distribution and in the worst case reliability issues. This is because some market designs cause the market function to act as a control element in a feedback control loop, whether intended or not. This loop is closed around a substantial portion of the power delivery system, including multiple operational tiers as illustrated in Figure 6.2 [113]. Note that feedback of state variables (not system outputs) causes the equilibrium price to move so as to re-establish the balance between supply and demand, and moves in the equilibrium price cause changes in available generation.

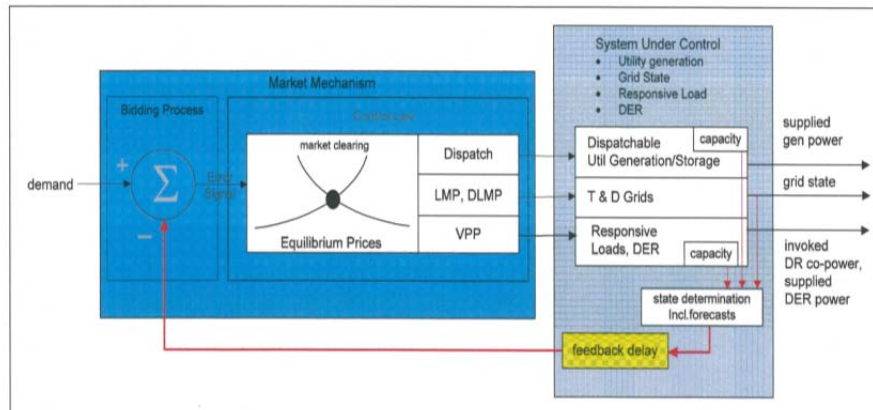


Figure 6.2 Market mechanisms in feedback control loop

6.5.1 CONTROL FRAMEWORK

Modern economies are not tolerant of grid disruptions and failure to achieve existing policy mandates related to renewable and distributed resources is not acceptable. Taft and Martini [113] propose three steps to resolve this. One of the steps proposed is to apply modern optimization methods to solve problems that allows for competing objectives, multiple constraints, and provides for both control federation and disaggregation so that each utility and energy service

organization has the ability to solve its local grid management problems, but within an overall framework that ensure grid stability. One such optimization strategy, a self-organizing strategy is proposed by Zhihua Qu et al [112].

6.6 TRANSITION IN CONTROL STRATEGY FOR INCREASED PENETRATION

The Optimal Power flow (OPF) strategy is the standard approach to dispatch and control of traditional generators in the transmission network [112]. The strategy has also been applied to distribution networks that have a few distributed generators. These results yield centralized controls (Figure 6.3b) by collecting the system-wide information and sending the command globally. For a power system whose transmission and distribution networks have numerous and geographically dispersed DGs, such centralized controls are too expensive to be implemented

A decentralized control mode (Figure 6.3a) such as the maximum photovoltaic power tracking (MPPT), constant VF (Voltage and Frequency) with droop mode, or the feeder power flow control mode, is useful in the distribution network if there are only a few DGs present [112]. However as PV penetration increases, intermittent changes of the PV outputs would also make a decentralized approach impractical to manage a distribution network.

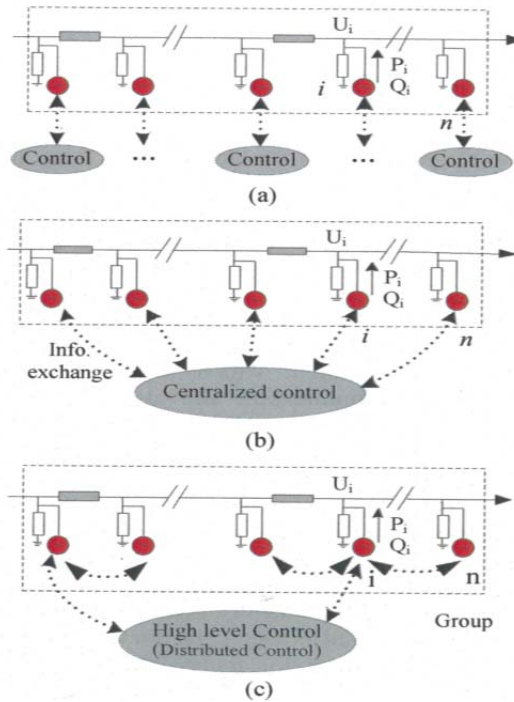


Figure 6.3 Control Architectures

A more practical, potentially feasible solution to adequately manage the voltage profile is a distributed control configuration [118] (Figure 6.2c) that uses local communication networks and hence combines the positive features of both centralized and decentralized controls. The distinctive feature is robust with respect to intermittency and latency of its feedbacks, and also tolerates connection and disconnection of network components [118]. In general, the desired control algorithm should be able to manage a large number of DGs but require only local information from neighboring units. By doing so, groups of DGs can be formed autonomously based on the presence of local communication networks, and the power in a distributed network can be more easily dispatched and controlled with the goal that large swings in power outputs can be tolerated. For instance, a solution to the power-output coordination problem is to prescribe a certain utilization profile for all PVs in a group. By applying cooperative control theory of networked systems to power distribution networks, the control can make the PVs in one group converge to any given utilization profile while providing the desired power being dispatched from the group [112].

The basic idea of the proposed distributed control is that by incorporating local communication networks that share information among neighboring units, numerous PV generators autonomously form a number of generation groups and that each group is represented by a virtual generation unit which aggregates all the power generated within. The outputs of these virtual generators can be dispatched and controlled by a high level control (which is equivalent to a

transmission and distribution control center). While the latter is similar to the centralized configuration, the proposed control configuration requires much less communication since the numerous distributed generators do not communicate with the higher-level control. Once the power output of each group is dispatched, the proposed cooperative control coordinates all the outputs of PV generators in the same group so that, even though the output capacity of individual PVs may have large swings, a given profile is achieved for their utilization and the sum of their outputs converges to the dispatched value. This makes it possible for all the active PVs to self-organize themselves and be controlled. The local information sharing within one group of PVs may be intermittent, asynchronous, and of varying topology. The proposed control is then robust with respect to possible variations and limitations of communication networks. The utilization profile for PVs in the group can be determined according to such considerations as economic and regulatory policies [112].

6.6.1 CASE STUDY OPTIMIZATION BASED ON COOPERATIVE CONTROL

In the case study outlined in [112] three problems were defined:

1. Problem 1 Design a cooperative control system based on a fair utilization profile such that all the PVs in the group are to be run at the same active and reactive power output ratios.
2. Problem 2 Design the local communication network among the PVs (the S matrix) in order to ensure efficiency and reliability of the network while minimizing economic costs.
3. Problem 3 Design a high level control based on the solutions of problems 1 and 2 such that, for each group of PVs, the voltage of a critical bus is of a specific value and the active power flow across certain transmission or distribution lines is a fixed amount.

6.6.1.1 COMMUNICATION TOPOLOGY

The topology of the local communication network among the PVs in one group can be time varying and asynchronous, in which case the communications matrix S describing the topology becomes piecewise constant. To ensure that a given utilization profile is achieved among one group of PVs, there needs to be local information sharing among them. The more communication channels there are, the more information propagates within the group, and the faster the convergence to the desired utilization profile. However this quickly becomes an uneconomical solution to the problem. From cooperative control theory [119], it follows that the minimum requirement on communication topologies is the so

called sequential completeness condition. For the purpose of distributed control design, the following rule is given for designing local communication networks and scheduling local communications.

Rule: The communication matrix S is piecewise constant, and the corresponding sequence $S_{\infty:0} = \{S(t_0), S(t_1), \dots\}$ is sequentially complete.

The sequential completeness condition is a very precise method to schedule local communication, and it is the necessary and sufficient condition for any properly-designed cooperative system to converge [119].

6.6.1.2 CASE STUDY RESULTS

Z. Qu et.al. [112] utilized the IEEE 34-bus distribution network to illustrate the effectiveness of the proposed distributed two-level control strategy. The network's main voltage is 24.9 kV and the network includes 16 PV generators and one gas turbine generator. Detailed results of the simulations are contained in [112]

In this distribution network, the distributed generators (including the gas turbine generator) provide power to not only the local loads but also the external main grid. In the simulation was done using Digsilent software and showed total penetration levels of PVs were increased up to about 220%.

Subsequent studies that were conducted verified the proposed distributed two-layer control can make the system operate well and all the PV generators converge according to the desired utilization profile for the following disturbances: 1- Short-circuit faults 2- Changes in sunlight 3- load changes and intermittent communication interruptions [112].

This proposed two-level control scheme for the power groups of PV generators in the distribution network can autonomously adjust itself to a feasible operating point (after disturbances occur) so that all the PV generators in one group converge to a prescribed utilization profile. The proposed controls require only intermittent information sharing among neighboring generators, and topologies of local communication networks can be time varying. As long as the communication networks meet the minimum information exchange requirement (of the matrix sequence being sequentially complete), the proposed controls ensures convergence. The proposed design methodology is also applicable to distribution networks with different types of DGs including wind [112].

6.6.2 OTHER FUTURE DISTRIBUTION SYSTEM CONFIGURATIONS AND CHARACTERISTICS

As part of Southern California Edison's (SCE) distribution Smart Grid initiatives, SCE has engaged in two projects involving advanced distribution automation and active voltage control that may provide insight into future distribution system designs [127]. The two projects are (1) Avanti circuit of the future [128], and (2) Irvine Smart Grid demonstration (ISGD) project [129].

The Avanti circuit design includes a distribution level dynamic reactive power compensator to provide voltage and VAR support. The circuit is also equipped with solid-state fault current limiter, remote control switches, and fault interrupters to facilitate integration of distributed generation and protection coordination. The project objective was to demonstrate an integrated design, interoperability of various control devices, and operational features that can be achieved in distribution circuits equipped with intelligent devices, coordinated and operated through a SCADA system [127].

The ISGD project serves customer loads distributed on two adjacent feeders that can be operated as a closed or an open loop. Universal remote control interruption devices with two-way communication infrastructure are provisioned to change circuit topology and transfer loads from one circuit to another during faults and contingency conditions. The project also targets specific Smart grid aspects such as (1) automatic volt/VAR control, (2) utilization of community-level energy storage for distribution constraint management, and (3) advanced control and protection strategies for self-healing circuits [129].

7.0 SUMMARY AND FUTURE WORK

More renewable energy sources and distributed generation sources are happening. They can reduce the need for long distance transmission systems, but they will cause increased stress on distribution networks.

RPS goals cannot ignore the reliability aspect of integrating renewables onto the grid. Future policy must consider reliability when developing RPS goals. It is recommended that future senate bills such SB1 (CSI) and SB2 (RPS) be reviewed together and preferably combined into a single initiative to account for all the renewables on the grid for reliability purposes.

Z. Qu et.al. [4] provide a control strategy for Fair Utilization and Control design for System Coordination based on the application of a cooperative control for power flow control of photovoltaic generators. Their study shows penetration levels can be increased up to about 220% provided that all the PVs are run according to the fair utilization profile and their power factors are also kept the same. This can be a tremendous benefit once it demonstrated on an actual system. It would also be very interesting to add some storage and repeat the simulations.

Water-borne PV systems can provide an alternative solution to land use environmental requirements in permitting solar projects. Water borne systems also augment solar rooftop initiatives to add additional distributed generation. Floating PV on WWT plant ponds can be a valuable energy efficiency strategy and can be an effective bridge to mitigate the high penetration issue of installing increasing amounts of renewable generation on distribution networks until new control strategies and storage are developed. The water-borne system can be integrated into the electric grid as well as act as a stand-alone system in behind the meter installations. Because of its unique features, the water-borne system requires 50-70% less area. These water-borne systems are geographically dispersed; therefore the high penetration issue is greatly reduced. Future articles will discuss design criteria for economical water-borne systems and discuss lesson learned from the pilot project installation.

Nonimaging optics is a wonderful development, and its application to CPV may provide path forward for the solar PV industry in conjunction with the continued improvement in efficiency of multijunction cells as discussed in Appendix A. The current low cost of silicon cells has dealt a blow to the CPV market. Flat panel designs are also gaining in efficiency; the latest designs have efficiency of 22%. Water-borne installations designs should consider the lowest

life cycle cost in the design approach. The Cost Benefit showed that behind the meter installations are approximately 10% less analysis costly than systems that are integrated on the transmission side of the meter due to wheeling and transmission access charges.

While Chapter 5 discussed the methodology for integrating renewables including PV into the transmission system, many DER installations are more likely to be integrated into the distribution network. The power flow type of analysis needs to solve large scale problems from transmission-level voltages down to secondary service points, including heavily meshed secondary distribution systems. The power flow analysis should address both steady-state and dynamic overload, voltage flicker and control concern. A power flow and voltage drop study should be performed to determine the steady-state loading profile of the system. The power flow should be capable of stepping through time-sequenced operations of the circuitry's active components, including rapid changes in loading such as system responses to changes in PV outputs and loading associated with rapid configuration changes [127]. New tools for planning engineers need to be developed to address these challenges.

As discussed in chapter 6, integrating renewables and PV into the distribution network can be very challenging. Some of the differences in analysis algorithms were compared for conducting power flow studies and were contrasted with those used in transmission planning studies. New algorithms and software tools will need to be developed for future high penetration because the definition of stability and reliability will include market and social networking variables. Distribution Engineers will need to become versed in alternative control strategies such as cooperative control theory as well as network engineering and cyber security. Market forces will have to be captured into the control system algorithm. As DER and distributed PV continue to gain momentum and increased market acceptance, new and improved control systems and regulatory requirements will become vital and very important. This was demonstrated by the IEEE bus simulation where penetration was able to increase to 220% using a two level cooperative control strategy implementing a fair optimization algorithm.

7.1 FUTURE RESEARCH

Further Areas of research to follow and develop:

1. Complete the list and ranking of the California WWT plant sites for potential installation of the water-borne systems. Expand the study to other western states.

2. Assist in the development of a PV water-borne system for installation in a WWT facility.
3. Determine the measures and scale factors to reduce the cost of the water-borne system below \$2.70/watt including the inverter.
4. Traditional grid planning is based on worst case deterministic “contingency” scenarios and related risk analyses as discussed in chapter 5. This approach focuses on the loading characteristics of transmission lines, distribution feeders, substations and transformers based on forecasts of generation and customer demand. Today transmission system modeling includes stochastic analysis, but not typically integrated with variable DER or distribution system analysis. Develop software analysis tools that provide numerous dynamic scenarios and energy flows moving in many directions at once across distribution and transmission. These tools also need to account and provide flexibility to include new control system designs and ability to include storage elements.
5. Grid operations in the coming decade will undergo a significant transformation due to increased variability in electric generation production from wind and solar as well as customer load becoming less predictable given onsite generation and responsive loads [140]. Controllability in the context of millions of dynamic resources in a market across transmission and distribution is not yet well understood. There is an urgent need to consider the interactions across the grid and the current operational systems to ensure grid stability and reliability.
6. Given these fundamental changes, can cooperative control be effectively applied to utility distribution networks with variable inputs. A two layer fair utilization profile using cooperative control was briefly discussed in chapter 6 that shows promise in a simulated case, but how does one determine the fair utilization profile to account for market reactions and social networking responses. Perhaps the related risk management techniques adapted from other mission-critical industries should be evaluated.
7. New control schemes as well as storage systems have been shown to help increase the penetration level of distributed renewables on distribution networks. What is the optimum, most efficient, and cost effective combination of these methods.
8. The three pillars of control: observability, controllability, and algorithms are helpful in considering changes to operational systems. Currently, the industry does not have either robust observability strategies or related measurement strategies. Phasor measurement units (PMUs), sensors that monitor power

characteristics in very small time increments-30-120 samples per second, are a vast improvement in the fidelity of information with traditional 4 second updates still widely used. A utility with 50 PMUs, 2.5 million smart meters and other sensors will accumulate about 20 billion pieces of grid state data each month [140]. Integrating this data with appropriate controls to see disturbances as they develop so proper corrective action can take place requires further development.

9. With increased penetration of distributed energy resources such as solar PV, treating distributed resources as negative load will not work as additional strain will be placed on transmission side resources to compensate for variability in DERs as well as physical problem on distribution circuits. There is also the potential for significant operational flexibility in the distribution system related to customer loads, which are currently underutilized, that may prove useful in buffering the effects of renewable source variability at the bulk system level. Further research is needed to resolve the questions related to how tightly or loosely coupled distributed resources (generation, storage and demand) should be to maintain overall grid reliability and power quality[140]. This involves the evolution of distributed controls talked about in Chapter 6.

10. The role of system checks, whether human or machine is an important consideration in the discussion of centralized and distributed market designs and possible links to dynamic price signals as significant system control inputs as alluded to in chapter 6. This is because of the potential to enable unintended effects like the financial market flash crashes that have occurred several times over the past five years. Since these can occur in seconds or less, there is a growing recognition that machine-to machine based systems leveraging expert systems and adaptive controls will be needed.

A number of architectural issues remain to be resolved including the role of market in grid control systems, multiple time scales, multiple granularity levels, and local versus wide-area controls.

Electric Utility company control centers are evolving from a human-centric operational model to a machine-centric model, much as the aviation industry has evolved to “fly-by-wire” systems [140]

11. Use the similarity measure described in the Southern California Edison High-Penetration Photovoltaic Project [127] to develop tools that utility distribution provides and Resource planners can use to analyze the penetration of DER on their distribution systems. The methodology uses geographic and statistical analysis to determine the similarity of a large set of non-studied feeders with respect to a small set of studied feeders.

12. How to manage the transition and related operational and market systems in a manner that doesn't result in an unstable and unmanageable system is a challenge. The likelihood is that for most of the next 20 years the electric system will evolve into a hybrid set of centrally controlled generation, storage and power management devices and a distributed set of resources managed on a more decentralized basis leveraging the self-managed capabilities of DER. A nice advantage of the water-borne system discussed in this Dissertation is that it helps fill the gaps during this transition time.

The current complexity and operational instability issues facing Germany's electric system may be a good example of challenges ahead [144]. The article [144] suggests that although PV may be able to give some relief to the grids, PV cannot reduce the need for peak capacity and additional PV will cause a considerable growth in the need for regulating capacity. The regulating work which must be made by controllable power sources grows considerably with the growth of wind power and PV. TenneT is one of Germany's four main grid operators. In the TenneT area, a calculation for April 2011 has shown that wind power alone would extend the regulating range by more than 50 percent, while the actual combination of wind power and PV has doubled the regulating range.

On November 4, 2006, a German 380-kilovolt line had to be temporarily disconnected. Due to insufficient coordination of protection systems, a circuit tripped and started cascading outages. The result was that the continental grid in Europe was divided into three islands and about 17 gigawatts of load was shed. The case demonstrates how a local event in Germany can turn into a widespread European disturbance [144]. Since the German system is heavily stressed, there is good reason for concern.

13. Work to integrate change in regard to integrating inverters into distribution system for voltage control, a key to increased levels of penetration of PV.

14. Increase the reliability of inverters [96] for 20 year life and oversized for grid application. Work to decrease the reluctance to adapt the existing infrastructure and modify traditional practices to allow this to happen through the implementation of successful demonstration projects in the field to show new practices are safe, reliable and beneficial.

15. The latest stage of electricity market evolution involves a thousand-fold increase in the number of spot markets in the largest U.S. markets. This results in creation of more than 20,000 Locational Marginal Pricing (LMP) nodes nationwide. The intent is to provide greater pricing fidelity to generation and transmission operation and investment decisions. LMP markets are spot markets intended to address bulk power system balancing needs that do not reflect appropriate price signals for distributed resource investment or for

investment in bulk power generation resources. As such, LMP markets have made large-scale generation resource allocation on shorter time scales quite difficult as both the unit commitment problem is very hard to solve exactly, and long-term capital investment isn't driven by short-term marginal pricing/profits. Neither investors in generation and transmission nor retail customers want to be exposed to levels of extreme variability and volatility. This is why more than 80% of the energy transacted in North American markets is through long-term bilateral contracts between producers and Load Serving Entities. These long term purchase contracts typically set the price by which new generation is built.

The use of dynamic wholesale spot pricing like LMP, for customer demand response, creates challenge. Wholesale spot prices sent to customer devices inherently creates a form of decentralized real-time control, where each customer or aggregator sets device response characteristics based on their preferences. The inherent closed-loop feedback between volatile spot price and aggregate demand could result in undesirable cycling of devices (and feedback into market pricing). These prices do not reflect distribution level information related to location, reliability or power quality considerations and will create issues for distribution systems [140].

Is LMP an appropriate market pricing mechanism for a hybrid electric system with tens of millions of distributed resource actors as envisioned by FERC? Appropriate price and market mechanisms to be developed to value energy at a particular point on a distribution system. New pricing mechanisms are needed to create effective closed loop systems that are tightly coupled with distribution control systems to ensure reliability and power quality as discussed in chapter 6.

16. Network design and new control strategies must be integrated in such a manner to protect against cyber attack. Increasing levels of DER and CPV on distribution networks will require more interconnected networks and control systems. The growing threat of cyber attack to energy related control systems is ever increasing and so cyber security will be vital for future new distribution control systems to accommodate high penetration levels of distributed renewable resources.

17. The U.S. electrical system serves more than 144 million customers through about 6 million miles of wire and cable and some 600,000 distribution circuits originating from an estimated 60,000 substations [145]. Unlike transmission planning, distribution system planning does not typically involve a multi-stakeholder process that considers various proposed uses for the system before engineering is conducted and investments determined. As such, the lack of insight on the potential use of the system can lead to a systematic under valuation and investment, resulting in a failure to achieve societal needs. An early indication of the challenge is the significant growth in the backlog of distributed generation applications [146]. Estimates for fully capable distribution

circuits suggest an additional cost of between \$2 million and \$3.5 million per circuit for physical upgrade and intelligent control systems [147]. Who should pay for these costs? A recent proposal by California utilities for a non-bypassable network use charge is an attempt to address this. However, it is not clear that this type of proposal alone will achieve energy policy objectives or the interests of the utility. For example, non-bypassable charges may accelerate the adoption of onsite energy storage combined with solar photovoltaic systems and home energy management systems. This may make it possible for a customer to leave the grid entirely, echoing another telecom phenomenon: the rise of mobile phone service-only households, which now exceed 30% of the u.S. market, and even higher globally. The paradox is that customers leaving the grid will compound the issue of fixed cost recovery driving rates higher on a declining delivery revenue leading to potentially more customers leaving and ultimately a “death spiral” [140]. Rate redesign is needed to separate fixed costs associated with grid infrastructure using fixed fees from variable costs like energy commodity that are more appropriate for volumetric pricing.

REFERENCES

- [1] U.S. Renewable Energy Technical Potentials: A GIS-Based Analysis
Lopez, A; Roberts, B; Heimiller, D; Blair, N; Porro, G
Technical Report
NREL/TP-6A20-51946
July 2012
Available electronically at <http://www.osti.gov/bridge>

- [2] Integrating Renewable Electricity on the Grid
A Report by the American Physical Society (APS) Panel on Public Affairs
February 2012
Pages: 2,8

- [3] Principles of Solar Engineering Second Edition
Goswami, D.; Kreith,F; Kreider J
Page: 13

- [4] Solar Shield- Protecting the North American Power Grid-NASA Science
Phillips, T.
October 26, 2010
Pages: 1-3
http://science.nasa.gov/science-news/science-at-nasa/2010/26oct_solarshield/

- [5] Solar Superstorm Could Knock Out US Power Grid – Experts
Reuters edited by Simao, P
October 2, 2012
Pages: 1-5
<http://www.reuters.com/article/2012/08/04/us-solar-superstorm-idUSBRE8721K820120804>

- [6] NERC 2012 Special Reliability Assessment Interim report: Effects of
Geomagnetic Disturbances on the Bulk Power System
February 2012
Pages: ii-iv

- [7] Nonimaging Optics
Winston, R.; Minano, F; Benitez P; contributions from Shatz, N.; Bortz,J
Pages: 46,99

- [8] High Collection Nonimaging Optics
Welford, W.T.; Winston, R
Pages: 115-116

- [9] Implications of Liouville's Theorem on The Apparent Brightness
Temperatures of Solar Radio Bursts
Solar Physics 116 (1988)
Melrose, D.B; Dulk G.A
Pages: 141-156
- [10] The 2011 Integrated Energy Policy Report
California Energy Commission CEC-100-001-CMF
<http://www.energy.ca.gov/2011publications/CEC-100-2011-001/CEC-100-2011-001-CMF.pdf>
- [11] [155] An Energy Policy Essay Renewable and Distributed Power in
California Simplifying the Regulatory Maze- Making the Path for the Future
Carl, J.; Grueneich, D.; Fedor, D.; Goldenberg, C
Shultz-Stephenson Task Force on Energy Policy
www.hoover.org/taskforces/energy-policy
pp 1-48
- [12] California Energy Efficiency Strategic Plan
Strategic Plan Progress Report
Energy Division, pursuant to D.09-09-047
October 2011
Pages: 1-14
- [13] How Updating climate-blind environmental laws could speed-up US Solar
Development
CSP Today (<http://social.csptoday.com>)
April 4, 2013
Pages: 1-4
- [14] Streamlining Solar Permitting and Overcoming Environmental Hurdles to
speed-up CSP development in the US
CSP Today (<http://social.csptoday.com>)
April 10, 2013
Pages: 1-4
- [15] 2010 CTPG Phase 1 Study Report
April 21, 2011
Pages: 3
The final 2010 CTPG Phase 1 Study Report is available at
<http://www.ctpg.us/archived-documents>

- [16] 2010 CTPG Final Study Report Phase 2
May 7, 2010
Pages: 3
The final 2010 CTPG Phase 2 Study Plan is available at
<http://www.ctpg.us/archived-documents>
- [17] 2010 CTPG Study Report Phase 3
September 10, 2011
Pages: 3
The final 2010 CTPG Phase 3 Study Plan is available at
<http://www.ctpg.us/archived-documents>
- [18] 2010 CTPG DRAFT Phase 4 Study Report DRAFT FINAL
February 2, 2011
Pages: 3
The final 2010 DRAFT CTPG Phase 4 Study Plan DRAFT FINAL is
available at <http://www.ctpg.us/archived-documents>
- [19] 136 FERC ¶ 61,051 UNITED STATES OF AMERICA FEDERAL ENERGY
REGULATORY COMMISSION
Transmission Planning and Cost Allocation by Transmission Owning and
Operating Public Utilities
Docket No. RM10-23-000
Pages: 1-15
- [20] Renewable Systems Interconnection Study:
Distributed Photovoltaic Systems Design and Technology Requirements
Whitaker C; Newmiller J; Ropp M; Norris B
Sandi Report SAN2008-0946P
February 2008
Pages: 4-11
- [21] Evaluating the Benefits and Costs of Net Energy Metering in California
Beach, R.; McGuire, P
Crossborder Energy
January 2013
- [22] California Energy Efficiency Strategic Plan
Strategic Plan Progress Report

Energy Division, pursuant to D.09-09-047
October 2011
Pages: 1-14

- [23] Reliability Standards for Geomagnetic Disturbances
United States of America Federal Energy Regulatory Commission
18 CFR Part 40 [Docket No. RM12-22-000; Order No. 779]
May 16, 2013

- [24] Principles of Solar Engineering Second Edition
Goswami, D.; Kreith,F; Kreider J
Page: 13-14

- [25] Offshore Membrane Enclosures For Growing Algae (OMEGA): A System
For Biofuel Production, Wastewater Treatment and CO₂ Sequestration
Trent et al.

- [26] Nonimaging Fresnel Lenses Design and Performance of Solar
Concentrators
Leutz, R.; Suzuki, A.
Pages 18-25

- [27] Nonimaging Optics
Winston, R.; Minano,F; Benitez P; contributions from Shatz, N.; Bortz,J
Page: 22

- [28] High Collection Nonimaging Optics
Welford, W.T.; Winston, R
Pages: 22-29, 223-230

- [29] Nonimaging Optics
Winston, R.; Minano,F; Benitez P; contributions from Shatz, N.; Bortz,J
Page: 115-116, 415-420

- [30] Implications of Liouville's Theorem on The Apparent Brightness
Temperatures of Solar Radio Bursts
Solar Physics 116 (1988)
Melrose, D.B; Dulk G.A
Pages: 154-155

- [31] API Conference Proceedings 1477, 98 (2012); doi: 10.1063/1.4753843
Solar Cells Design For Low and Medium Concentrating Photovoltaic
Systems
Baig,H.; Heasman, k; Sarmah, N; Mallick,

Page:1

- [32] Nonimaging Fresnel Lenses Design and Performance of Solar Concentrators
Leutz, R.; Suzuki, A.
Page: 77

- [33] Optical Design using Fresnel Lenses Basic Principles and Some Practical Examples
Davis, A.; Kuhnlenz, F
Page: 1-8

- [34] Nonimaging Fresnel Lens Concentrators For Photovoltaic Applications
Leutz, R.; Suzuki, A.; Akisawa, A; Kahiwagi T

- [35] Optical Design using Fresnel Lenses Basic Principles and Some Practical Examples
Davis, A.; Kuhnlenz, F
Pages: 50-51

- [36] Principles of Optics
Born, M.; Wolf, E.
Pergamon, Oxford, 6th edition 1989

- [37] Nonimaging Fresnel Lenses Design and Performance of Solar Concentrators
Leutz, R.; Suzuki, A.
Pages: 41-44

- [38] Nonimaging Fresnel Lenses Design and Performance of Solar Concentrators
Leutz, R.; Suzuki, A.
Pages: 51-52,77-92

- [39] Nonimaging Fresnel Lenses Design and Performance of Solar Concentrators
Leutz, R.; Suzuki, A.
Pages: 101-110,179-181

- [40] Nonimaging Fresnel Lens Concentrator-The Prototype
Leutz, R.; Suzuki, A.; Akisawa, A.; Kashiwaga, T
Pages: 5-

- [41] Active Solar Collectors and Their Applications
Rabl, A
Oxford, New York, 1985
- [42] Nonimaging Fresnel Lenses Design and Performance of Solar Concentrators
Leutz, R.; Suzuki, A.
Pages: 184-195
- [43] Nonimaging Fresnel Lenses Design and Performance of Solar Concentrators
Leutz, R.; Suzuki, A.
Pages: 45-49
- [44] Acrylic Polymers for Optical Applications
Jans, R.W
In *Proceedings of the SPIE, Physical Properties of Optical Materials*, volume 204, San Diego, California, August 1979
Pages: 1-8
- [45] Schott Computer Gaskatalog version 1.0
Schott Glaswerke, Mainz, 1992
- [46] Step Lenses and Step Prisms for Utilization of Solar energy
Oshida, I
In *New Sources of Energy, Proceedings of the Conference, United Nations*, volume 4, August 1961, Rome Italy
Pages: S/22. 598-603
- [47] Fundamentals of Photovoltaic Conversion of Concentrated Sunlight
Photovoltaic Conversion of Concentrated Sunlight Wiley, Chichester, 1997
Grilikhes, V.A.; Andreev, V.M.; Rummyantsev, V.D. editors
- [48] Transfer and Distribution of radiant Energy in Concentration Systems
Photovoltaic Conversion of Concentrated Sunlight Wiley, Chichester, 1997
Andreev, V.M; Grilikhes, V.A.; Rummyantsev, V.D. editors

- [49] Parameter Analysis on Solar Concentrator Cells Under Nonuniform Illumination In *16th European Photovoltaic Conference and Exhibition*, Glasgow, United Kingdom, May 2000
Araki, K.; Yamaguchi, Y.
- [50] Estimating and Controlling Chromatic Aberration Losses For Two-Junction, Two Terminal Devices in Refractive Concentrator Systems In *Proceedings of the 25th IEEE Photovoltaic Specialists Conference*, Washington, D.C. May 1996
Pages: 361-364
- [51] Concentrator Multijunction Solar Cell Characteristics Under Variable Intensity and Temperature
Kinsey, G; Hebert, P; Barbour, K; Krut, D; Cotal, H; Sherif, R
Spectrolab Inc.
- [52] Optical Design Using Fresnel Lenses Basic Principles and Some Practical Examples
Davis, A; Kuhnlenz, F
Reflexite Optical Solutions Business
Page 2
- [53] Concentrator Multijunction Solar Cell Characteristics under Variable Intensity and Temperature
Kinsey, G.S.; Hebert, P.H.; Barbour, K.E; Krut, D. D.; Cotal, H.L.; Sherif, R.A
- [54] Reduced Temperature Coefficients for Recent High-Performance Silicon Solar Cells
Prog. in Photovoltaics" Research and Applications, v.2, n.3 1994
Pages:221-225
- [55] Reduced Temperature Dependence of High-Concentration photovoltaic Solar Cell Open-Circuit Voltage (V_{oc}) at High Concentration Levels
24th IEEE Photovoltaic Specialists Conf, v.2 1994
Pages: 1500-1504
- [56] Pathways to 40%-Efficient Concentrator Photovoltaics
Presented at the 20th European Photovoltaic Solar Energy Conference and Exhibition, Barcelona, Spain, 6-10 June 2005
King, R.; Law, D; Fetzer, C.; Sherif, R; Edmondson, K.; Kurtz, S.; Kinsey, G; Cotal, H; Krut, D; Ermer, J; Karam, N

- [57] Solar Cell Generations over 40% Efficiency
 Published online in Wiley Online library (wileyonlinelibrary.com)
 DOI:10.1002/pip.1255
 King, R.; Bhusari, D.; Larrabee, D.; Liu, X.; Rehder, E.; Edmondson, K.;
 Cottal, H.; Jones, R.; Ermer, J.; Fetzer, D.; Law, D.; Karam, N.
 Presented at 26th EU PVSEC, Hamburg, Germany 2011
- [58] III-V Multijunction Solar Cells For Concentrating Photovoltaics
 Cotal, Hector; Fetzer, C; Boisvert, J.; Kinsey, G.; Hebert, P.; Yoon, H.;
 Karam, N
 Energy Environ. Sci 2009 2
 Pages: 174-192
- [59] Physics of Semiconductors, Wiley, New York, 2nd edn, 1981
 Sze, S.M
 Pages: 245-311
- [60] J. Electr, Mater., 1991, 20
 Ren, A.; Emerson, A.B; Pearton, S. J.;Hobson, W.S.; Fullowan, T.R.;
 Lothian, J.
 Page: 595
- [61] Appl. Phys. Lett., 1976, 29
 Wada, O.; Yanagisawa,S.; Takanashi, H.
 Pages: 263-265
- [62] J. Appl. Phys. 1986, 60
 Lahav ,A.; Eizenberg, M.; Komem, Y.
 Page:99
- [63] Semicond. Sci. Technol., 1999, 14
 Nuhoglu, C.; Saglam, M.; Turut, A.
 Pages:114-117
- [64] Appl. Phys. Lett., 1982, 42
 Waldrop, J.R.
 Page: 350
- [65] Appl. Phys. Lett., 1984, 44
 Waldrop, J.R.
 Page: 1002
- [66] Progress In High-Efficiency Terrestrial Concentrator Solar Cells
 Jones, R.K.; Hebert, P.; King, R.R.; Bhusare, D.; Brandt, R.; Al-Taher, O.;

Fetzer,C.;Ermer.J

- [67] Solar Cells: Operating Principle, Technology and System Applications,
Green
Prentice Hall, 1982
- [68] Advances in High Efficiency III-V Multijunction Concentrator Cells
King et al.
Advances in OptoElectronics, 2007
- [69] Advances in OptoElectronics, 2007
King et al.
- [70] http://www.fraunhofer.org/News/ISE_PI_e_World%20Recod.pdf
- [71] New Horizons in III-V Multijunction Terrestrial
King, R. et al.
- [72] High Collection Nonimaging Optics
Welford, W.T.; Winston, R
Pages: 192-195
- [73] Energy Baseline For Municipal Wastewater Treatment Plants
Prepared for Pacific Gas and Electric Company New Construction Energy
Efficiency Program
Prepared by: BASE Energy, Inc
San Francisco California
September 2006
- [74] Municipal Wastewater Treatment Plant Energy Baseline Study
Prepared for Pacific Gas and Electric Company New Construction Energy
Efficiency Program
Prepared by: M/J Industrial Solutions
San Francisco California
June 2003
- [75] Benefits of a Water-Borne CPV System
8th International Conference on Concentrating Photovoltaic Systems
AIP Conf. Proc. 1477
Rosenthal, S.; Earl, D
Pages: 297-300
- [76] Under Obama, 11,327 Pages of Federal Regulations Added
cnsnews.com

September 12, 2012

- [77] Handout Congressional Research Service Analysis of a 2008 Study commissioned by the Small Business Administration
September 7, 2012
- [78] The Importance of Cost-Benefit Analysis in Financial Regulation
U.S Chamber of Commerce Center For Capital Markets and Competitive Fairness
Rose, P; Walker, C
March 2013
- [79] Moritz Professors Present Findings On Cost-Benefit Analysis in Rulemaking to U.S. Chamber of Commerce
The Ohio State University Moritz College of Law
March 12, 2013
- [80] US Army Cost Benefit Analysis Guide 2nd edition
April 8, 2011
Page 19
- [81] Principles Of Engineering Economy 6th edition
Grant, E; Ireson, W; Leavenworth, R
Pages: 132-141
- [82] An Introduction To Cost Benefit Analysis
Thayer Watkins
<http://www.sjsu.edu/faculty/watkins/cba.htm>
- [83] Energy Production by Microbial Photosynthesis
Beneman, J.R; Weissman, J.C.; Koopman, B.L; Oswald, W. J.
Nature, Vol 268, No. 5615, July 7, 1977
Pages: 19-23
- [84] Photosynthesis In Sewage Treatment
Oswald, W.J; Gotaas, M.
American Society of Civil Engineers Transactions Paper No. 2849
- [85] Interconnection Facilities Study Report Generation Interconnection Northern California Power Agency Lodi Energy Center Final Report Completed in coordination with Pacific Gas & Electric
January 20, 2009

- [86] NCPA CIP:002-3 Compliance Project
System Studies Report-Summer Peak and Off Peak
Final Report Revision 1.1
January 13, 2013
- [87] Solar Plant Modeling Impacts on Distribution Systems PV Case Study
Shirek, G.J.; Lassiter, B.A
- [88] Solar Energy Grid Integration Systems "SEGIS"
Sandia National Laboratories, U.S. Department of Energy Efficiency and
Renewable Energy Program Concept Paper October, 2007
- [89] Investigation of Voltage Stability for Residential Customers Due to High
Photovoltaic Penetrations
Yan, R.; Saha, T.K
IEEE TRANSACTIONS OF POWER SYSTEMS, vol 27, no 2 May 2012
- [90] Effects of Large-scale photovoltaic Power Integration on Electricity
Distribution Networks
Paatero, J.; Lund, P
ScienceDirect available online March 22, 2006 at www.sciencedirect.com
- [91] Integration of Photovoltaic Power Systems In High Penetration
Clusters For Distribution Networks and Minigrids
Katiraei, F.; Mauch, K; Dignard-Bailey, L
International Journal of Distributed Energy Resources,
Vol 3 Num 3 July-September 2007
- [92] Not Used
- [93] Secondary Network Distribution Systems Background and Issues Related
to The interconnection of Distributed Resources
Behnke, M; Erdman, W; Horgan, S; Dawson, D; Feero, W; Soudi,
F.,Smith, D; Whitaker, C; Kroposki, B
Technical Report NREL/TP-560-38079 July 2005
- [94] Not Used
- [95] Interconnecting PV on New York City's Secondary Network Distribution
System
Anderson, K; Coddington, M; Burman, K; Hayter, S; Kroposki, B;
Watson, A
Technical Report NREL/TP-7A2-46902 November 2009

- [96] Renewable Systems Interconnection Study: Distributed Photovoltaic Systems Design and Technology Requirements
Whitaker, C; Newmiller, J.; Ropp, M; Norris, B
Sandia Report SAND2008-0946 P February 2008
- [97] Not Used
- [98] Comparison of Distribution Systems Power Flow Algorithms For Voltage Dependent Loads
Eminoglu, U; Hocaoglu, M.H
- [99] The Effect of Photovoltaic Power Generation on Utility Operation
Chalmers, S.; Hitt, M.; Underhill, J.; Anderson, P.; Vogt, P.; Ingersoll, R.
IEEE Transactions on Power Apparatus and Systems; PAS-104,1985
Pages: 524-530
- [100] A Study of Dispersed PV Generation on the PSO System
Jewell, W.; Ramakumar, R.; Hill, S.
IEEE Transactions on Energy Conversion; Vol. 3, 1988
pp.473-478
- [101] Not Used
- [102] Not Used
- [103] Limits on Cloud-Induced Fluctuation in photovoltaic Generation
Jewell, W.; Unruh, T.
IEEE Transactions Energy Conversion; Vol. 5, 1990
pp. 8-14
- [104] Not Used
- [105] Influence of Photovoltaic Power Generation on Required Capacity for Load Frequency Control
Asno, H.; Yajima, K.; Kaya, Y.
IEEE Transactions on Energy Conversion; Vol. 11, 1996
pp.188-193
- [106] International Energy Agency Report IEA PVPS T5-10:2002, February 2002,
Povlsen, A.
Available online at [www. iea.org](http://www.iea.org)
- [107] Not Used

- [108] Not Used
- [109] Not Used
- [110] Utility Interconnection Experience with an Operating Central Station MW-Sized Photovoltaic Plant
Patapoff, N.; Mattijetz, D.
IEEE Transactions on Power Systems and Apparatus, PAS-104, 1985
pp. 2020-2024
- [111] An Effective Approach for Distribution System Power Flow Solution
Alsaadi, A.; Gholami, B
World Academy of Science, Engineering and Technology 28 2009
pp. 732-736
- [112] A Self Organizing Strategy for Power Flow Control of Photovoltaic Generators in a Distribution Network
Xin, H.; Qu, Z., Sueuss, J.; Maknouninejad, A.
- [113] Ultra Large Scale Power System Control Structure
A Strategic Framework For Integrating Advanced Grid Functionality
Taft, J.; De Martini, P
October 2012
- [114] Control of Utility Interactive Inverters
Sozer, Y.; Torrey D
Pp 1-13
- [115] Decoupling Control of d and q Current Components in Three-Phase Voltage Source Inverter
Milosevic, M.
pp. 1-11
- [116] United States Congress, 2007 Energy Independence & Security act, Title XIII-Smart Grid, Section 1301- Statement on Policy on Modernization of Electricity Grid
- [117] National Energy Technology Lab, Modern grid Strategy: Smart Grid Concepts Presentation
US DOE, September 2009
- [118] Distributed Control for Identical Dynamically Coupled Systems: A decomposition Approach
Massioni, P.; Verhaegen, M.
IEEE Transactions on Automatic Control, vol. 54, no 1 January 2009
Pages: 124-135

- [119] Cooperative Control of Dynamical Systems
 Qu, Z.
 Springer 2009
- [120] Evaluation of anti-islanding schemes based on non detection zone concept
 Ye, Z.; Kolwalkar, A.; Zhang, Y.; Du, P.; Walling, R.
 IEEE Trans. On Power Electronics, Vol. 19, No.5 September 2004
 Pages: 1171-1176
- [121] Development of Testing of Anti-Islanding in Utility-Interconnected Photovoltaic Systems
 Stevens, J.; Bonn, R.; Ginn, J.; Gonzalez, S.
 Sandia National Laboratories, SAND 2000-1939 Report, August 2000
- [122] Impact on the Power System of a Large Penetration of Photovoltaic Generation
 Yun Tiam, T; Kirschen, D.
 In Proc. IEEE Power Eng. Soc. General Meeting, 2007
 Pages:1-8
- [123] Voltage Regulation in Radial Distribution Feeders With High Penetration of Photovoltaic
 Tonkoski, R., Lopes, L.
 In Proc. IEEE Energy 2030 Conf., 2008
 Pages: 1-7
- [124] The Effects of Moving Clouds On Electric Utilities with Dispersed Photovoltaic Generation
 Jewell, W.; Ramakumar, R.
 IEEE Transactions on Energy Conversion, Vol. EC-2, No. 4, December 1987
- [125] Factors Relevant to Utility Integration of Intermittent Renewable Technologies
 Yih-huei, W.; Parsons, B
 National Renewable Energy Laboratory, August 1993
- [126] Digital Control of Dynamic Systems 2nd Edition
 Franklin, G.; Powell, J.; Workman, M
 ADDISON-WESLEY PUBLISHING COMPANY
- [127] Southern California Edison High-Penetration Photovoltaic Project –Year 1

Mather, B.; Kroposki, B.; Neal, R.; Katiraei, F; Yazdani, A.; Agüero, J.; Hoff, T.; Norris, B.; Parkins, A.; Seguin, R; Schauder, C
Technical Report NREL/TP-5500-50875 Prepared under Task No.
ARPB.HT22 June 2011

- [128] Circuit of the Future: Interoperability and SCE's DER Program
Hamilton, S., et al
In Proceedings of Bulk power System Dynamics and control Conference,
August 19-24, 2007
http://www.cems.uvm.edu/~phines/publications/2007/Hamiltron_2007_IRE_P.pdf
- [129] SCE press release for Avanti circuit;
http://www.edison.com/files/0607_sce_avanti.pdf
- [130] SCE Interconnection Handbook; available online
http://www.sce.com/NR/rdonlyres/851128D1-6820-43DD-BAD4-B30DE27B0F35/0/Inconnection_Handbook_090317.pdf
- [131] California's Rule 21; available online
http://www.energy.ca.gov/distgen/interconnection/california_requirements.html
<http://www.sce.com/NR/sce/tm2/pdf/Rule21.pdf>
- [132] Carrier Based Single-state PWM Technique In multilevel inverter
Van Nho, N.; Hai, Q; Lee, H
- [133] 2 Space Vector Modulation for Three-Leg Voltage Source Inverters
Prasad, V.
1997
scholar.lib.vt.edu/theses/available/etd-2798-1216/.../chap2.pdf
- [134] Space Vector Modulation-An introduction
Neacsu, D.
The 27th Annual Conference of the IEEE Industrial Electronics Society
pp. 1583-1592
- [135] Space Vector Modulation in 3-Level Voltage Sourced Neutral Point
Clamped Inverter
Durma, E.
PQ-Digital Power, March 23, 1013
- [136] Review of multilevel voltage source inverter topologies and control
schemes
Colak, I.et. al.

Energy Conversion and Manage(2010),doi:10.101/
j.enconman.2010.09.006

- [137] Space Vector Pulse Width Modulation of Three-Level Inverter Extending Operation Into Overmodulation Region
Mondal, S.; Bose, B.; Oleshuk,V.; Pinto
IEEE Transactions on Power Electronics, Vol. 18, No.2, March 2003
- [138] Optimised Space Vector Switching sequences for Multilevel Inverters
McGrath, B.; Holmes,D.; Lipo, T.
Wisconsin Electric Machines & Power Electronics Consortium 2001
- [139] Novel Multilevel Inverter Carrier-Based PWM Methods
Tolbert, L; Habetler, T
IEEE IAS 1998 Annual Meeting, St Louis, Missouri, October 10-15,1998
pp. 1424-1431
- [140] Grid 2020: Towards a Policy of Renewable and Distributed Energy Resources
California Institute of Technology Resnick Institute Report
September 2012
- [141] Current Control of a Voltage Source Inverter connected to the Grid via LCL Filter
Papavasiliou, A.; Papathanassiou, S.; Manias, S.;Demetriadis, G.
- [142] Advanced Integrated Wastewater Pond Systems
Ertas, T; Ponce, V
<http://ponce.sdsu.edu/aiwps.html>
- [143] U.S. Congress. 2007. Energy Independence & Security Act, Title XIII- Smart Grid, Section 1301-Statement of Policy on Modernization of Electricity Grid
- [144] Germany Faces a growing Risk of Disastrous Power Blackouts
Bach, P
GreenTech Media
<http://www.greentechmedia.com/articles/read/guest-post-germany-faces-a-growing-risk-of-disastrous-power-blackouts/>, May 30, 2012
- [145] National Rural Electric Cooperative Association. March 2012. Fact Sheet.
<http://www.nreca.coop/members/CoopFacts/Documents/AnnualMeetingFactSheet.pdf>

ABB Inc. August 2008. Hard to Find Information About Distribution Systems.

[http://www05.abb.com/global/scot/scot235.nsf/veritydisplay/91ad329a50978bf85256c550053db0d/\\$file/hard.to.find.6th.pdf](http://www05.abb.com/global/scot/scot235.nsf/veritydisplay/91ad329a50978bf85256c550053db0d/$file/hard.to.find.6th.pdf)

- [146] Solar Energy Industries Association. February 16, 2012. Petition on Federal Energy Regulatory Commission Interconnection Standards. <http://www.seia.org/researchresources/solar-industry-ferc-filing-small-generator-interconnection-procedure>
- [147] Estimating the Costs and Benefits of the Smart Grid: A Preliminary Estimate of the Investment Requirements and the Resultant Benefits of a Fully Functioning Smart Grid. Product ID 1022519. Electric Power Research Institute. April, 2011
http://my.epri.com/portal/server.pt?space=CommunityPage&cached=true&parentname=ObjMgr&parentid=2&control=SetCommunity&CommunityID=404&RaiseDocID=00000000001022519&RaiseDocType=Abstract_id
Cisco Systems. September 2011. Gridonomics.
http://www.cisco.com/web/strategy/docs/energy/gridonomics_white_paper.pdf
- [148] Solar PV Carousel Trackers For Building Flat Rooftops: Three Case Studies
Frass, L.; Avery, J.; Minkin, L.; Luang, H.; Schneider, H; Larson, D
- [149] The Solar Island : A Groundbreaking CSP Technology
CSP Today Technology
Muirhead, J
March 28, 2013
- [150] Performance Evaluation of Sun Tracking Photovoltaic Systems in Canada
Mehrtash, M.; Quesada, G.; Dutil, Y; Rousse, D
20th Annual International Conference on Mechanical Engineering-
ISME20112-2329 May 16-18, 2012
pp. 1-4
- [151] Tracking and Ground Cover Ratio
Narvarte, L.; Lorenzo, E.
Progress in Photovoltaics: Research and Applications 2008; 16:703-714
Published online August 7, 2008 in Wiley InterScience
(www.interscience.wiley.com) DOI: 10.1002/pip.847
- [152] Feasibility Study of One Axis Three Positions Tracking Solar PV with Low Concentration ratio Reflector
Huang, B.; Sun, F.

Science Direct Energy Conversion and Management 48 (2007) 1273-1280
Available online at www.sciencedirect.com November 29, 2006

- [153] 2012 Special Reliability Assessment Interim Report: Effects of Geomagnetic Disturbances on the Bulk Power System February 2012
North American Electric Reliability Corporation

- [154] Calculation Techniques and Results of Effects of GIC Currents as Applied to Two Large Power Transformers
Girgis, R.; Chung-Duck, K.).
IEEE Transactions on Power Delivery, vol 7, no.2, April 1992
pp.699-705

- [155] Capital Costs For Transmission and Substations Recommendations for WECC Transmission Expansion Planning
Black & Veatch Project No. 176322
Mason, T.; Curry, T.; Wilson, D
October 2012

- [156] San Diego Gas & Electric's Sunrise Powerlink
www.cpuc.ca.gov/environmental/info/aspensunrise/sunrise.htm

- [157] New Transmission Project will help California Meet Summer Electric Demand
U.S. Energy Information Administration Today In Energy
July 11, 2012
www.eia.gov/todayinenergy/detail.cfm?id=7050

- [158] Advanced Integrated Wastewater Pond Systems For Nitrogen Removal
Oswald, W.J.; Green, F. B.; Lundquist, T.J.
EPAA National Wastewater Treatment Technology Transfer Workshop
Kansas City Missouri, June 8, 1994

- [159] 2012 Special Reliability Assessment Interim Report: Effects of Geomagnetic Disturbances on the Bulk Power System
February 2012
http://www.nerc.com/pa/Stand/Geomagnetic%20Disturbance%20Resources%20DL/2012_GMD_Report_112012.pdf

- [160] Residential, Commercial, and Utility-Scale Prices in the United States: Current Drivers and Cost-Reduction Opportunities
Goodrich, A.; James, T.; Woodhouse, M.
Technical Report NREL/TP-6A20-53347

February 2012
Available electronically at <http://www.osti.gov/bridge>

- [161] Life Cycle Inventories and Life Cycle Assessments of Photovoltaic Systems
Fthenakis, V.; Kim, H.; Frischknecht, R.; Raugei, M.; Parikhit, S; Stucki, M.
International Energy Agency Photovoltaic Power Systems Programme
IEA PVPS Task 12, Subtask 20, LCA
Report IEA-PVPS T12-02:2011
October 2011

- [162] Energy Payback and Life-cycle CO₂ Emissions of the BOS in an Optimized 3.5 MW PV installation
Maon, J. et al.
Progress in Photovoltaics: Research and Applications, 2006. 14 pp. 179-190

- [163] New Transmission Project will help California Meet Summer Electric Demand
U.S. Energy Information Administration Today In Energy
July 11, 2012
www.eia.gov/todayinenergy/detail.cfm?id=7050

- [164] Empirical Research on the efficiency of Floating PV Systems Compared with Overland PV Systems
Choi, Y.; Lee, N.; Kim, K.

- [165] From Land to Water
Thurston, C
PV-Magazine Applications & Installations April 2012
<http://www.pv-magazine.com/archive/articles/beitrag/from-land-to-water-/100006317/501/>

APPENDIX A CONCENTRATION AND EFFICIENCY IN SOLAR PHOTOVOLTAIC APPLICATIONS

A.1 BACKGROUND

The sun is a 13.9×10^5 km diameter sphere comprised of many layers of gases, which become hotter toward its center. The surface is approximately at an equivalent black-body temperature of 5760 °K; however at its center it may be at 20×10^6 °K. The rate of energy emission from the sun is 3.8×10^{23} kW, which results from the conversion of 4.3×10^9 g/sec (4.7×10^6 ton/sec) of mass to energy [24]. Based on this rate, scientists believe the sun to have a life span of 10 billion years and that it has been burning for approximately 5 billion years. Of this total energy emission from the sun, only a tiny fraction, approximately 1.7×10^{14} kW, is intercepted by the earth, which is located about 150 million km from the sun [24]. This could also be stated as the amount of energy from the sun striking the earth is over 1.5×10^{22} J (15,000 EJ) each day, more than 10^4 times the 1.3 EJ daily energy consumption by human activity [72]. Clearly, solar energy is a sustainable resource, with energy input far exceeding the rate it is consumed. It is also, however a dilute source of energy, requiring relatively large collector areas to generate solar electricity compared with the lighting, appliances, vehicles and manufacturing processes that use it.

For solar energy collection we have a source essentially at infinity that subtends a semi-angle (or half angle) of approximately 0.005 radians ($\frac{1^\circ}{4}$), approximately half of the 0.53° shown below [24]. This is the given value of the collection angle and is important in understanding the development of solar concentrators and determination of maximum concentration values.

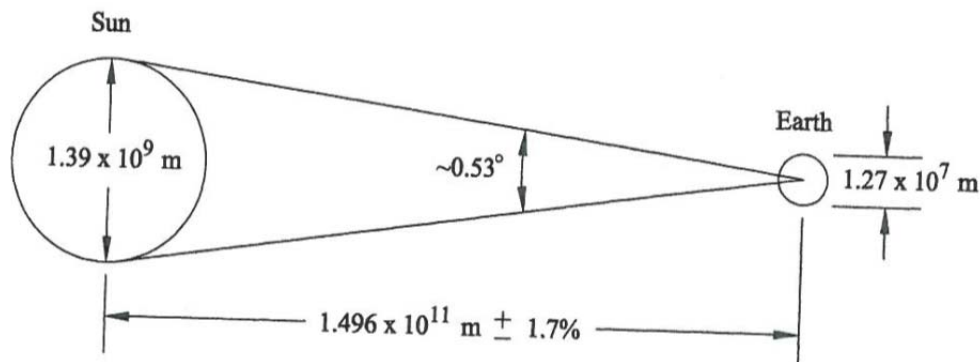


Figure A.1 Relationship between sun and earth

The two motivations for using concentration in solar collectors are: 1) to improve performance (higher efficiency) and 2) to improve the economics by reducing cost. The economic motivation for employing concentration for PV applications is to reduce overall system cost. Solar cells are quite expensive, and if one has to cover large areas with these expensive transducers, the cost can be prohibitive. However, if one can reduce the area of expensive material per unit aperture area, this cost can be substantially reduced [24].

High efficiency (achieved through concentration) is one of the few effective ways to reduce the module packaging and support costs of solar electricity. A 10% efficient module technology requires 10 m^2 worth of materials and manufacturing for module packaging and support to generate 1 kW of electricity under 1000 W/m^2 incident intensity, whereas a 25% efficient module requires 2.5 times less, or only 4 m^2 . As a result and somewhat counter-intuitively, more complicated and expensive PV cell technologies that also confer higher efficiency can frequently be less expensive at the module or full PV system level than modules based on lower efficiency cells [71].

Since the term concentration ratio will be used throughout this dissertation, it is important to distinguish between several important definitions. The limits for the concentration ratio in 2D (two dimensions) and 3D (three dimensions) systems are described in equations A.1 and A.2 below. These upper limits depend only on the input angle and the input and output refractive indices and can be called the **theoretical maximum concentration ratio**.

An actual system will have entry and exit apertures of dimensions $2a$ and $2a'$ as shown in Figure A.2. These can be width or diameter for linear or rotational systems, respectively. The exit aperture may or may not transmit all

rays that reach it, but in any case the ratios $\left(\frac{a}{a'}\right)$ or $\left(\frac{a}{a'}\right)^2$ define a **geometrical concentration ratio**.

The **optical concentration ratio** is the proportion of incident rays within the collecting angle that emerge from the exit aperture [28].

In the geometrical optics approximation, the propagation of the totality of light is as if it were a fluid flow in six-dimensional phase. This flow is subject to conservation theorems that are essentially geometric and follow from the law of propagation of light rays. These are loosely referred to as Liouville's theorem, but they are more properly called the integral invariants of Poincare [7][8]. Liouville's theorem for radiation implies that the extension in phase along the trajectory through phase space is conserved. For an optical system this may be expressed in terms of the conservation of the generalized *étendue* along the ray path. This is an important principle in understanding solar concentration.

The goal is to closely approach the theoretical sine law limit to concentration while maintaining high throughput or *étendue* (optical equivalent of mechanical volume). A useful representation to show this is in "phase space" which is an analogy used both in fluid dynamics as well as optics. Phase space has twice the dimensions of ordinary space and consists of both the positions and momenta of elements of the fluid. In optics, the momenta are the directions of light rays (direction cosines) multiplied by the index of refraction of the medium. In optics, as in fluid dynamics, the volume in this phase space is conserved.

A simple analogy is in transporting a container (the volume in phase space) filled with alphabet blocks spelling out a message illustrates the difference between imaging and nonimaging optics. If the message needs to be preserved, one would have to take care not to shake the container and thereby scramble the blocks and hence the message. But if one merely needs to transport the blocks without regard to the message, the task is easier. This simple analogy distinguishes the difference between using imaging optics (preserving the message of the blocks) versus non-imaging optics (just moving the blocks) for solar concentration.

Concentrator PV systems have several advantages over flat-plate systems. First, concentrator systems reduce the size or number of cells needed. This allows certain designs to use more expensive semiconductor materials which would otherwise be cost prohibitive. Second, a solar cell's efficiency increases under concentrated light. How much that efficiency increases depends largely on the design of the solar cell and the material used to make it. Third, a concentrator can be made of small individual cells. This is an advantage because

it is harder to produce large-area, high-efficiency solar cells than it is to produce small-area cells.

Concentrator photovoltaic (PV) systems use less solar cell material than other PV systems. PV cells are the most expensive components of a PV system, on a per-area basis. A concentrator makes use of relatively inexpensive materials such as plastic lenses and metal housings to capture the solar energy shining on a fairly large area and focuses that energy onto a smaller area—the solar cell. One measure of the effectiveness of this approach is the concentration ratio—in other words, how much concentration the cell is receiving. The real key measure however is how the increased concentration produces an increase in efficiency.

Most concentrators must track the sun throughout the day and year to be effective; thus, achieving higher concentration ratios means using tracking mechanisms that require precise controls.

A.2 NONIMAGING OPTICS

Nonimaging optics is an approach to the collection, concentration and transport of light, largely developed by physicists from the University of Chicago over the past 35 years. The goal of nonimaging optics is not to create an image of the object for photographic accuracy, but the collection of rays incident at the first (entry) aperture of the optical system [7,8]. Nonimaging optics and solar energy go well together because solar energy does not demand imaging qualities, but instead requires flexible designs of highly uniform flux concentrators coping with solar disk size, solar spectrum and tracking errors.

The basic idea is to relax the constraints of point-to point mapping of imaging optics. This permits the design of optical systems that achieve or closely achieve the maximum geometric concentration for a given field of view. Low to moderate concentrations 2x through 4x can be achieved with stationary (fixed year round) collectors. Slightly higher levels (3x-10x) will usually require occasional (seasonal) adjustment. Higher concentrations (10x-40,000x) will require tracking. In general, wherever concentration of sunlight is desired, nonimaging optics can achieve the highest possible levels with the most relaxed optical tolerances [25].

Figure A.2 shows a generalized schematic of any two-dimensional solar energy optical system where the geometrical concentration ratio $C = \left(\frac{a}{a'}\right)^2$ [7,8]. The power accepted by the optical system is determined by the radius of the entry aperture a and the acceptance angle θ , which is the semiangle of the beams accepted. The refractive indices of the material before the entry aperture

of the transparent material filling the concentrator are marked n and n' respectively [26].

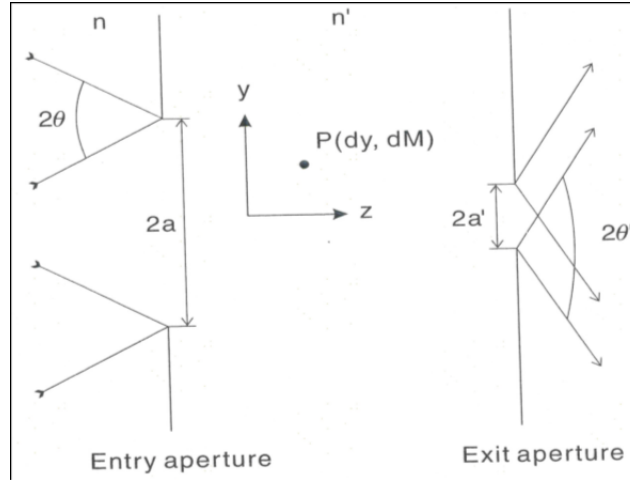


Figure A.2 Concept of *étendue* and maximum 2D concentration

In 2D geometry, if the plane in which all the rays are contained is an $x =$ constant plane, then the differential of *étendue* can be written as $dE = ndy dM$. Setting a point $P(y,z)$ of a ray with direction cosines (M,N) anywhere in front of the entry aperture, the movement of P along the y axis, which is the axis of concentration can be written as dy . The changes of direction of the ray relative to the same axis may be written as dM . The influence of the refractive index n is considered, and the generalized *étendue* (or Langrange invariant) for any ray bundle that transverses the system can be written as

$$ndy dM = n' dy' dM', \quad (\text{A.0})$$

integrating over y and M yields

$4n a \sin \theta = 4n' a' \sin \theta'$; therefore, the geometrical concentration ratio as can be written as $\left(\frac{a}{a'}\right) = \frac{n' \sin \theta'}{n \sin \theta}$. Clearly θ' cannot exceed $\pi/2$, so the theoretical maximum concentration ratio is the result shown in equation A.1 [7,8,26].

$$CR_{max,2D} = \frac{n'}{n \sin \theta_{max}} \quad (\text{A.1})$$

For the 3D case, the input ray segment can be represented by the coordinates of $P(x,y,z)$, and by direction cosines of the ray (L,M,N) . The output ray is similarly specified. Small displacements of P can be represented by

increments dx and dy to its x and y coordinates. Small changes in the direction of the ray can be represented by increments of dL and dM to the direction cosines for the x and y axes. This generates a beam of area dx dy and angular extent of dL dM for the y section and yields:

$$n^2 dy dz dM dN = n'^2 dy' dz' dM' dN'. [7, 8, 28]$$

Proof or derivation of the generalized *étendue* theorem (Lagrange Invariant) has been accomplished in different ways. References [7][8] [28][29] give a proof based directly on optical principles that follow closely the method of Welford (1986), which makes use of the point-eikonal, or characteristic, function of Hamilton. Reference [30] contains a derivation of the Generalized *étendue* based on Liouville's theorem or more specifically one of the Invariants of Poincare.

$$CR_{max,3D} = \left(\frac{n'}{n \sin \theta_{max}} \right)^2 \quad (A.2)$$

Of interest are the upper and lower limits of concentration defined by practical viewing angle limits-the maximum CR is limited only by the size of the sun's disk and achieved by continuous tracking. The upper limit of concentration for two and three- dimensional concentrators is as follows [7, 8, 26, 27]:

$$CR_{max,2D} = \frac{1}{\sin^2 \frac{1}{4}} \cong 208 \text{ in air}$$

$$\frac{1.5}{\sin(.275 \cong \frac{1}{4})} \cong 312 \text{ in glass } (n = 1.5)$$

$$CR_{max,3D} = \frac{1}{\sin^2 \frac{1}{4}} \cong 43,300 \text{ in air}$$

$$\frac{1.5^2}{\sin^2 \frac{1}{4}} \cong 98,650 \text{ in glass}$$

The thermodynamic limit of solar concentration can also be deduced with the help of Figure A.1 and yields the same equations for determining the ideal concentration ratio of solar concentrators as the geometrical approach just described utilizing the application of the edge ray principle.

Assuming that the sun is a blackbody radiator of temperature T_s , the temperature of the sun's surface (5777 K), the amount of radiation incident on the earth on the first aperture of the concentrator is

$$q_{s \rightarrow a} = \sigma A_a T_s^4 \left(\frac{r_s}{l} \right)^2 \quad [26] \quad (\text{A.3a})$$

where r_s is the radius of the sun, l the distance sun-to-earth, and $\sigma = 5.67 * 10^{-8} \text{Wm}^{-2}\text{K}^{-4}$ is the Stefan-Boltzmann constant. The size of the solar disk observed by the collector can be expressed in angular terms as [26]

$$q_{s \rightarrow a} = \sigma A_a T_s^4 \sin^2 \theta_s \quad (\text{A.3b})$$

where $\theta_s = 0.275^\circ$ is the half-angle of the sun. Imagine an ideal black absorber emits radiation at a temperature T_{abs} . This radiation is thought to be completely received at the sun, so that

$$q_{abs \rightarrow s} = \sigma A_{abs} T_{abs}^4 \quad (\text{A.3c})$$

The thermodynamic maximum of concentration can only be reached if $T_{abs} = T_s$ and $q_{s \rightarrow a} = q_{abs \rightarrow s}$. By setting A.3 b equal to A.3 c it follows that the maximum concentration of the solar image on the absorber of a three-dimensional concentrator is

$$C_{3D,max} = \frac{A_a}{A_{abs}} = \frac{1}{\sin^2 \theta_s} \approx 43,400 \quad \text{which is identical to equation A.2 [26].}$$

In practice, these levels of concentration are very difficult to achieve because of the effects of tracking errors and imperfections in the reflecting or refracting element surface. In an experiment carried out at the University of Chicago where a combination of a paraboloidal concentrator as primary and an ideal nonimaging secondary concentrator were utilized, a concentration ratio of 102,000 was achieved and a higher density than that on the surface of the sun was observed. Even though the energy density was higher than on the surface of the sun, the receiver's temperature cannot exceed the sun's temperature [24].

Concentrating photovoltaic (CPV) systems are starting to challenge traditional flat panel PV modules in terms of cost. Depending on the concentration ratio, application and the type of concentrator, different types of solar cells are utilized for achieving an optimum performance and reliability of the system. The type of Solar cells to be used in the CPV system can be single junction silicon cells, thin films or multi-junction cells [31].

For applications demanding high concentrations like point focused systems, multi-junction solar cells are needed which can perform under high concentration and extreme temperatures [31].

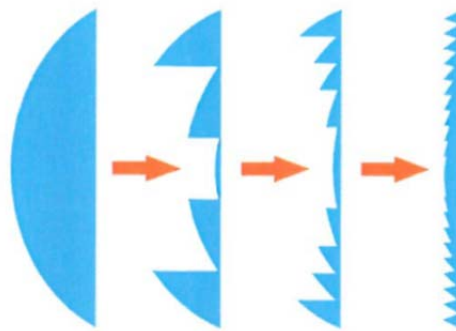
In high concentration photovoltaic systems, quality optics are key components towards high module efficiency. Fresnel lenses are usually selected for their potential due to low cost and high scale production with plastic injection

technology. A Fresnel lens is essentially a chain of prisms. The nonimaging Fresnel lens is designed with the objective of concentrating light rather than forming an image. The main goal of the design of a nonimaging Fresnel lens is to maximize the amount (energy) and quality (flux uniformity) of solar radiation concentrated by the lens [32].

A.3 FRESNEL LENS DESIGN

Both reflectors and lenses have been used to concentrate light for PV systems. The Fresnel lens, uses a miniature sawtooth design to focus incoming light. When the teeth run in straight rows, the lenses act as line-focusing concentrators. When the teeth are arranged in concentric circles, light is focused at a central point. However, no lens can transmit 100% of the incident light. The best that lenses can transmit is 90% to 95%, and in practice, most transmit less.

A Fresnel lens is an optical component which can be used as a cost effective, lightweight alternative to conventional continuous surface optics. The principle of operation is given in that the refractive power of a lens is contained only at the optical interfaces (lens surfaces); therefore the goal is to remove as much of the optical material as possible while still maintaining the surface curvature. Another way to consider it is that the continuous surface of the lens is “collapsed” onto a plane as shown in Figure A.3 [33].



Conceptual illustration (in side-profile) of collapsing a continuous surface aspheric lens into an equivalent power Fresnel lens.

Figure A.3 Conceptual illustration of Fresnel lens

The practical aspect of compressing the lens surface power into a plane surface requires a finite prism pitch, a slope angle component (which acts to refract the rays in the prescribed manner) and a draft component (optically inactive, but necessary to return the surface profile back to the plane) as depicted in Figure A.4. [33]

Typical for solar lens concentrators is to orient the grooves towards the solar cell. This minimizes the impingement of solar radiation of the draft and avoids buildup of dirt and debris within the facets [27, 33].

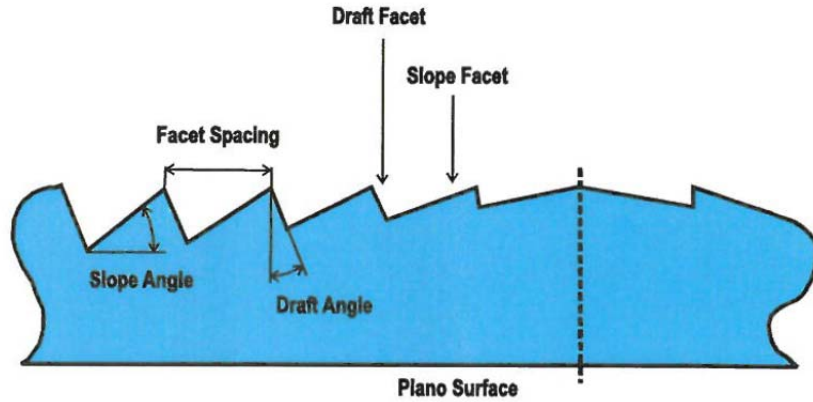


Figure A.4 Fresnel lens details

A.3.1 MINIMUM DEVIATION

Solar light is polychromatic light. The dispersion of a prism is of interest for solar concentration. It can be shown that minimum dispersion occurs at minimum deviation. The minimum deviation prism is to be preferred for solar applications so as to keep the absorber as small as possible [35]. A proof for the congruence of minimum dispersion and minimum deviation is given by Born and Wolf [35][36].

The two surfaces of a prism form the prism angle β (Figure 2.5). Due to this angle the deviation produced by the refraction at the first surface is not annulled by the refraction at the second surface as in the case of refraction of the plane-parallel plate, but is further increased. Increasing deviation increases both the chances for total reflection and chromatic dispersion. The total deviation for the two-dimensional prism shown in Figure A.5 is calculated as the sum of the deviations produced at each surface as shown in equation 2.3 [37].

$$\delta = \phi_1 - \phi'_1 + \phi_2 - \phi'_2 = \phi_1 + \phi_2 - \beta \quad (\text{A.3})$$

Equation A.3 does not hold true for the three-dimensional prism since the angles to be added no longer lie in one plane [37].

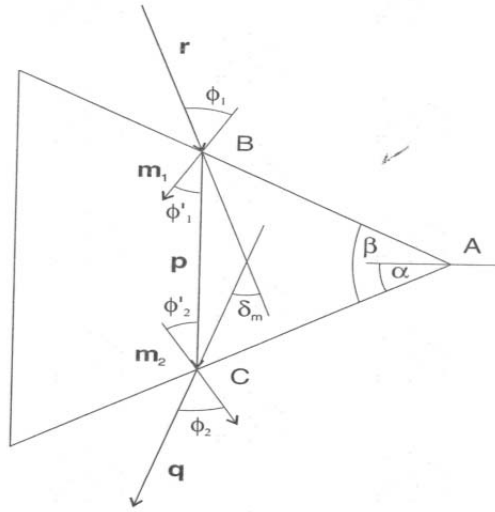


Figure A.5 Maximum Deviation Prism

Minimum deviation exists and can be proved from equation A.3 for the two dimensional case [35, 36]. The deviation reaches a minimum when the rays pass through the prism in a symmetrical way. Every prism has one and only one angle of incidence, for which $\phi_1 = \phi_2$, that results in minimum deviation [37].

Minimum deviation is also understood as a consequence of the principle of the reversibility of light. If reversed in its direction, the ray will follow the same passage through the prism as on its initial pass. There will be only one angle of incidence resulting in minimum deviation. The principle of the reversibility of light is equally true for the three-dimensional case: there can be only one angle of incidence giving minimum deviation [37].

Dispersion occurs due to the color-dependent refraction. Shorter wavelengths (ultraviolet, blue) are refracted further away from the surface normal than longer wavelengths (red, infrared). The speed of light in a medium varies with color. Since the refractive index n of a material is defined as ratio of the speed of light in vacuum to the speed of light in the material, the refractive index is a function of the color of light, i.e. its wavelength [43]:

$$n = n(\lambda). \tag{A.4}$$

A beam of light with a uniform wavefront BB' incident on the prism shown in Figure A.6 [38] produces a refracted ray bundle CC' which will no longer have a uniform wavefront, but will be a function of the wavelength λ . It therefore follows that the deviation δ depends on the wavelength λ [38]:

$$\delta = \delta(\lambda) \tag{A.5}$$

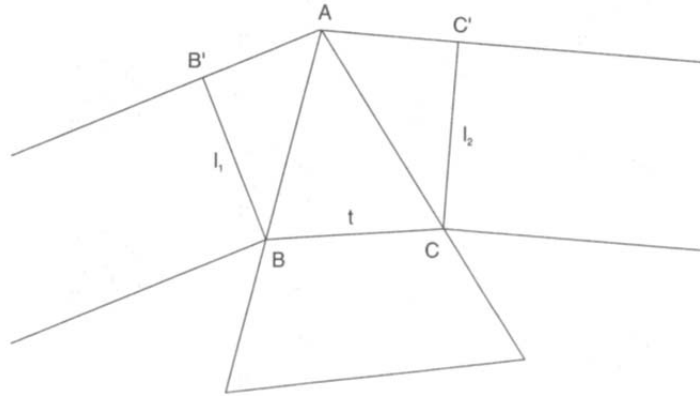


Figure A.6 Dispersion of a prism

The dependence of the deviation on wavelength can by the chain rule be expressed as

$$\frac{d\delta}{d\lambda} = \frac{d\delta}{dn} \frac{dn}{d\lambda} \quad (\text{A.6})$$

This deviation can be evaluated in two factors. The first factor, $\frac{d\delta}{dn}$, depends completely on the geometry of the ray and the prisms. The second factor, $\frac{dn}{d\lambda}$, characterizes the dispersive power of the prism material.

For the two-dimensional case, the general equation for the angle of deviation δ (A.3) expressed by the outer angles of incidence and refraction is [38]

$$\delta + \beta = \phi_1 + \phi_2, \quad (\text{A.7})$$

and for the inner angles of refraction and incidence is

$$\beta = \phi'_1 + \phi'_2 \quad (\text{A.8})$$

Keeping the angle of incidence ϕ_1 constant and using the equations for the angle of deviation in equations A.7 and A.8 above [38],

$$\frac{d\delta}{dn} = \frac{d\phi_2}{dn}, \quad (\text{A.9})$$

$$\frac{d\phi'_1}{dn} = -\frac{d\phi'_2}{dn},$$

Snell's law of refraction can be written as:

$$\sin\phi_1 = n' \sin\phi'_1 \quad (\text{A.10a})$$

$$\sin\phi_2 = n' \sin\phi'_2 \quad (\text{A.10b})$$

Since ϕ_1 is constant, Snell's law of refraction yields the differentiations

$$\sin\phi'_1 + n \cos\phi'_1 \frac{d\phi'_1}{dn} = 0 \quad (\text{A.11a})$$

$$\cos\phi_2 \frac{d\phi_2}{dn} = \sin\phi'_2 + n \cos\phi'_2 \frac{d\phi'_2}{dn} \quad (\text{A.11b})$$

Combining the equations of A.9 and A.11 yields [38]

$$\frac{d\delta}{dn} = \frac{d\phi_2}{dn}$$

$$\frac{d\phi'_1}{dn} = -\frac{d\phi'_2}{dn} = -\frac{\sin\phi'_1}{\cos\phi'_1}$$

$$\begin{aligned} \frac{d\phi_2}{dn} &= \frac{\sin\phi'_2 + n \cos\phi'_2 \frac{d\phi'_2}{dn}}{\cos\phi_2} = \left(\frac{\sin\phi'_2 + n \cos\phi'_2}{\cos\phi_2} \right) \left(\frac{\sin\phi'_1}{\cos\phi'_1} \right) \\ &= \frac{\sin(\phi'_1 + \phi'_2)}{\cos\phi_2 \cos\phi'_1} = \frac{\sin\beta}{\cos\phi_2 \cos\phi'_1} \end{aligned} \quad (\text{A.11c})$$

For the triangle ABC shown in Figures A.5 and A.6 above and utilizing the Law of Sines:

$$\frac{p \text{ (or } t \text{ (2.7))}}{\sin\beta} = \frac{AC}{\sin(90 - \phi'_1)} = \frac{AC}{\cos\phi'_1}$$

$$AC = \frac{\cos\phi'_1}{\sin\beta} t \quad (\text{A.12})$$

For the triangle ACC' shown in Figures A.5 and A.6 above

$$AC = l_2 \frac{1}{\cos\phi_2} \quad (\text{A.13})$$

The deviation depending on the wavelength reaches a minimum when $l_1 = l_2$. The principle of the reversibility of light requires this symmetry. The same argument from the reversibility of light also requires minimum deviation. Minimum deviation requires minimum dispersion. Every wavelength has its own angle of minimum deviation dependent on its refractive index. Choosing an average wavelength and refractive index for the design of the prisms will

minimize the beam spread of white light due to dispersion. In solar energy applications this allows for an absorber of minimum size to be installed.

Using (A.6), (A.11c), (A.12) and (A.13) results in

$$\frac{d\delta}{dn} = \frac{t}{l_2} \text{ and } \frac{d\delta}{d\lambda} = \frac{t}{l_2} \frac{dn}{d\lambda} \quad (\text{A.14})$$

The angular dispersion (the angle by which the emergent wave front (l_2) is rotated when the wavelength is changed by $\Delta \lambda$ is [38]

$$\Delta \delta = \frac{t}{l_2} \frac{dn}{d\lambda} \Delta \lambda \quad (\text{A.15})$$

If the beam of light completely fills the prism, then $t = b$, where b is the base of the prism. The design of the base of a prism is thus defined by the angle of incidence, and the refractive index of the prism material. Or the design of the shape of a prism should depend on its refractive power [38].

In contrast to the performance of crystalline silicon concentrator cells, the performance of multijunction devices is sensitive to both nonuniform flux and nonuniform color distribution. Flux uniformity over the area of the multijunction device and color flux homogeneity penetrating the cell layers are distinguished as “parallel” and “series” connection types. Both types of intensities are crucial for the optimum performance of the multijunction device. Flux density is defined as the radiant energy crossing an area element. The flux density ratio is for the absorber what the optical concentration ratio is for the lens. But while it may be sensible to average concentration ratio of the lens over the whole lens and still obtain a meaningful figure, the flux density should always be a distribution, with some maxima and an extension [39].

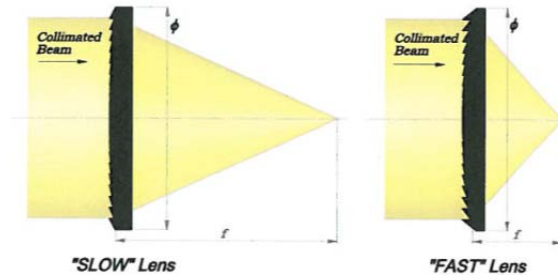
The width d of the absorber of the nonimaging Fresnel lens is correlated with the lens height f and the cross-sectional acceptance half angle θ [40]

$$f = \frac{d}{\tan\theta} \quad (\text{A.16})$$

In the nonimaging 2D lens, the absorber width is usually greater than the cross-section of the area filled by refracted light originally incident at a combination of rays θ_{in}/ψ_{in} . The size of the fraction filled and its location on the absorber must be known in order to evaluate the suitability of the lens for photovoltaic applications, where homogeneous illumination of the absorber in terms of both flux density, and color spectrum is essential for the performance of the system [40].

Focal length and f-number also specify a Fresnel lens. For a lens with prism facets on one side and a flat plane surface on the other (Fresnel lens) the effective focal length is the distance from the prism surface of the lens to the

focal point. The f -number is the ratio of the lens focal length f to the clear aperture diameter of the lens. A lens of smaller f -number will concentrate light faster than an equivalent diameter lens of larger f -number (Figure A.7) [26].



Demonstration of f -number. The lens focal length is f . The lens diameter is ϕ . The “fast” lens has a lower f -number than the “slow” lens.

Figure A.7 Demonstration of f -number

A.3.2 NONIMAGING FRESNEL LENS DESIGN

The nonimaging Fresnel lens is defined as optimum if the following conditions are fulfilled, resulting in an arched linear lens:

- The simulation has to yield minimum deviation prisms for minimum dispersion, and the smallest possible absorber size;
- The outer surface of the lens must be smooth to eliminate blocking losses on the outside. Also this allows for cleaning of the lens.

The parameters to control during the design of the nonimaging lens are the following:

- The cross-sectional acceptance half-angle pair $\pm\theta$;
- The perpendicular acceptance half-angle pair $\pm\psi$;
- The (horizontal) prism inclination α for each prism;
- The average refractive index of the material n ;
- An error margin ΔE for the numerical solution;
- The angle ω that divides the aperture of the lens into equal segments (like the spokes of a wheel) and subsequently defines the pitch Δx by which

the projected width of a prism is defined. This also limits the number of prisms constituting the lens. The designer may later set a fraction of this angle ω as a backstepping angle to start a new prism on the face of the one just finished, thus achieving a finite thickness of the lens

These parameters can be set to fulfill the conditions given above, and define a two-dimensional, convex shaped, optimum nonimaging Fresnel lens of finite thickness. The nonimaging lens of finite thickness cannot be completely described in analytical terms, and a numerical solution has to be found [38].

Shaped nonimaging Fresnel lenses have been designed according to the edge ray principle, incorporating any combination of two acceptance half angle pairs. Kritchmann et al dismiss the use of nonimaging flat Fresnel lenses on technical grounds; however a flat nonimaging Fresnel lens is possible and represents the logical extreme of a curved lens [38]. Refraction, or the design of lenses may take advantage of nonimaging principles. Lenses have a unique advantage over mirrors in due to prisms' partial self correction of errors. The refracted ray is affected little, while the reflected ray's direction angle is changed by double the slope orientation. New plastic materials for lenses offer high transmittance and durability for common wavelengths, while keeping the system inexpensive and lightweight.

Various designs have been researched: point-focus, fixed focal area (blue-edge, and red-edge), statistical or folding focus design, to name a few. However, it is important to remember that the irradiance distribution on the target depends on three factors, the cosine of the impinging ray (its projected width), the dispersion of the lens (the beam width depends on the spectrum of the incident light, and the prism material and angle), and the divergence angle of the source and that the half angle of the solar disk is 0.275° [29].

A.3.3 FLUX DENSITY

The flux density on the absorber of the linear nonimaging Fresnel lens can be calculated by tracing incident edge rays from each prism of the lens to the absorber. The edge (outermost) rays for any combination of angles of incidence are traced, and their intersections with the absorber plane are found in a cross-sectional projection, resulting in a part of the absorber plane ΔD being illuminated. Depending on the distance of the prism from the absorber, a factor s describing the spread of the refracted beam is calculated. The prism's height over the absorber plane defines the cosine losses of the beam when hitting the absorber at an angle β other than normal [40]. Figure A.8 below illustrates cosine loss [41][138].

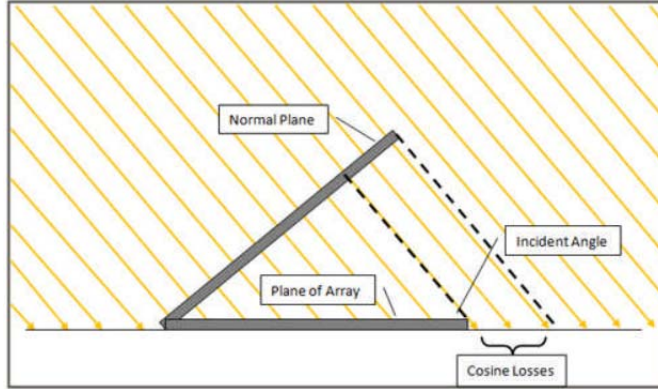


Figure A.8 Cosine loss

The procedure is repeated for each prism i on both sides of the 2D lens. The two sides are not symmetric for any any combination of incidence other than normal incidence. The flux density $\delta\xi$ on any part of the absorber plane is a function of the angles of incidence representing the relative position of the sun over the concentrator, and is found as [40]

$$\delta\xi_{\delta d}(\theta_{in}, \psi_{in}) = \sum_{-i}^i \omega_{e,i} \tau_i S_i \cos\beta \quad (\text{A.17})$$

Where the geometrical losses (tip and blocking losses, but not absorber misses) are discounted, resulting in an effective width $\omega_{e,i}$ of the prism i (Figure A.9) [39].

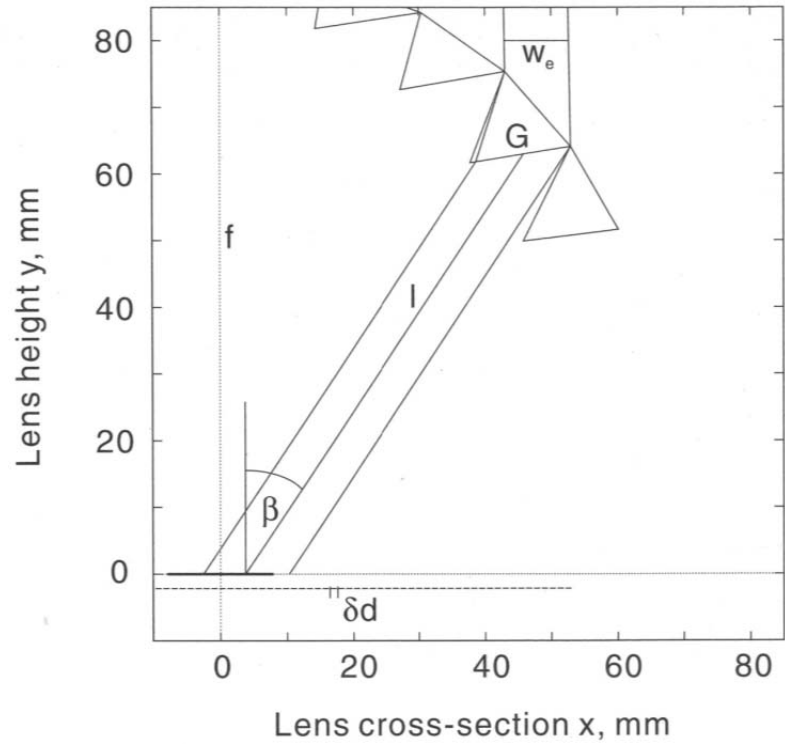


Figure A.9 Flux Density factor

Transmittance losses τ accounting for first order reflections are deducted. Depending on the distance of the prism from the absorber, a factor s describing the intensity of the refracted beam on the absorber is calculated as

$$s = \Delta D \cos \beta l \quad (\text{A.18})$$

Closer distance means higher flux density. A factor l is introduced to describe this distance, normalized in respect to the lens height f [39].

A.3.4 SOLAR DISK SIZE AND BRIGHTNESS

The influence of the solar disk size on the flux density at the absorber of a concentrator can be simulated by ray tracing. Proper simulations for both imaging and nonimaging concentrators with acceptance half-angles approaching θ_s (recall that the radius of the solar disk is, corresponding to the solar disk half-angle $\theta_s = 0.275^\circ$) incorporate the brightness distribution of the solar disk, plotted in Figure 2.10 from Rabl [41,42]. The diffusion over the edge of the solar disk is

caused by absorption and scattering of radiation in the photosphere of the sun and the atmosphere of the earth [42].

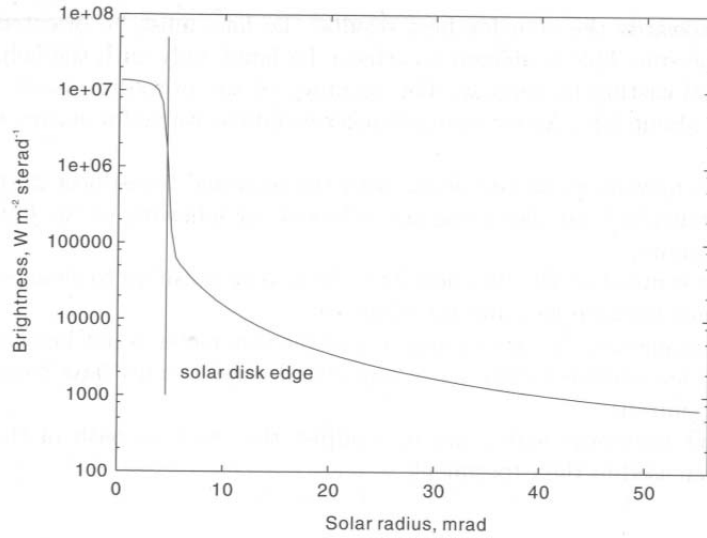


Figure A.10 Brightness distribution of solar flux

An example showing the insensitivity to solar disk size effects for a lens where the acceptance half-angle is larger than the half-angle of the sun is also shown in Figure A.11 for a lens of acceptance half-angle pairs $\theta = \pm 2^\circ$ and $\psi = \pm 12^\circ$ [42]

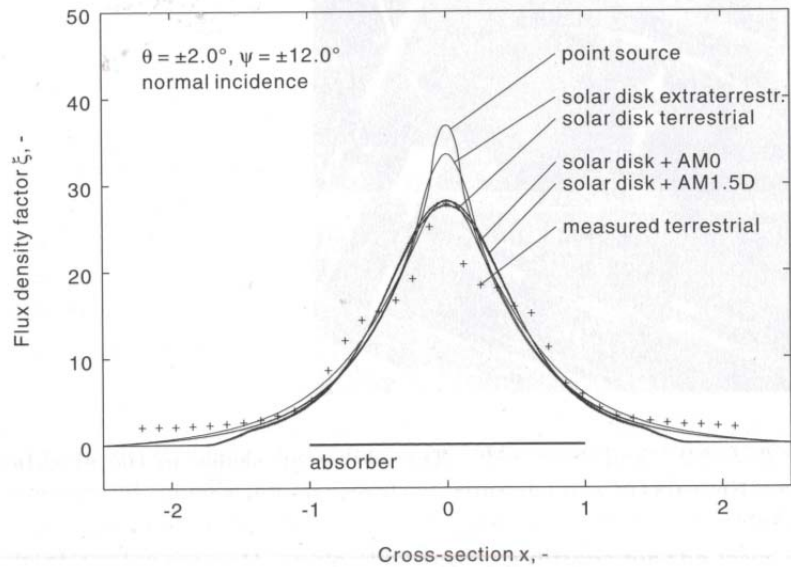


Figure A.11 Flux density factors for non-imaging Fresnel lens

The solar spectrum is thought to originate equally from all over the solar disk (and circumsolar radiation). Ultraviolet radiation appears to be more strongly attenuated in the sun's photosphere than infrared, thus the rim of the solar disk appears darker and redder than its center. Giving an example, Grilikhes [47] describes the radiance of the solar disk to decrease towards the edge by 50% in the wavelength range 450-500 nm, and by 30% in the wavelength range 700-1000 nm. This wavelength-specific description of the sun shape is not reported to have any significant influence on the performance of solar concentrators; the spectral brightness distribution induces errors which are small in comparison to optical distortions [42].

A.3.5 REFRACTIVE INDICES

Borosilicate crown glass (e.g. BK7) is an optical glass that has a relatively low refraction index, low ABBE number and can be produced in large quantities at moderate cost. BK7 is optically very homogeneous and offers transmission rates up to 95% over a bandwidth of $350 < 2700 \text{ nm}$. This is desirable for solar applications, since the solar spectrum covers approximately a range of 250 – 8000 nm, with 93% of the energy transmitted in the band covered by the borosilicate glass [43].

Polymethylmethacrylate (PMMA) is a low cost acrylic that almost reaches the transmittance of BK7 glass over the solar spectrum. Reflection at the surface and not absorption within the material, is the leading cause for transmission losses. Reflection losses account for less than 10% of transmission if the angle of incidence is kept below 55° [43, 44].

The refractive index can be plotted as a function of the wavelength for the material. The Sellmeier formula is the common approach and industrial standard to make this kind of plot for glass [43].

$$n = \sqrt{1 + \sum_{j=1}^3 \frac{a_j \lambda^2}{\lambda^2 - b_j}} \quad (\text{A.19})$$

Where the wavelength λ is in μm . Six constants are needed to calculate the Sellmeier formula for three combinations of refractive indices and wavelengths.

The electronic Schott glass catalog [45] contains data for various glasses.

The refractive index of PMMA is slightly smaller than the one shown for BK7 glass in Figure A.12 [43]. The wavelength-dependent refractive index may be calculated with the Cauchy formula or with the empirical Hartmann formula.

Equation A.20 is a formula for PMMA, based on Cauchy with λ in angstroms [43]:

$$n = 1.4779 + \frac{5.0496 \times 10^5}{\lambda^2} + \frac{6.9486 \times 10^{11}}{\lambda^4} \quad (\text{A.20})$$

The Hartmann formula is explained for PMMA by Oshida [43, 46] with the constants for acrylic (λ in angstroms):

$$n = n_0 + \frac{c}{\lambda - \lambda_0} = 1.4681 + \frac{93.42}{\lambda - 1,235} \quad (\text{A.21})$$

Data obtained with the Hartmann's formula has been plotted in Figure A.12

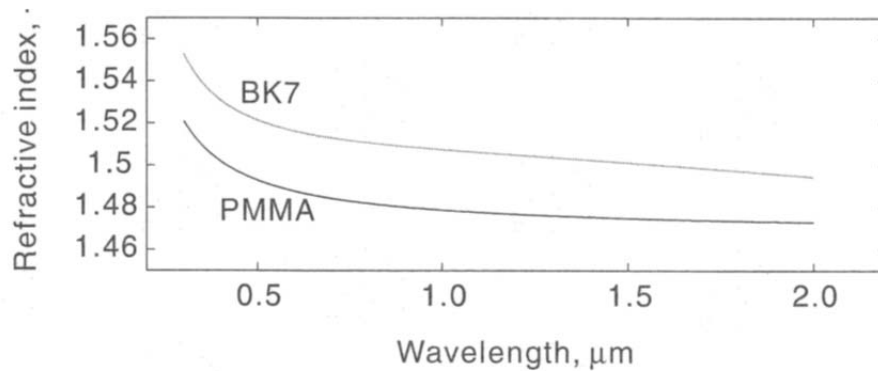


Figure A.12 Refractive indices BK 7 glass & PMMA

A.3.6 SPECTRAL COLOR DISPERSION

In refractive solar concentrators, color dispersion will have an influence on total flux intensity. Ray bundles may be refracted in such a way that they miss the absorber, or concentrate on a “hot spot”, leading to partial illumination of the absorber or photovoltaic cell. Color behavior, or dispersive power, depends on the refractive index of the lens material, here polymethylacrylate (PMMA) with $n=1.49$ for yellow light. The refractive index is wavelength-dependent, for PMMA over the range of 1.515 to 1.470 from blue to red light [42]. The refractive index can be calculated from the formulas in equations A.20 and A.21 and plotted in Figure A.11.

The photon energy in radiation follows the relation [48]

$$h\nu = h \frac{c}{\lambda} = \frac{1.24}{\lambda[\mu m]} [eV], \quad (\text{A.22})$$

where c is the velocity of light, $h\nu$ the energy of one photon, $h = 6.6260755 * 10^{-34} \text{Ws}^2$ is the Planck constant, ν is the frequency of a spectral component of the radiation, and λ is the wavelength. Therefore, the longest wavelength λ_g below which photons can contribute to the photovoltaic effect in a semiconductor material of band gap E_g is

$$\lambda_g = \frac{1.24}{E_g} \quad (\text{A.23})$$

Longer wavelengths are not absorbed as they do not carry enough energy to produce carriers in the semiconductor. Shorter wavelengths, or photons of higher kinetic energy than required to produce electron hole pairs in the semiconductor, will lose the excess kinetic energy as heat in the lattice. Thus the conversion efficiency of photons of wavelengths shorter than λ_g must be reduced by a factor λ_g/λ [42].

Color dispersion changes the resulting flux densities quite significantly, once the acceptance half-angle of the concentrator gets close to the radius of the solar disk [42].

A.3.7 SUMMARY OF FRESNEL LENS CONCENTRATORS FOR PHOTOVOLTAIC APPLICATIONS

The PMMA lens material, has insignificant temperature and humidity induced changes in its refractive index. Changes in the refractive index due to wavelengths of the solar spectrum are more relevant for practical lens design because dispersion occurs due to the color-dependent refraction [34].

Color aberration is not a major problem with a non-imaging 2D Fresnel concentrator. Lorenzo (1981) evaluated chromatic aberrations in solar energy systems using Fresnel lenses. He found that lenses with acceptance half angles $\theta < 5^\circ$ may lead to the refracted ray being spread wider than the width of the absorber. However rays missing the absorber are only a minor problem for photovoltaics. Incomplete illumination of the absorber due to shading rather than color induced inhomogeneous illumination, must be regarded as being of prime importance, since colors separated by refraction at the prisms are usually mixed at the absorber level, when the perpendicular incidence of the 2D lens is taken into account. [34]

The incomplete illumination of the absorber may call for the use of a secondary concentrator.

Solar cells have to be manufactured according to the flux they will receive under a concentrator. The ability of solar cells to convert concentrated sunlight is limited by their base series resistance, by the contact resistance between the grids and the semiconductor material, and by the emitter resistance caused by the spaces between the grid lines.

Two rules of thumb related to the performance of solar cells under concentrated radiation can be given as:

- The product of concentration ratio and cell series resistance is a constant. Additionally, the resistance increases proportionally to cell width; therefore small concentrator cells are desirable.
- Solar cells under concentration potentially see their efficiency increase by a factor $\ln(C)$ [42].

A.4 CONCENTRATOR CELL EFFICIENCY

The conversion efficiency of a solar cell under nonconcentrated radiation can be expressed as [42]

$$\eta = \frac{I_{sc}V_{oc}FF}{P_{in}/A} \quad (\text{A.24})$$

Where A is the area of the cell, I_{sc} is the short-circuit current of the cell. The fill factor FF describes the quality of the I-V characteristics of the solar cell. The more rectangular the curve for current and voltage appears, the higher FF , which is given by [42]

$$FF = \frac{I_{mpp} V_{mpp}}{I_{sc} V_{oc}} \quad (\text{2.25})$$

Where the subscript mpp corresponds to the maximum power point, or the point for which the area of the rectangle $P = IV$ is a maximum. The fill factor describes the “squareness” of the graphs in Figure 2.13 [42].

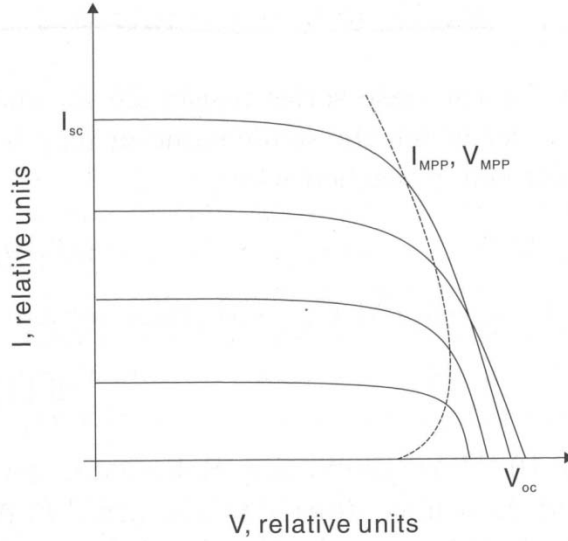


Figure A.13 I-V characteristic of solar cells

Values for FF decrease rapidly with increasing ohmic losses of higher series resistance due to the concentration [3,18]. Under concentration, the current increases linearly with irradiance (or optical input power P_{in}) as

$$I_{sc} = CI_{sc_0} \quad (\text{A.26})$$

The open-circuit voltage V_{oc} increases logarithmically as

$$V_{oc} = V_{oc_0} + nV_{th} \ln(C) \quad (\text{A.27})$$

For a photovoltaic cell under concentrated light, kept at constant temperature (A.21) can be expressed as a function of concentration by

$$\eta(C) = \frac{CI_{sc}V_{oc}(C)FF(C)}{CP_{in_0}/A} \quad (\text{A.28})$$

where the fill factor FF is a strong function of the concentration ratio C , as given by $FF(C) = FF_0(V_{mpp})$,

$$V_{mpp} = V_{mpp_0} + nV_{th} \ln(C) - R_s CI_{mpp} \quad (\text{A.29})$$

In the dominant factor $R_s CI_{mpp}$, I_{mpp} may be approximated by I_{sc} . The expression for V_{mpp} has to be inserted in (A.22) to obtain the value for FF used in (A.25).

From equation (A.26), the efficiency of a solar cell under concentrated light has the potential to increase by a factor $\ln(C)$; however concentration also produces effects that diminish this positive effect such as [42]:

- Increasing R_s : this resistance can be reduced by closer arrangement of the top contacts, but this results in blocking incoming radiation. Secondary concentrators can help with this, but optical losses as well as the added complexity increase.
- Temperature dependency: The temperature limit for operation of high quality cells is in the region is $120^\circ C$.
- Distributed diode effects: under concentration these degrade the fill factor [49, 50]
- Effects of inhomogeneous illumination, both in terms of flux and color.

A.5 GEOMETRICAL LOSSES

Losses due to optical design of the lens are evaluated with the help of ray tracing. Three types of losses can be evaluated by tracing rays through each prism of the lens i.e. tip losses, blocking losses and absorber misses [39].

A.6 MULTIJUNCTION DEVICES

Multijunction solar cells were first introduced by the Research Triangle Institute and by Varian Research Center in the late 1970s to mid 1980s when dual junction devices were formed from an AlGaAs junction stacked or grown on top of a GaAs junction and interconnected by a semiconductor tunnel junction. Later in the 1990s, changes in the top cell thickness led to record efficiencies for dual-junction and triple junction solar cells with GaInP and GaAs both grown on top of an active Ge Bottom cell substrate. It had long been realized that the high efficiency structure of multijunction solar cells makes them highly attractive for cost-effective terrestrial concentrator systems [58].

Solar cell efficiencies can be dramatically improved by dividing the broad solar spectrum up into smaller wavelength ranges, each of which can be converted more efficiently, through the use of multijunction cells. Multijunction CPV solar cells are only the third-generation photovoltaic technology cells that double or triple the efficiencies of the first and second generation PV cells and are able to overcome the Shockley-Queisser efficiency limit for single-junction cells that are now in production. The 3-junction GaInP/GaInAs/Ge concentrator solar cell technology is the first to reach over 40% efficiency and is now the baseline technology for 40% efficiency production CPV cells. However, the baseline 3-junction design is still far from the optimum combination of subcell bandgaps, and far from its efficiency potential [57].

Ideal efficiencies of over 59% are possible for 4 junction cells, and for 5-junction and 6-junction terrestrial concentrator cells, efficiencies over 60% are achievable [57]. The 5- and 6- junction cell designs partition the solar spectrum into narrower wavelength ranges than 3-junction cells, allowing all the subcells to be current matched to the low-current-producing GaInNAs subcell. Additionally, the finer division of the incident spectrum reduces thermalization losses from electron-hole pairs photo generated by photons with energy far above the bandgap energy, and the smaller current density in 5- and 6- junction cells lowers resistive I^2R losses [56]. Figure A.14 charts efficiency histograms of the last five generations of Spectrolab's terrestrial production terrestrial concentrator cells at 500 suns : C1MJ Cella-36.9% average production efficiency, C2MJ with 37.7%, C3MJ with 38.8%, C3MJ+ with 39.3%, and the newly introduced upright metamorphic C4MJ solar cell at 38.8%. The C4MJ is anticipated to reach 40% with continued refinement of production processes [57].

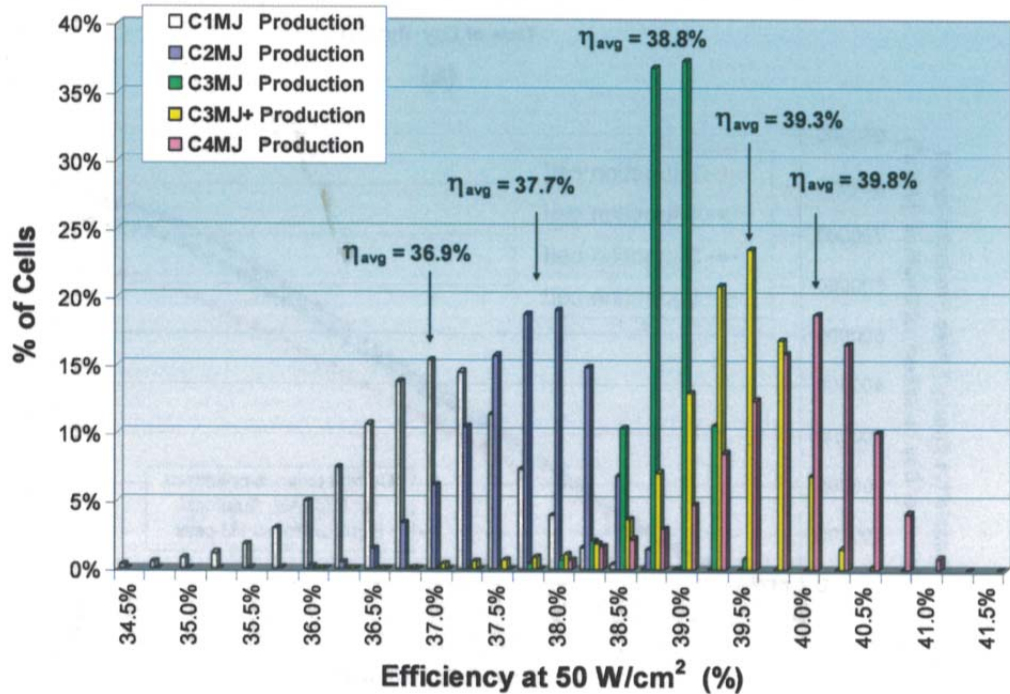


Figure A.14 Efficiency histograms of last 5 generations of terrestrial cells

Efficiency histograms of the last five generations of Spectrolab's terrestrial concentrator cell products, from the C1MJ cell with 36.9% average production efficiency, C2MJ with 37.7 %, C3MJ with 38.8%, C3MJ+ with 39.3%, and production data for the upright metamorphic C4Mj . Average efficiency for the C4MJ is anticipated to reach 40%

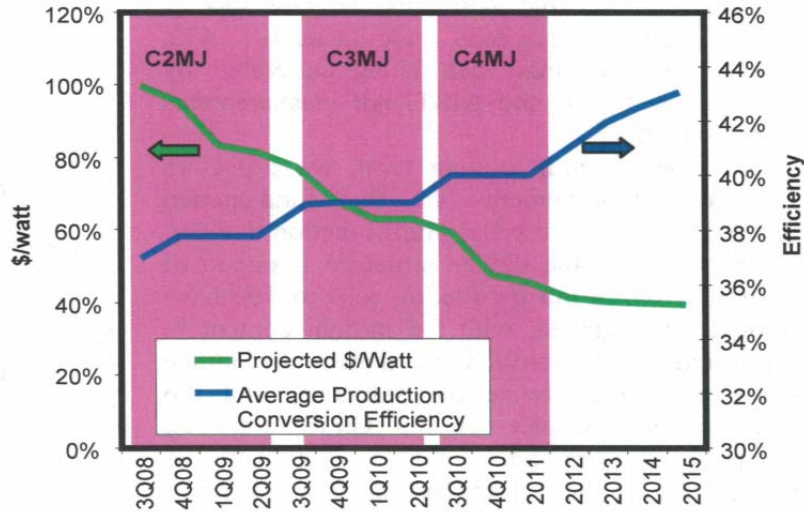


Figure A.15 Planned improvement in economics of multijunction cells

Figure A.15 summarizes the planned improvements in the economics of Spectrolab’s multi-junction cells. This reflects both efficiency improvements, which leverage the cost of the entire system by increasing the power output of the system in proportion to efficiency, and cost improvements, which are themselves also leveraged by efficiency improvements. The efficiency improvements will be achieved through fundamental improvements in the epitaxial device structure and through various improvements in processing at the wafer level [66].

The design improvements for the C2MJ process consisted of improvements in front metal patterning. The shadowing of the semiconductor surface by the metal fingers that collect and conduct the photocurrent to the external circuit is an important loss mechanism [67]. This is particularly true for cells designed for high concentration, since the current and hence metal density are correspondingly higher [68]. Photoresist and metal deposition processes were modified to increase gridline aspect ratio (height/ width). This allows grids to conduct equivalent or higher current while also admitting more light to the active layers. C2MJ uses the same epitaxial wafer as C1MJ, but generates extra current as a result of the reduced gridline shadowing. The C3MJ design retains the same wafer metallization processes that were qualified in the C2JM process, but also incorporates an improved epitaxial design. The C3MJ top cell band gap is higher than that of the C1MJ/C2MJ process but the top cell is thicker, resulting in a more sharply defined absorption [66].

The current path from 40% to 50% terrestrial concentrator cell efficiency is shown to markedly widen the geographic areas for which solar electricity can be generated cost effectively in the US as shown in Figure A.16 [57]

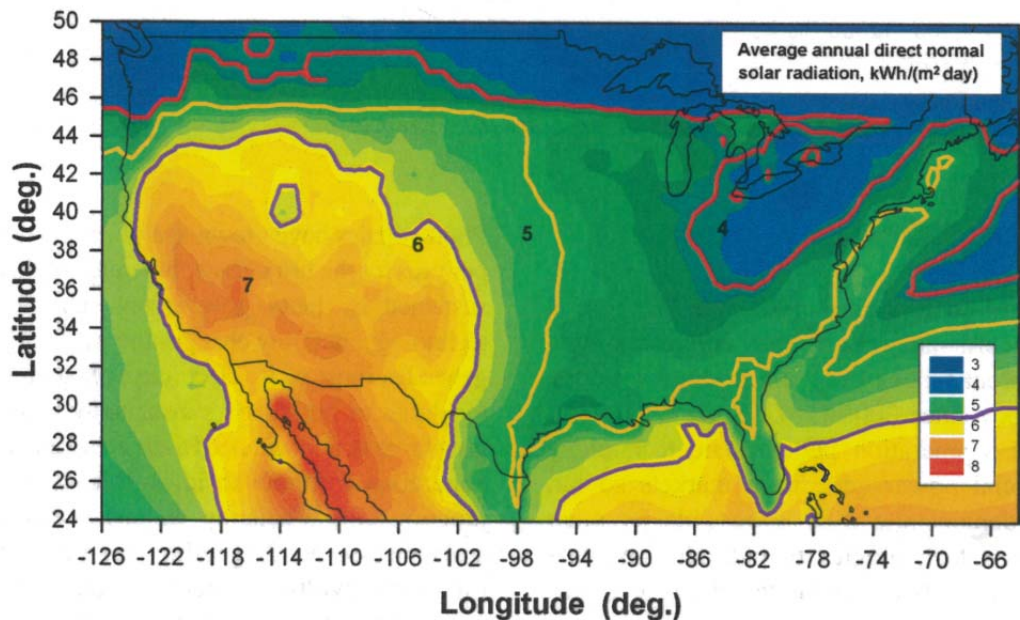


Figure A.16 Contour map showing cost with improvements in cell efficiency

Map of the continental US with filled contours indicated annual average direct normal solar radiation, in units of kWh/m² day, as well as colored line contours indicating regions of cost effectiveness for three cases of CPV systems:

Case 1 (purple)	40% cell and 80% optical eff., 50W/cm ² on cell → 5.8 kWh/m ² day
Case 2 (orange)	50% cell and 80% optical eff., 50W/cm ² on cell → 4.8 kWh/m ² day
Case 3 (red)	50% cell and 85% optical eff., 85W/cm ² on cell → 4.1 kWh/m ² day

Multijunction photovoltaic cells are used with medium and highly concentrated sunlight. The conversion efficiency of concentrator cells increases with the concentration ratio, but the fill factor is degraded by increasing resistance losses. For state-of-the-art multijunction cells in concentrator systems, the flux characteristics of the concentrated sunlight must be accurately controlled to ensure optimum performance. The irradiation over the cell area should be kept constant.

Color effects, or the spectral mismatch between the cells in the multijunction device, can be expressed by a rule of thumb: if the spectral

mismatch between cells in a multijunction device amounts to 20%, the total performance of the device is cut by 10% [42,50].

A.5.1 DEVICE ARCHITECTURES

Modern multijunction solar cells begin with taking a raw wafer and forming individual layers of crystalline semiconductor on the substrate. This process of crystal growth known as epitaxy employs a number of techniques. The oldest is liquid phase epitaxy (LPE); the current favored technique is organometallic vapor phase epitaxy (OMVPE). There are many variants of these techniques such as MBF, MOMB, ALE, HVPE, etc.; however they all deliver atoms to the crystalline substrate [58].

In designing multijunction solar cells, two or more semiconducting layers are stacked as p-n junctions to collect light. A typical 3-junction solar cell structure comprised three n-p junctions made from GaInP, GaInAs and Ge stacked on top of each other—each layer with a bandgap energy higher than the layer below it and assembled with low resistive tunnel junctions [58].

Figure A.17 [66] illustrates the improvements to the fundamental epitaxial structures used in Spectrolab's multijunction devices. The production devices to date have been lattice-matched, with the indium content in the middle cell selected to match the lattice constant of the germanium substrate, and the compositional balance of the GaInP top cell similarly constrained. This still allows engineering of the top cell bandgap by means of controlled disordering of the (In, Ga) sublattice [69]. Lattice matched cells have the advantage of being a proven technology with the ability to grow structures of very high crystal quality [66].

While further evolution of the lattice-matched approach is possible, with promising candidate device architectures in 4, 5 and 6-junction configurations, Spectrolab has selected the metamorphic technology as the baseline approach to reach the 40% production efficiency goal. The metamorphic cell has a step-graded buffer layer between the bottom germanium cell and the middle cell to transition to a slightly larger lattice constant Ga(In)As middle cell, upon which is grown a lattice matched GaInP top cell; the middle and top cells more closely match the optimum bandgap combination for the solar spectrum, and higher efficiency cells in this configuration have been demonstrated [69, 70]. In the longer term, several promising research vectors exist for higher efficiency cells. These include inverted metamorphic [71], as well as upright metamorphic and lattice matched approaches [66].

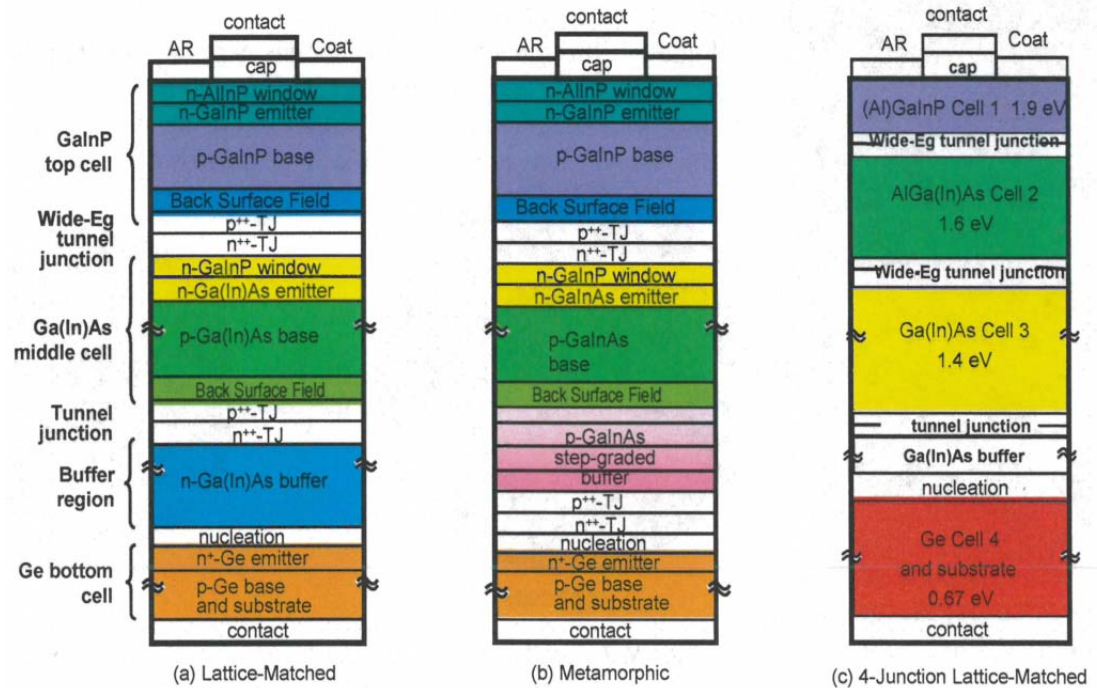


Figure A.17 Epitaxial structure improvements

A.7 METAL SEMICONDUCTOR CONTACTS

To effectively draw the current from the device, the formation of a low resistive interface at the metal-semiconductor junction is necessary. For high current devices as in the case of concentrator cells, quasi-ohmic contacts are imperative for high performance device operation. This means that for a highly doped semiconductor, the Schottky depletion region becomes quite narrow and therefore, the width of the barrier becomes thin enough to allow electrons to be injected in the metal through thermionic-field emission. This process takes place by quantum mechanical tunneling [58].

The higher the doping concentration in the semiconductor, the narrower the barrier width and higher the probability of the electron tunneling through the barrier regardless of the barrier height. A low resistance “ohmic contact” is obtained from the Schottky interface with the semiconductor heavily doped because of the low junction resistance encountered by the electrons. It takes less energy to tunnel through the junction than to surmount the junction barrier. Current flows through the device with little parasitic voltage losses and obeys Ohm’s law where these losses scale with the amount of current flow; this is

because the current-voltage characteristic is linear. Ideally low work function and high dopant concentrations in an n-type semiconductor are desired for low resistance ohmic contacts. Preferably, the metal work function should be less than or equal to the work function of the semiconductor, however, such a contact is practically nonexistent. For p-type material, the metal work function should be equal or greater than that of the semiconductor to form a good ohmic contact. High doping in the semiconductor is also favorable to obtain good ohmic behavior. An issue is that there are not high enough work function metals that are suitable for making good contacts to a p-type semiconductor [58]

Table A.1 depicts the work functions, $q\phi_m$ of common metal contacts and their measured Schottky barrier heights for some technologically important semiconductors [58, 59].

Table A.1 Work Function for metallic contacts

Work function of each metal is shown. (Values from ref 59 and from others as noted: ^a Ref 60, ^b Ref 61, ^c Ref 62, ^d Ref 63, ^e Ref 64, ^f Ref 65)

Metal contact	Work function ($q\phi_m$; eV)	n-Type semiconductor			p-Type semiconductor		
		Barrier height ($q\phi_{Bn}$; eV)			Barrier height ($q\phi_{Bp}$; eV)		
		GaAs	Ge	Si	GaAs	Ge	Si
Ag	4.26	0.88	0.54	0.78	0.63	0.50	0.54
Au	4.80	0.90	0.59	0.80	0.43	0.30	0.34
Al	4.25	0.80	0.48	0.72	0.61 ^f		0.58
Pt	5.30	0.98 ^a		0.90			0.22
Cr	4.50	0.80 ^b		0.61			0.50
Ni	4.50	0.83 ^c		0.61			0.51
Pd	5.12	0.78		0.81			0.42
Ti	4.33	0.75 ^d					
W	4.60	0.90 ^e	0.48	0.67			0.45

Surface states at the metal-semiconductor interfaces are predominant in all semiconductors due to the periodicity of the crystal lattice terminating at the surface with dangling bonds. Suffice it to say that the amount of surface states that are created become significantly high and their effects on the barrier height cannot be ignored. Typically dangling bonds deplete the surface charge of the semiconductor causing band bending even in the absence of a metal contact, which makes it cumbersome to form extremely low resistive ohmic contacts. Fermi level pinning occurs at these surface states within a narrow energy distribution in the band gap. In GaAs, for example, Fermi level pinning to surface

states fixes the barrier height between 0.7 to 0.9 eV below the conduction band at the interface regardless of the value of the metal work function. There are methods to lessen pinning at the surface, but typically entail elaborate and expensive cleanly recipes [58].

Low resistance contacts schemes include: using multilayer metals in metal stacking schemes, using heterojunction techniques, forming low band gap material, and using gold-germanium front contacts and Ti/Ni/Au back contacts.

Contact design depends on many factors such as contact metal, semiconductor material, dopant concentration, deposition technology, and contact fabrication process; all of which influence ρ_c , the specific contact resistivity (in $\Omega \text{ cm}^2$), with values ranging from 10^{-3} to $10^{-7} \Omega \text{ cm}^2$. An example of the importance of ρ_c for a $1 \times 1 \text{ cm}^2$ concentrator solar cell with $\rho_c = 10^{-3} \Omega \text{ cm}^2$ operating at 50 W cm^{-2} of incident sunlight that is 35% efficient can boost the efficiency to 37% for $\rho_c = 10^{-5} \Omega \text{ cm}^2$ [58].

A.8 PRINCIPLES OF OPERATION UNDER CONCENTRATED SUNLIGHT

One of the most important design goals of concentrator systems is to minimize electrical resistance where the electrical contacts on the cell carry off the current generated by the cell. In general, cell conversion efficiency will increase with concentration until series resistance begins to limit performance. In order to translate the high multijunction cell performance into low system-level energy costs, a convergence of multijunction cell and CPV system design must be obtained. Candidate CPV systems typically become more economically viable as the concentration design point is increased, to 300 suns and above [51, 52]

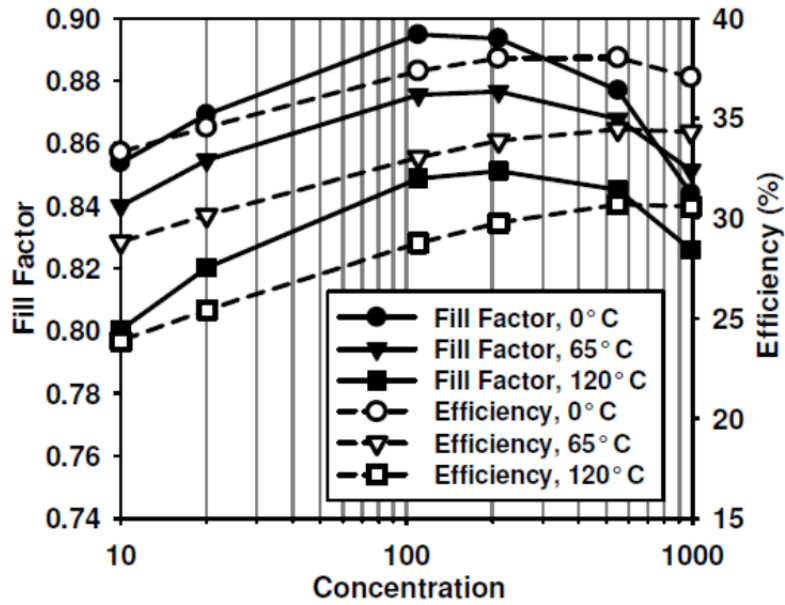


Figure A.18 Curves for cell fill factor and efficiency as a function of concentration

Representative curves for cell fill factor and efficiency (C1MJ cells) as a function of concentration are shown in Fig. A.18. Up to approximately 200x concentration, the fill factor increases, proportional to the increase in open-circuit voltage. At higher concentrations, series resistance limits fill factor. In contrast, the efficiency peaks at 500x, as designed. This is due to the fact that the metal contact grid coverage fraction and resistive power loss can be optimized for a given target concentration. However, as a result of the fill factor limitation, the highest overall efficiencies are typically obtained below 300x, even with such grid optimization. Since CPV systems using multijunction cells become economical only at higher concentration, a principal focus of ongoing cell development is to minimize the various contributors of internal and external series resistance that contribute to fill factor limitations. [53]

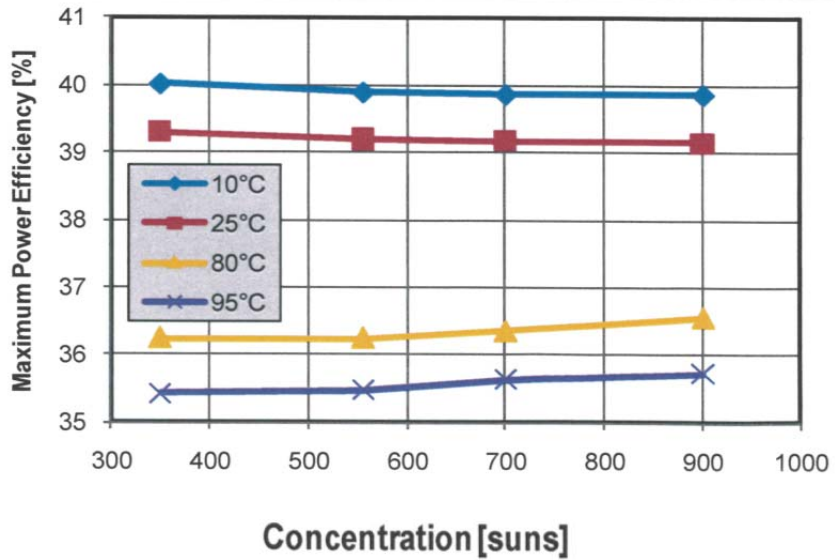


Figure A.19 Maximum power efficiency vs. concentration

Plotting the maximum power efficiency as a function of temperature and concentration is shown in Figure A.19. Figure A.20 plots open circuit voltage as a function of concentration and temperature.

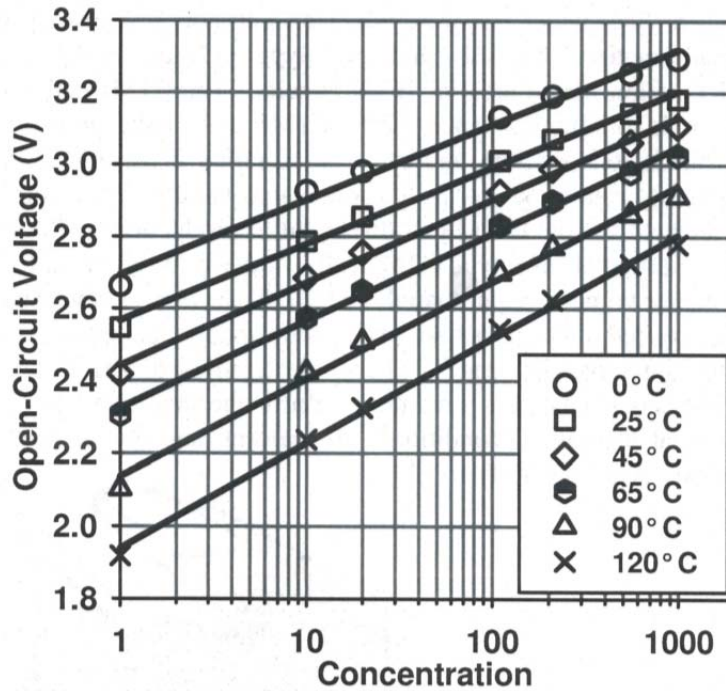


Figure A.20 Open Circuit voltage vs. temperature and concentration

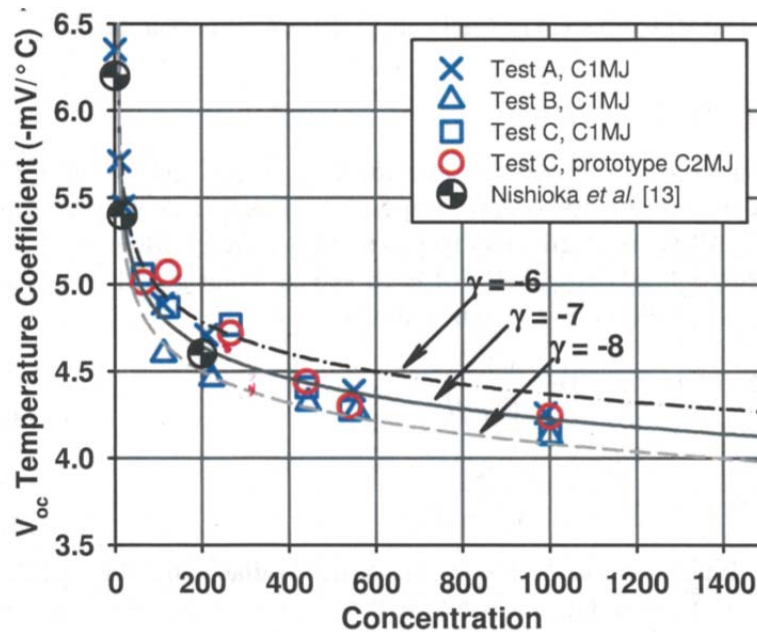


Figure A.21 Open circuit temperature coefficients vs. concentration

Figure A.21 allows for the extraction of the open circuit voltage temperature coefficients as various concentrations. The range of curves provides some prediction of cell performance above 1000x, where many future CPV systems are expected to operate [53].

Overall, the voltage temperature coefficients exhibit a decrease with concentration. This bodes well for future, high-concentration systems and implies a sub cell performance advantage with respect to silicon single-junction cells in these operating ranges [54] [55]. As an example, at 65°C and 250 x, a multijunction V_{oc} temperature coefficient of $-4.6 \text{ mV}/^\circ\text{C}$ implies a 1.5% decrease in voltage with respect to that at 25°C; for a crystalline silicon cell under similar conditions, a 1.7% decrease is expected [55]. Given the larger voltage of the multijunction, this differential will widen at higher concentrations.

A pattern using wide grid lines, known as fingers, in the contacting grid on top of the cell are ideal for low resistance, but they block too much light from reaching the cell because of their shadow. One solution to the problems of resistance and shadowing is prismatic covers. These special covers act like a prism and direct incoming light to parts of the cell's surface that are between the metal fingers of the electrical contacts.

The advantages of the nonimaging design are its reduced tracking requirements, and color mixing, but the price that is paid is incomplete illumination. A secondary concentrator may be called for in photovoltaic applications to alleviate “hot spots”.

The development of concentrators for PV systems incurs the following dilemma. The higher the geometrical concentration ratio of the concentrator, the smaller is the solar cell needed to generate a fixed amount of electricity, but the higher the system complexity, mainly in terms of the tracking accuracy and the related mechanics and controls.

A.9 NONIMAGING SECONDARY CONCENTRATORS FOR PHOTOVOLTAIC APPLICATIONS

The same principles of nonimaging optics used for the design of reflector shapes of the CPC family to attain maximum allowable geometric concentration for a given angular field of view can be used to design secondary elements (Rabl and Winston, 1976). Applications of two-stage designs lie in the higher-concentration small-angular regime where the geometry of a single stage CPC becomes impractical. The fundamental advantage is the same as in lower-concentration applications and may be expressed in complementary ways: either significant additional system concentration can be attained (i.e., a smaller lower cost absorber) or the angular tolerances and precision can be relaxed while maintaining the same level of concentration [72].

Two-stage nonimaging concentrators employing Fresnel lenses as the primaries and dielectric totally internally reflecting concentrators as the secondaries offer a means of achieving concentrations in the high concentration region (500-1000x), and in more moderate concentration regime (80-100x), it can provide the maximum possible acceptance angle (Ning *et al.* 1987a,b). In photovoltaic applications, these concentrators provide much larger acceptance angles than conventional lens-cell systems with the same geometrical concentrations. It has also been shown that a two-stage concentrator provides a more uniform and consistent flux distribution on the cell surface and, therefore, the cell's electrical performance can be enhanced [72].

A potential utility scale CPV installation that provides a concentration of greater than 1000x uses a Fresnel lens as a primary coupled with a secondary optic is discussed in Chapters 2 and 4.

A.10 ENVIRONMENTAL TESTING AND RELIABILITY

The long term reliability field data of III-V multijunction cells in terrestrial concentrator systems is unknown, but there is good reason to believe they will perform well. This is because their device relatives have performed superbly in space for over a decade.

Some design considerations to improve reliability are listed below:

- Substrate assembly coefficient of thermal expansion matched to Ge
- Stress relief at interfaces
- Uniform and low thermal resistance to heat sink
Isolation of mechanical stresses (interconnection, secondary optics, etc.)
- Moisture protection for cell and connections
- Reduction of polymers in optical path

The best test and the longest, is exposure to real operating conditions [58].

APPENDIX B WASTE WATER TREATMENT PLANTS IN CALIFORNIA

Agency	Facility Name	Facility Address
3441 South Willow Investments, LP	CANYON FORK WWTF	AUBERRY & MORGAN CANYON RDS, Prather, CA 93651
39th District Agricultural Association	Calaveras Cnty Fairgrounds (aka Frogtown)	Hwy 49, Angels Camp, CA 95222
AITCHISON, SCOTT	Sandy Point & River Bend MHPs	17604 EAST KINGS CANYON Road, Sanger, CA 93657
AMERICAN CANYON CITY	AMERICAN CANYON WWTP	151 Mezzetta Court, American Canyon, CA 94503
ASPEN EDUCATION GROUP, INC	ACADEMY OF SIERRAS - OWTS	42657 ROAD 44, Reedley, CA 93654
AUBERGE DU SOLEIL	AUBERGE DU SOLEIL SEWAGE PONDS	180 RUTHERFORD HILL Road, Rutherford, CA
Aetna Springs Resort Inc	Aetna Springs Resort	1600 Aetna Springs, Pope Valley, CA 94567
Alameda County Public Works Agency	CENTRAL MARIN SAN. AGCY. WWTP	1301 Anderson Drive, San Rafael, CA 94901
Almanor Lakeside Villas HOA	Almanor Lakeside Villas WWTF	452 Peninsula Drive, Lake Almanor, CA 96137
Alturas City	Alturas Municipal WWTP	200 North Street, Alturas, CA 96101
Amador City	Amador City WW Export System	Off Hwy 49, W of Town, Amador City, CA
Amador Water Agency	Buckhorn WTP	26810 Meadow Vista, Pioneer, CA 95666
Amador Water Agency	Wildwood Est Leachfield	12970 Burnt Cedar, Pine Grove, CA 95665
Amador Water Agency	Pine Grove Community Leachfield System	12800 Ridge Road, Sutter Creek, CA 95685
Amador Water Agency	CSA 3-Lake Camanche WWTP	2901 Camanche, Lake Camanche Village, CA
Amador Water Agency	Gayla Manor WWTP	Gayla Dr and Hwy 88, Pine Grove, CA
Amador Water Agency	Eagles Nest Leachfield	Lambert, Lone, CA
Amador Water Agency	Mace Meadows Leachfield/Fairway Pines L	Creekside, Pioneer, CA 95666
American River Resort	American River Resort WWTP	6019 New River Road, Coloma, CA 95613
Amiri, Haleh	Amiri Oil Company Dunnigan Station	28700 Road 6, Dunnigan, CA 95987
Anderson City	Anderson WPCP	3701 Rupert Road, Anderson, CA 96007
Angels City	Angels City WWTP	3000 Centennial Road, Angels Camp, CA 95222
Ankoor/Jack in the Box/Mumma	Best Western Hotel/Jib/Mumma	County Rd 6 & County Rd 89, Dunnigan, CA 95737
Arbuckle PUD	Arbuckle WWTP	Bailey Rd. & Salt Creek, Arbuckle, CA
Arcata City	Arcata City WWTF	600 South G Street, Arcata, CA 95521
Armona CSD	ARMONA CSD WWTF	SOUTH OF ARMONA, Armona, CA 93202
Arvin City	ARVIN WWTF	PO BOX 548, Arvin, CA 93203
Asti Winery (Beringer Blass) Onsite Domestic System	Asti Winery Domestic Waste	26150 Asti Road, Cloverdale, CA 95425
Atascadero City	ATASCADERO WWTP	6500 Palma Ave., Atascadero, CA 93422
Atwater City	ATWATER REGIONAL WWTF	South Bert Crane Road (Near Lisbon Road) Road, Atwater, C
Auburn City	Auburn WWTP	10441 Ophir Road, Auburn, CA 95603
Auburn Country Club Inc	Auburn Valley Community Services Dist	8815 Auburn Valley, Auburn, CA 95604
Auburn Valley Community Services District	Auburn Valley Community Services Dist	8815 Auburn Valley, Auburn, CA 95604
Avenal City	AVENAL WWTF	1 EFFLUENT WY, Avenal, CA 93204
Avila Beach CSD	AVILA WWTP	END OF SAN MIGUEL ST, Avila Beach, CA 93424
BAPTIST SUGAR PINE CONF	CAMP SUGAR PINE	48478 MILL CANYON, Oakhurst, CA 93644
BEAL PROPERTIES, INC	Beal Properties Facility	AVE 12 & HWY 99, Madera, CA
BIG CREEK SCHOOL DISTRICT	BIG CREEK SCHOOL WWTF	BIG CREEK SCHOOL, Big Creek, CA 93605
BLUE MNTN CNTR OF MEDITATION	BLUE MNTN CNTR SEWAGE PONDS	3600 TOMALES-PETALUMA, Tomales, CA 94971
BOLINAS COMMUNITY P.U.D.	BOLINAS SEWAGE POND SYSTEM	270 ELM, Bolinas, CA 94924
BORELLO PONDS	HOMESTEAD RANCH SEWAGE POND SYSTE	14990 STATE ROUTE 1, Point Reyes Station, CA 94956
BRIDGEPORT PUD	BRIDGEPORT PUD TREATMENT PLANT	PO BOX 91, Bridgeport, CA 93517
Baer, William	Black Oak General Store	3460 HWY 132, Coulterville, CA 95311
Bailey, Fritz	Yosemite-Mariposa KOA WWTF	6323 HWY 140, Midpines, CA 95345
Bakersfield City	BAKERSFIELD WWTP #2	1700 PLANZ, Bakersfield, CA 93307
Bakersfield City	BAKERSFIELD WWTP #3	8101 ASHE Road, Bakersfield, CA 93313
Bay City Flower Company, Inc	BAY CITY FLOWER COMPANY WWTP	2265 Cabrillo Highway South, Half Moon Bay, CA 94109
Beale AFB	Beale AFB WWTP	6451 B, Beale Air Force Base, CA 95903
Bear Valley CMSD	BEAR VALLEY CSD WWTP	29851 LOWER VALLEY, Tehachapi, CA 93561
Bear Valley Water District (Bear Valley, CA)	Bear Valley WWTP	441 Creekside, Bear Valley, CA 95223
Benicia City	BENICIA WWTP	614 East 5th Street, Benicia, CA 94510
Berrendos CSD	Berrendos CSD Treatment System	Berrendos Avenue, Red Bluff, CA 96080
Berryessa Pines & Spanish Flat	Berryessa Pines WWTF	4326 Knoxville, Napa, CA 94558
Biggs City	Biggs WWTP	3016 Sixth Street, Biggs, CA 95917
Bill and Kathy's Inc	Bill/Kathy's WWTF	Rd 89, Dunnigan, CA
Biola CSD	Biola WWTF	PO BOX 57, Biola, CA 93606
Bitney Springs LLC	Bitney Springs WWTF	12398 Bitney Springs, Nevada City, CA 95959
Blue Lake City	Blue Lake City POTW	Highway 299, Blue Lake, CA 95525
Bodega Bay PUD	Bodega Bay Wastewater Reclamation Facili	Highway 1 Just South of Bodega, Bodega Bay, CA 94923
Bowling, Rick & Cathy	Chico Mobile Country Club WWTP	1901 Dayton Place, Chico, CA 95926
Brentwood City	Brentwood WWTP	2251 Elkins Way, Brentwood, CA 94513
Brentwood City	Brentwood Master Reclamation Permit	Brentwood, CA 94513
Brown-Foreman Corporation	Sonoma-Cutrer Vineyards, Inc. Domestic W	4405 Slusser Road, Windsor, CA 95492
Browns Valley ID	Collins Lake Recreational Area	7530 Collins Lake, Oregon House, CA 95962

Buellton City	BUELLTON WWTP	79 INDUSTRIAL WY, Buellton, CA 93427
Burlingame City	BURLINGAME WWTP	1103 AIRPORT Road, Burlingame, CA 94010
Burney WD	Burney STP	20222 Hudson Street, Burney, CA 96013
Butte Community College District	Butte College WWTP	3536 Butte Campus Drive, Oroville, CA 95965
Buttonwillow CWD	Buttonwillow WWTF	1/2 MI N OF BUTTONWILLOW, Buttonwillow, CA 93206
Byron Sanitary District	Byron Sanitary District WWTF	4200 Camino Diablo Road, Byron, CA 94514
CA Dept of Corrections	CCC @ SUSANVILLE, CSP-LC WTF	PO BOX 790, Susanville, CA 96130
CA Dept of Corrections	CDC Pelican Bay Prison WWTP	Lake Earl Drive, Crescent City, CA 95531
CA Dept of Corrections	Deuel Vocational Institution	23500 Kasson Road, Tracy, CA 95376
CA Dept of Corrections	Kern Valley State Prison WWTF	29393 CECIL AVENUE, Delano, CA 93215
CA Dept of Corrections	Avenal Effluent Storage Reservoir	1 Kings, Avenal, CA 93204
CA Dept of Corrections	Sierra Conservation Center WTP (NPDES)	5100 O'Byrnes Ferry Road, Jamestown, CA 95327
CA Dept of Corrections	Wasco State Prison WWTF	15215 SCOFIELD, Wasco, CA 93280
CA Dept of Corrections	Tehachapi Correctional Inst WWTF	End of Highway 202, Tehachapi, CA 93561
CA Dept of Corrections	Sierra Conservation CTR-WWTP-1 (NON15)	5100 O'BYRNES FERRY, Jamestown, CA 95327
CA Dept of Corrections	CDCR - Mule Creek State Prison WWTP	4001 State Hwy 104, Lone, CA 95640
CA Dept of Corrections Corcoran	Corcoran State Prison WWTF	4001 KING, Corcoran, CA 93212
CA Dept of Parks & Rec Sacramento	Malakoff Diggins Historic Park	Nevada, CA
CA Dept of Parks & Rec Sacramento	Millerton Lake State Rec Area	PO BOX 205, Friant, CA 93626
CALIF HOT SPRINGS WATER CO	CALIF HOT SPRINGS WATER CO WWTF	42177 HOT SPRINGS, Calif Hot Springs, CA 93207
CALIFORNIA UTILITIES SERVICE	California Utilities	RESERVATION RD/HWY 68, Salinas, CA 93900
CAMBRIA CSD	CAMBRIA CSD WWTP	1316 TAMSOM DR, STE 201, Cambria, CA 93428
CARMEL AREA WWD	CARMEL AREA WWTP	1/4 M W HWY 1, S SDE CARMEL RD, Carmel, CA 93922
CARUTHERS CSD	Caruthers WWTF	CLEMENSEAU, Caruthers, CA 93609
CATE SCHOOL CORP	CATE SCHOOL WWTP	1960 CATE MESA RD, Carpinteria, CA 93013
COARSEGOLD VILLAGE LP	Oak Creek MHP WWTF	46041 Road 415, Coarsegold, CA 93614
COURTRIGHT LAKE MUTUAL WTR CO	COURTRIGHT LAKE SUBDIV 1862	44066 P.O.BOX, Lemon Cove, CA 93244
CULINARY INSTITUTE OF AMERICA	CWMS WWTP (CULINARY INST OF AMERIC	2812 MAIN Street, St. Helena, CA 94574
CUYAMA COMMUNITY SERVICES DIST	CUYAMA CSD WWTP	null
Ca Dept of Corrections Chowchilla	CDC CCWF & VSP WWTF	AVE 24 & RD 22, Fairmead, CA 93610
Ca Dept of Corrections Coalinga	Pleasant Valley State Prison WWTF	24863 West Jayne Avenue, Coalinga, CA 93210
Ca Dept of Corrections San Luis Obispo	California Men's Colony WWTP	CAMP SAN LUIS OBISPO, San Luis Obispo, CA 93409
Ca Dept of Forestry Georgetown Calfire	Growlerburg Conservation Camp	Resevior, Georgetown, CA
Ca Dept of Forestry Jamestown	Peoria Flat Baseline Conservation Camp	16809 PEORIA FLAT, Jamestown, CA 95327
Ca Dept of Forestry Sacramento	Chamberlain Creek Conservation Camp	15800 Highway 20, Fort Bragg, CA 95437
Ca Dept of Forestry Sanger	Miramonte Conservation Camp	49039 ORCHARD, Miramonte, CA 93641
Ca Dept of Forestry Sanger	Mount Bullion YCC	PO Box 5006, Mariposa, CA 95338
Ca Dept of Forestry Springville	Mountain Home Conservation Camp	45260 BEAR CREEK, Springville, CA 93265
Ca Dept of Parks & Rec Big Sur	PFEIFFER BIG SUR STATE PARK	Big Sur, CA 93920
Ca Dept of Parks & Rec Folsom	Granite Bay State Park	7806 Folsom-Auburn Road, Folsom, CA 95630
Ca Dept of Parks & Rec Gustine	San Luis Rec Area/Basalt Camp	31426 HWY 152, Santa Nella, CA 95322
Ca Dept of Parks & Rec La Honda	PORTOLA REDWOODS ST PARK WWTP	9000 PORTOLA ST. PARK, La Honda, CA 94020
Ca Dept of Parks & Rec Lebec	Colonel Allensworth State Historic Park	STAR ROUTE 1, Earlimart, CA 93219
Ca Dept of Parks & Rec Marin District	ANGEL ISLAND STATE PK - WWTP	ANGEL ISLAND, Angel Island, CA
Ca Dept of Parks & Rec Marin District	SAMUEL P TAYLOR ST PK WW Systm	SIR FRANCIS DRAKE BLVD, Lagunitas, CA 94901
Ca Dept of Parks & Rec Orick	CDPR Prairie Creek Redwoods (WDR)	127011 Dewton B Durury Scenic Drive, Klamath, CA 95548
Ca Dept of Parks & Rec State Parks	BIG BASIN WWTP	21600 Big Basin Way, Boulder Creek, CA 95006
Ca Dept of Transportation District 10 R55	Camp Connell Maintenance Sta.	Meko Dr. NR RT 4, Calaveras County, CA
Ca Dept of Transportation District 10 R55	Caples Lake Maint Station	Hwy 88, Alpine County, CA 95221
Ca Dept of Transportation District 3 R55	Dunnigan Roadside Rest WWTF	Interstate 5, Dunnigan, CA
Ca Dept of Transportation District 3 R55	Gold Run Roadside Rests	Hwy 80, Gold Run, CA
Ca Dept of Transportation District 3 R55	Elkhorn Safety Roadside Rest Area	624 North East Street, Woodland, CA 95776
Ca Dept of Transportation District 3 R55	Maxwell Roadside Rest Station	HWY 5, Colusa (County), CA
Ca Dept of Transportation District 3 R55	Whitmore Maintenance Station	Interstate 80 4mi E of Baxter, Baxter, CA
Ca Dept of Transportation District 6 Bakersfield R5F	PHILIP S RAINE SRRA	FWY 99 TIPTON, CA
Ca Dept of Transportation District 6 Fresno	COALINGA AVENUE SRRA	15 Hwy 5, one mile North of Hwy 269, Fresno County, CA
Ca Dept of Transportation District 6 Fresno	LASSEN AVE ROADSIDE REST	Fresno County, CA
Ca Dept of Transportation District 6 Sacramento R5F	LEBEC SRRA (TEJON PASS)	I-5 NEAR LEBEC, Lebec, CA
Ca Dept of Water Resources Santa Nella	Gianelli (San Luis) Pump-Generate Plant W	31770 HWY 152, Santa Nella, CA 95322
Ca Pines CSD	Ca Pines STP	County Rd 71, Alturas, CA 96101
Cain-Papais Trust	Forest Meadows WWRP	1040 Forest Meadows Drive, Murphys, CA 95247
Calaveras Cnty Fairgrounds	Calaveras Cnty Fairgrounds (aka Frogtown)	Hwy 49, Angels Camp, CA 95222
Calaveras Cnty Water District	Arnold WWTP	3294 HWY 4, Arnold, CA 95223
Calaveras Cnty Water District	Forest Meadows WWRP	1040 Forest Meadows Drive, Murphys, CA 95247
Calaveras Cnty Water District	Wilseyville Comm. Sewage System	Railroad Flat, Wilseyville, CA
Calaveras Cnty Water District	West Point WWTP	Hwy 26 @ Sandy Gulch Rd, Wilseyville, CA 95255
Calaveras Cnty Water District	Wallace Wastewater Treatment Facility	Wallace, CA 95254
Calaveras Cnty Water District	Southworth Ranch Estates WWTF	Southworth, Wallace, CA 95254
Calaveras Cnty Water District	Sequoia Woods/Mountain Retreat	Cypress, Arnold, CA 95223
Calaveras Cnty Water District	Copper Cove WWRP	5130 Kiva Place, Copperopolis, CA 95228
Calaveras Cnty Water District	Mill Woods WWTF	Manvel Rd, Off Hwy 4, Arnold, CA 95223

Calaveras Cnty Water District	La Contenta WWT & RF	1525 Campbell Court, Valley Springs, CA 95252
Calaveras Cnty Water District	Indian Rock Vineyards WWTP	Pennsylvania Gulch, Murphys, CA 95247
Calaveras Cnty Water District	Forest Meadows WWT & RP	1040 Forest Meadows Drive, Murphys, CA 95247
Calaveras Cnty Water District	Douglas Flat/Vallecito WWTP	1901 Holiday Mine Road off State Route 4, Douglas Flat, CA
Calaveras Cnty Water District	Copper Cove WWRF	5130 Kiva Place, Copperopolis, CA 95228
Calaveras Cnty Water District	Big Trees County Houses WWTP	Hoopa, Camp Connell, CA 95223
Calaveras Timber Trails, Assoc	Calaveras Timber Trails WWTF & Disposal F	1071 Avery Sheep Ranch, Avery, CA
Calaveras Unified SD	Jenny Lind Elementary School	Star Route 26, Rancho Calaveras, CA
Calaveras Unified SD	Toyon Middle School	San Andreas, CA 95249
California American Water Co Monterey	INDIAN SPRINGS STP	RIVER RD, Salinas, CA 93900
California American Water Co Monterey	LAS PALMAS RANCH WWTP	21702 River Road, Salinas, CA 93901
California American Water Co Monterey	OAK HILLS DEVELOPMENT WWTP	Castroville, CA 95012
California National Guard	CAMP ROBERTS STP	US 101, CAMP ROBERTS EXIT, CA 93451
California State Parks Foundation	MARCONI CONFERENCE CENTER WWTP	HIGHWAY One, Marshall, CA 94940
Calistoga City	Calistoga City Dunaweal WWTP	1185 Dunaweal Lane, Calistoga, CA 94515
Calpella CWD	Calpella CWD WWTP	5681 North State Street, Calpella, CA 95418
Calvin Harwood	Harwood Products Branscomb Mill	14210 Branscomb Road, Branscomb, CA 95417
Camp Sierra Association	Camp Sierra, Big Creek	52000 Camp Sierra Road, Shaver Lake, CA 93664
Canada Woods Reclamation Facility	CANADA WOODS RECLAMATION FACILITY	ESTE MADERA/CANDA SEGUNDA, Carmel, CA 93923
Canyon Fork Properties	CANYON FORK WWTF	AUBERRY & MORGAN CANYON RDS, Prather, CA 93651
Carneros Partnership LLC	CARNEROS INN WASTEWATER SYSTEM	4048 SONOMA HIGHWAY, Napa, CA 94558
Carpinteria SD	CARPINTERIA SD WWTP	5351 Sixth Street, Carpinteria, CA 93013
Cascade Partners, LLC	Cascade MHP WWTP	18330 Wards Ferry Road, Sonora, CA 95370
Castro Valley Sanitary District	ORO LOMA/CASTRO VALLEY SD WPCP	2600 GRANT Avenue, San Lorenzo, CA 94580
Central Contra Costa Sanitary District	CENTRAL CONTRA COSTA SD WWTP	5019 IMHOFF, Martinez, CA 94553
Central Marin Sanitation Agency	CENTRAL MARIN SAN. AGCY. WWTP	1301 Anderson Drive, San Rafael, CA 94901
Ceres City	Ceres WWTP	4200 Morgan, Ceres, CA 95307
Chateau St Jean Winery	CHATEAU ST JEAN WINERY WW Ponds	8555 SONOMA Highway, Kenwood, CA 95452
Chawanakke Unified School District	Minarets High School WWTP	N of Madera Co Rd 200 & East of Outback Industrial Rd, Nort
Chester PUD	Chester STP	881 First Avenue, Chester, CA 96020
Chico City	Chico Water Pollution Control Plant	4827 Chico River Road, Chico, CA 95927
Children's Hospital Central California	Children's Hospital WWTF	9300 Valley Children's Place, Madera, CA 93636
Chowchilla City	Chowchilla WWTF	AVE 24 1/2 & RD 16, Chowchilla, CA 93610
Christian Outreach Ministries	Honey Rock STP - Ponds	3945 Oro-Bangor Highway, Oroville, CA 95966
Circle Oaks Cnty Water Dist	Circle Oaks WWTF	Napa (County), CA
Clearlake Oaks Cnty Water Dist	Clearlake Oaks Co WTR Dis WWTP	Lake County, CA
Cloverdale City	Cloverdale City WWTP	700 Asti Road, Cloverdale, CA 95425
Clovis City	Clovis WWTF	9700 EAST ASHLAN Avenue, Clovis, CA 93619
Coalinga City	COALINGA WWTF	South of Los Gatos Creek, 1000 feet East of Wartham Creek,
Coit Ginning Company	Coit Ginning Company WWTF	2578 LYON, Mendota, CA 93640
Colfax City	Colfax WWTP	23550 Grandview Avenue, Colfax, CA 95713
College of the Redwoods	College of the Redwoods, POTW	7351 Tompkins Hill Road, Eureka, CA 95501
Colusa City	Colusa WWTP	2820 Will S Green Road, Colusa, CA 95932
Colusa Cnty	Migrant Housing Camp	401 Theater, Williams, CA
Consolidated Tribal Health Project, Inc.	Consolidated Tribal Health Project, Inc.	6991 North State Street, Redwood Valley, CA 95470
Contra Costa County SD No 5	PORT COSTA WWTP	CANYON LAKE DRIVE, Port Costa, CA 94569
Contra Costa County SD No 6	Contra Costa Co.SD#6 WWTP (Stonehurst)	ALHAMBRA VALLEY ROAD, Martinez, CA 94533
Contra Costa Water Authority (a Partnership)	Randall Bold WTP	3760 Neroly Road, Oakley, CA
Contra Costa Water District	Randall Bold WTP	3760 Neroly Road, Oakley, CA
Cool Village Investments, LLC	Cool Village WWTF	Cool, CA
Corcoran City	CORCORAN WWTF	Pueblo Avenue and 5th Avenue, Corcoran, CA 93212
Cordell, Carlene dba C Arrow B Recreational Center	Black Oak General Store	3460 HWY 132, Coulterville, CA 95311
Corning City	Corning WWTP	25010 Gardiner Ferry Road, Corning, CA 96021
Covelo CSD	Covelo POTW	76001 Commercial Street, Covelo, CA 95428
Cox, Randy and Diane	Deer Creek RV Park	10679 Orange Belt Drive, Terra Bella, CA 93270
Crescent City	Crescent City WWTP	210 Battery, Crescent City, CA 95531
Critchfield, OC and Harry	Roll-in MHP WWTF	22466 AIRPORT, Sonora, CA 95370
Crockett CSD	PORT COSTA WWTP	CANYON LAKE DRIVE, Port Costa, CA 94569
Cutler-Orosi JT Powers WW Authority	CUTLER-OROSI WWTF	40401 RD 120, Cutler, CA 93615
Cypress Ridge Limited Partnership	CYPRESS RIDGE SEWER FACILITY	950 CYPRESS RIDGE PKWY, Arroyo Grande, CA 93420
D-Q University	D-Q University WWTF	Davis, CA
DAVENPORT CO SD	DAVENPORT WWTP	NONE, Santa Cruz, CA 95017
DEER MEADOW LEACHFIELD SERVICE	DEER MEADOW LEACHFIELD	THREE RIVERS, Three Rivers, CA 93271
DELHI CWD	DELHI WWTF	CANAL DR & SOUTH AVE, Delhi, CA 95315
DISINGER, MARGARET	LEMON COVE/SEQUOIA CAMPGROUND	SIERRA DR (HWY 198), Lemon Cove, CA 93244
DNC Parks & Resorts at Tenya Inc	Tenaya Lodge At Yosemite	1122 HWY 41, PO BOX 159, Fish Camp, CA 93623
DUBLIN SAN RAMON SERVICES DISTRICT (WWTP NPDE	DUBLIN SAN RAMON SD WWTP	7399 JOHNSON Drive, Pleasanton, CA 94588
DUBLIN SAN RAMON SERVICES DISTRICT (WWTP NPDE	City of Livermore Water Reclamation Plant	101 West JACK LONDON Boulevard, Livermore, CA 94551
DUFFY'S MYRTLEDALE	DUFFY'S MYRTLEDALE WW PONDS	3076 MYRTLEDALE, Calistoga, CA 94515
Danco Builders	Willow Creek Apartments	51 Brannon Mountain Road, Willow Creek, CA 95573
Davis City	Davis WWTP	Davis, CA

Garberville Sanitary District	Garberville POTW	Old Marshall Ranch, Garberville, CA 95542
Georgetown Divide PUD	Auburn LK Onsite WW Disp	1.5 Miles E Of Cool, on Hwy 49, Cool, CA 95614
Gerber-Las Flores CSD	Gerber STP	Levee Road, Gerber, CA 96035
Gilardis Resort	PAPAS TAVERNA Wastewater Systm	5688 LAKEVILLE Road, Petaluma, CA 94954
Glenos, David & Maria	Roll-in MHP WWTF	22466 AIRPORT, Sonora, CA 95370
Gold Beach Park	Gold Beach Park WTF	8201 Hwy 49, Box #5, El Dorado, CA 95623
Gold Mountain CSD	Gold Mountain WWTF	HWY A13, Blairsden, CA 96103
Golden Hills Sanitation Co, Inc	Golden Hills WWTF	Tehachapi, CA 93561
Golden Meadows CSD	Golden Meadows STP (sand filter)	22572 Fisher Road, Red Bluff, CA 96080
Grass Valley City	Grass Valley City WWTP	556 Freeman Lane, Grass Valley, CA 95945
Graton CSD	SCWA Graton CSD	Ross, Graton, CA 95444
Grayson CSD	Grayson Comm Serv Dist WTF	Grayson, CA
Greenstone Estates MHP	Greenstone Estates MHP - WWTF	4700 Old Frenchtown, Shingle Springs, CA 95682
Grenada Sanitary District	Grenada Sanitary District STP	Grenada-Road A-12, Grenada, CA 96038
Gridley City	Gridley WWTF	East Gridley Place, Gridley, CA 95948
Grizzly Lake Resort Imp Dist	Crocker Mountain Estates STP	Grizzly Road, Portola, CA 96122
Grizzly Lake Resort Imp Dist	Delleker WWTP	73821 Industrial Way, Portola, CA 96122
Groveland CSD	GROVELAND STP	18966 FERRETTI Road, Groveland, CA 95321
Gualala CSD	Gualala WWTF	42455 State Highway 1, Gualala, CA 95445
Gustine City	Gustine WWTF	CARNATION, Gustine, CA 95322
HANNEGAN, JOE & HANNEGAN, BRAD	Lakeside Trailer Park	29198 HWY 190, Porterville, CA 93257
HARRIS FARMS, INC	Harris Farms Farm Labor Housing Facility	ROUTE 1, BOX 420, Coalinga, CA 93210
HARRIS FARMS, INC DBA HARRIS RANCH	I-5 & Dorris Avenue Rest Stop WWTF	ROUTE 1, BOX 777, Coalinga, CA 93210
HARTLAND CHRISTIAN ASSOCIATION	Hartland Christian OWTS	57611 ESHOM VALLEY, Badger, CA 93603
HAYWARD CITY	HAYWARD WPCF	3700 ENTERPRISE, Hayward, CA 94545
HCRID #1	Shelter Cove POTW	9126 Shelter Cove Dr, Shelter Cove, CA
HERITAGE RANCH CSD	HERITAGE RANCH WWTP	4870 HERITAGE RD, Paso Robles, CA 93446
HILMAR CWD	Hilmar CWD WWTF	NR GRIFFITH & WILLIAMS, Hilmar, CA 95324
HOLCOMB, C.P.	Yosemite Cattle Company	24025 State Highway 120, Groveland, CA 95321
HOVANNISIAN, JOHN	North Fork Mill Housing Facility	PO BOX 943, North Fork, CA 93643
HUDSON, EDGAR	Kings Canyon MHP	35671 Kings Canyon Road, Dunlap, CA 93621
HUME LAKE CHRISTIAN CAMPS	HUME LAKE WWTF	64144 HUME LAKE, Hume, CA 93628
Hageman Properties LLC	Creekside RV Park	4949 Dennis McCarthy Drive, Bakersfield, CA 93307
Hamilton City CSD	Hamilton City CSD WWTP	Hamilton City, CA
Hanford City	HANFORD WWTF	10555 HOUSTON, Hanford, CA 93230
Happy Camp Sanitation District	Happy Camp WWTP	Highway 96, Happy Camp, CA 96039
Harwood Products, Inc.	Harwood Products Branscomb Mill	14210 Branscomb Road, Branscomb, CA 95417
Healdsburg City	Healdsburg City WWTP	Felta Road, Healdsburg, CA 95448
Herlong PUD	Herlong Utilities Cooperative WW Reclama	POLELINE RD, Herlong, CA
Hess Collection Winery	HESS WINERY WW Pond System	4411 REDWOOD, Napa, CA 94558
Hidden Valley Lake CSD	Hidden Valley Lake WRF	19400 Hartman Road, Middletown, CA 95461
Hoberg's Club Resort	Hoberg's Club Resort	15205 Hwy 175, Cobb, CA 95426
Hollister City	HOLLISTER DOMESTIC WWTP	N SIDE HWY 156, W SAN BENITO R, Hollister, CA 95023
Homestead Ranch LLC	HOMESTEAD RANCH SEWAGE POND SYSTE	14990 STATE ROUTE 1, Point Reyes Station, CA 94956
Hopland Public Utility District	Hopland Public Utilities District	Highway 101, Hopland, CA 95449
Hughson City	Hughson WWTF	6700 Leedom Road, Hughson, CA 95326
Huron City	HURON WWTF	CA
I-5 PROPERTY SERVICE, INC	I-5 & Panoche Road WWTF	HC-1 BOX 1, Fresno County, CA
I-5 PROPERTY SERVICES, INC	I-5 & Dorris Avenue WWTF	I-5 & DORRIS, Huron, CA
I-5 UTILITY COMPANY, INC	I-5 & Highway 58 WWTF	HWY 58 AT I-5, Buttonwillow, CA 93206
INSTITUTE OF NOETIC SCIENCES	Inst Noetic Science WW System	101 SAN ANTONIO ROAD, Petaluma, CA 94952
IVANHOE PUD	IVANHOE WWTF	PO BOX A, Ivanhoe, CA 93235
Indian Valley CSD	Greenville WW Ponds	Hot Springs Road, Greenville, CA 95947
Indian Valley CSD	Taylorville STP	Taylorville Road, Taylorville, CA 95971
Ione City	Ione City Secondary WWTP	1600 West Marlette Street, Ione, CA 95640
Ironhouse Sanitary District	Ironhouse WWTF	450 Walnut Meadows Drive, Oakley, CA 94561
Isleton City	Isleton WWTP	210 Jackson, Isleton, CA 95641
JHAJ, GURVINDER S.	COMANCHE SHELL STATION - OWTS	Intersection of Comanche & Edison HWY, Bakersfield, CA 93
JUNEJA INTERNATIONAL LLC	FIREBAUGH TRUCK & AUTO PLAZA	I-5 & NEES AVE, Merced County, CA
Jackson City	Jackson City WWTP	39 North Highway 49-88, Jackson, CA 95642
Jackson Valley Industries LLC	Harwood Products Branscomb Mill	14210 Branscomb Road, Branscomb, CA 95417
Jamestown SD	JAMESTOWN SANITARY DISTRICT WWTF	CA
Joahannine Daist Communion	Mountain of Attn Sanctuary	12040 North Seigler Springs Road, Middletown, CA 95461
Jordan Winery	Jordan Vineyard and Winery (Domestic Wa	1474 Alexander Valley Road, Healdsburg, CA 95448
KELLEHER CORPORATION	BRIX RESTAURANT WW PONDS	7331 ST. HELENA, Yountville, CA
Kelseyville Cnty Waterworks, District 3	Lake Cnty SD Kelseyville WWD No. 3 Kelsey	4395 Gaddy Lane, Kelseyville, CA 95451
Kendall-Jackson Winery LTD	Kendall-Jackson Wine Center Domestic Wa	5007 Fulton Road, Santa Rosa, CA 95403
Kerman City	KERMAN WWTF	15480 CHURCH, Kerman, CA 93630
Kern Cnty Eng & Surveying Services Dept	Kern Cnty CSA 39-Zone 2	ADJ HWY 178, Lake Isabella, CA 93240
Kern Cnty Housing Authority	North Shafter Farm Labor Camp	P O BOX 638 (CENTRAL VALLEY H, Shafter, CA 93263
Kern Cnty Waste Mgmt Dept	Kern Cnty Buena Vista Aquatic Rec Area	Kern County, CA

Kern Cnty Waste Mgmt Dept	Kern Cnty Sheriff's Lerdo WWTF	N/E LERDO HIGHWAY & QUALITY RD, Shafter, CA
Kern Sanitation Authority	Kern Sanitation Authority WWTF	HWY 58 & QUANTICO, Bakersfield, CA
Kern Valley Hospital District	Kern Valley Hospital WWTF	6412 LAUREL, Mountain Mesa, CA 93240
Kettleman City Csd	KETTLEMAN CITY WWTF	CA
King City	KING CITY DOMESTIC WWTF	CEMETARY RD & SALINAS RIVER, Salinas, CA 93930
Kings River Union Elementary School District	Kings River UESD OWTS	3961 Avenue 400, Kingsburg, CA 93631
Kingsbury Greens CSD	Kingsbury Greens CSD WWTP	15460 Kingsbury, Grass Valley, CA 95949
Kirkwood Meadows P.U.D.	Kirkwood Meadows WWTF	33540 Loop Road, Kirkwood, CA 95667
Klamath CSD Del Norte Community Development	Klamath STP (Del Norte Community Develo	New Klamath Townsite, Klamath, CA 95548
Knights Landing Service Dist	Knights Landing CSD WWTP	1/2 M south of Cnty Rd 116, just east of Knights Landing, Kni
LAGUNA SANITATION	LAGUNA COUNTY SD	3500 BLACK RD, Santa Maria, CA 93455
LAKE CANYON COMMUNITY SRVS DIS	LAKE CANYON COMMUNITY WWTP	19025 LAUREL, Los Gatos, CA 95030
LAKE DON PEDRO OWNERS ASSOCIATION	HACIENDA WWTP	2211 LA GRANGE, La Grange, CA 95329
LAKESHORE RESORT	LAKESHORE RESORT WWTF	HUNTINGTON, Lakeshore, CA 93634
LAMONT PUD	LAMONT WWTF	6525 East Bear Mountain Road, Lamont, CA 93241
LATON CSD	LATON WWTF	PO BOX 447, Laton, CA 93242
LE GRAND CSD	LE GRAND WWTF	13038 JEFFERSON, Le Grand, CA 95333
LEAVITT LAKE CSD	LEAVITT LAKE SEW TRT PONDS	471-830 BUFFUM LN, Susanville, CA 96130
LEMON COVE SANITARY DISTRICT	Lemon Cove WWTF	NORTH OF TOWN, Lemon Cove, CA 93244
LITTLE BEAR WATER CO., INC.	LITTLE BEAR WATER CO WWTP	PINE CANYON RD, King City, CA 93930
LIVERMORE CITY	DUBLIN SAN RAMON SD WWTP	7399 JOHNSON Drive, Pleasanton, CA 94588
LIVERMORE CITY	City of Livermore Water Reclamation Plant	101 West JACK LONDON Boulevard, Livermore, CA 94551
LIVERMORE-AMADOR VALLEY WATER MANAGEMENT	DUBLIN SAN RAMON SD WWTP	7399 JOHNSON Drive, Pleasanton, CA 94588
LIVERMORE-AMADOR VALLEY WATER MANAGEMENT	City of Livermore Water Reclamation Plant	101 West JACK LONDON Boulevard, Livermore, CA 94551
LONDON CSD	LONDON WWTF	RD 60 AVE 376, Dinuba, CA 93618
LOS ALAMOS CSD	LOS ALAMOS WWTP	2 M NW LOS ALAMOS, SE OF 101, Los Alamos, CA 93440
LOST HILLS UTILITY DISTRICT	LOST HILLS WWTF	21331 HWY 46, Lost Hills, CA 93249
Lagunitas School District	Lagunitas School WW System	Sir Francis Drake Boulevard, San Geronimo, CA
Lake Almanor Lakeside LLC	Almanor Lakeside Villas WWTF	452 Penninsula Drive, Lake Almanor, CA 96137
Lake Berryessa Resort Improvement District	Lake Berryessa Resort Improvement Distric	2446 Stagecoach Canyon Road, Pope Valley, CA 94567
Lake Cnty	Middletown STP (SD 2-2)	20126 Hwy 175, Middletown, CA 95461
Lake Cnty	NW Regional Waste Disp Fac	CA
Lake Cnty	Southeast Regional WW System	Lake County, CA
Lake Isabella Water Facility, LLC	ECSSCO Lake Isabella WWTF	Erskine Creek and Lake Isabella Boulevard, Lake Isabella, CA
Lake Shastina CSD	Lake Shastina CSD STP	County Road 20, Weed, CA 96094
Lakeport City Municipal Sewer District	Lakeport City WWTP	795 Linda Lane, Lakeport, CA 95453
Las Gollinas Valley Sanitary District	LAS GALLINAS WWTP	300 SMITH RANCH Road, San Rafael, CA 94903
Lassen Co Waterworks Dist #1	Bieber STP	HWY 299E, Bieber, CA 96009
Lathrop City	Lathrop Industrial WWTP	Howland, Lathrop, CA 95330
Lathrop City	City of Lathrop Water Recycling Plant (WRP	18800 Christopher Way, Lathrop, CA
Lathrop City/Califia LLC	City of Lathrop Water Recycling Plant (WRP	18800 Christopher Way, Lathrop, CA
Lawton Power Inc	FIVE AND FORTY SIX WWTF	HWY 46 & I-5, Lost Hills, CA 93249
Lawton Power Inc	Stoco WWTF	Kern County, CA
Lehigh Southwest Cement Company, Permanente Facili	LEHIGH PERMANENTE CEMENT-WWTP & R	24001 STEVENS CREEK Boulevard, Cupertino, CA 95014
Leland Meadow Water District	Leland Meadow WWTP	33887 Leland Road, Strawberry, CA 95375
Lemoore City	Lemoore WWTF	VINE, Lemoore, CA 93245
Leprino Foods Company	Tracy WWTP	3900 Holly Drive, Tracy, CA 95376
Lewis Carroll School Assn	Lewis Carroll School	9841 Texas Hill Road, Oregon House, CA 95962
Lewiston Park Mutual Water Co	Lewiston Park Water Company, POTW	Old Lewiston Rd at Viola Lane, Lewiston, CA 96052
Lewiston Valley Water Company Inc	Lewiston Community Services District POT	W831 B Trinity Dam Boulevard, Lewiston, CA 96052
Lincoln City	Lincoln City WWTF	1245 Fiddymont Road, Lincoln, CA 95648
Linda Cnty Water District	Linda Cnty Water District WWTP	909 Myrna Avenue, Marysville, CA 95901
Linden Cnty Water District	LINDEN CO WATER DIST WWTF	18243 HWY 26, Linden, CA 95236
Lindsay City	Lindsay WWTF	23611 Road 196, Lindsay, CA 93247
Live Oak City	Live Oak City WWTP	3450 Treatment Road, Live Oak, CA 95953
Livingston City	Livingston Domestic WWTF	7160 North Gallo Road, Livingston, CA 95334
Lockeford CSD	Lockeford CSD WWTP	17725 North Tully Road, Lockeford, CA 95237
Lodi City	White Slough Water Pollution Control Facil	12751 North Thornton Road, Lodi, CA 95242
Loleta CSD	Loleta WWTF	2656 Eel River Drive, Loleta, CA 95551
Lompoc City	LOMPOC REGIONAL WWTP	West 1801 Central Avenue, Lompoc, CA 93436
Los Banos City	Los Banos WWTF	OLD SANTE FE GRADE, Los Banos, CA 93635
Los Brez's Park Mutual Water	Windflower Point STP	9597 Windflower Point, Clearlake, CA 95422
Loyalton City	City of Loyalton and Grandi Ranch WWTF	403 Poole Lane, Loyalton, CA 96118
Lucasfilm Ltd/Skywalker Ranch	SKYWALKER RANCH WW SYSTEMS	5858 LUCAS VALLEY, Nicasio, CA 94946
MARIN CO OFFICE OF EDUCATION	WALKER CREEK RANCH WWTP	1700 MARSHALL-PETALUMA, Petaluma, CA 94952
MARIN COUNTY EHS (Marshall WWTP)	Marshall Community WWWTP (Phase1)	Barinaga Ranch, Marshall, CA
MARIN COUNTY Sanitary District #5	MARIN CSD 5 - TIBURON WWTP	MAR WEST ST & PARADISE DRIVE, Tiburon, CA 94920
MARIN COUNTY Sanitary District #5	MARIN CSD 5 PARADISE COVE WWTP	PARADISE DRIVE, Tiburon, CA 94920
MARIPOSA PUD	Mariposa WWTP	4956 MILLER, Mariposa, CA 95338
MARKLEEVILLE PUD	MARKLEEVILLE WSTWTR TRTMNT SYS	Markleeville, CA 96120
MARTINEZ SHELL REFINING CO	SHELL MARTINEZ REFINERY WWTP	MARINA VISTA AVENUE, Martinez, CA 94553

MATA AMRITANANDAMAYI CENTER	MATA AMRITANANDAMAYI WW System	10200 CROW CANYON, Castro Valley, CA 94552
MELLENMIUM PACIFIC ASSET	Hi-Ho Lodge & MHP	11901 Sierra, Kernville, CA 93238
MERCED CO CORR FACILITY	Sandy Mush WWTF	SANDY MUSH, Merced County, CA
MERCED ID	BARRET COVE	9014 VILLAGE, Snelling, CA 95369
MERCED ID	McSwain Rec Area WWTF	9014 VILLAGE, Snelling, CA 95369
MERCED ID	McClure Pt Rec Area	9014 VILLAGE, Snelling, CA 95369
MERCED ID	HORSESHOE BEND REC AREA	9014 VILLAGE, Snelling, CA 95369
MHC NAC Inc	New Don Pedro WW Facilities	Moccasin Point, Jamestown, CA 95327
MHC NAC Inc	Naco West Waste Disposal	41776 Yuba Gap, Emigrant Gap, CA 95715
MICHAEL HAMILTON RIVERSIDE RV	Yosemite Lakes Campground	31191 HARDIN FLAT Road, Groveland, CA 95321
MINTER FIELD AIRPORT DISTRICT	RIVERSIDE R.V. PARK WWTP	576 MONTEREY, San Jose, CA 95038
MISSION HILLS CSD	Shafter Airport WWTF	201 Aviation Street, Shafter, CA 93263
MONTEREY CSA - CHUALAR	MISSION HILLS LA PURISIMA WWTP	1500 East Burton Mesa Boulevard, Lompoc, CA 93436
MONTEREY REGIONAL WPCA	MONTEREY CSA - CHUALAR WWTP	CHUALAR RIVER ROAD, (2 MI W), Chualar, CA 93925
MONTEREY REGIONAL WPCA	MRWPCA REG TRTMT & OUTFALL SYS	PO BOX 1790, Marina, CA 93933
MOORES RESORT	Monterey Regional Reclamation (Producer) CA	
MORRO BAY SD	MOORES RESORT WASTEWATER PONDS	6 CUTTINGS WHARF, Napa, CA 94558
MT. VIEW SANITARY DISTRICT	MORRO BAY/CAYUCOS WWTP	160 ATASCADERO RD, Morro Bay, CA 93442
MYERS, DON	MT. VIEW SANITARY DISTRICT WWTP	END OF ARTHUR ROAD, Martinez, CA 94553
Madera City	SHADY LAKES MHP	5665 South CHESTNUT Avenue, Fresno, CA 93725
Madera Cnty Eng & Gen Services	Madera WWTF	AVE 13 & RD 21 1/2, Madera, CA 93637
Madera Cnty Eng & Gen Services	Madera Cnty #19-Parkwood WWTF	RD 27 & AVE 12, Madera, CA 93637
Madera Cnty Eng & Gen Services	Madera Cnty #37-La Vina WWTF	AVE 9, Madera, CA 93637
Madera Cnty Eng & Gen Services	Madera Cnty #2-Bass Lake WWTF	Bass Lake, CA 93604
Madera Cnty Eng & Gen Services	Madera Cnty #7-Marina View Heights WW	CO RD 274, Bass Lake, CA 93604
Madera Cnty Eng & Gen Services	Madera Cnty #8A-North Fork WWTF	North Fork, CA 93643
Madera Cnty Eng & Gen Services	Madera Cnty #14-Chukchase WWTF	AVE 19 1/2 at RD 28 1/2 NE, Madera, CA 93637
Madera Cnty Eng & Gen Services	Madera Cnty #6-Lake Shore Park WWTF	CO RD 274, Bass Lake, CA 93604
Madera Cnty Eng & Gen Services	Madera Cnty #22A-Oakhurst WWTF	HWY 41 / OAKHURST, Oakhurst, CA 93644
Madera Cnty Eng & Gen Services	Madera Cnty #24 Teaford Meadow Lakes W	Bass Lake, CA 93604
Madera Cnty Eng & Gen Services	Madera Cnty #27-Goldside Estates WWTF	BEECHWOOD, Madera County, CA
Madera Cnty Eng & Gen Services	Madera Cnty #28 Ripperdan WWTF	NR RIPPERDAN ON MADERA, Ripperdan, CA
Madison Service District	Madison WWTF	9 Hwy 16 & Co Rd 89, Madison, CA 95653
Maharishi Global Admin Law	Hoberg?s Club Resort	15205 Hwy 175, Cobb, CA 95426
Majistee Corporation	Yosemite Pine RV Park	20450 OLD HWY 120, Groveland, CA 95321
Malaga CWD	Malaga CWD WWTF	3749 MAPLE, Fresno, CA 93725
Manila CSD	Manila CSD WWTP	Foot of Lupin Street, Manila, CA 95521
Manteca City	Manteca WW Quality Control Facility	2450 West Yosemite Avenue, Manteca, CA 95337
Maricopa City	Maricopa Wastewater Disposal Facility	SECT 7,T11N,R23W,SBM, Maricopa, CA
Mariposa Cnty DPW	COULTERVILLE WWTF	10113 Old Highway 49, Coulterville, CA 95338
Mariposa Cnty DPW	DON PEDRO SEWER ZONE 1	RANCHITO, Mariposa County, CA
Mariposa Cnty DPW	Yosemite West MD WWTF	INDIAN CREEK, Wawona, CA 95389
Mariposa Cnty DPW	Mariposa Pines WWTF	Mariposa, CA 95338
Markham Vineyards	CWMS WWTP (CULINARY INST OF AMERIC	2812 MAIN Street, St. Helena, CA 94574
Marysville City	Marysville WWTP	Marysville, CA
Maxwell PUD	Maxwell PUD WWTF	Intersection of East Ave and South Ave, Maxwell, CA 95955
Maxwell PUD	Maxwell PUD	3755 Hwy 99, Maxwell, CA 95955
Mayacama Golf Club LLC	Mayacama Golf Club LLC	525 Mayacama Club Drive, Santa Rosa, CA 95403
McClory Properties	EL DORADO MHP WWTF	9630 HWY 41, Lemoore, CA 93245
McCloud Community Services District	McCloud WWTF	Squaw Valley Road, Mccloud, CA 96057
McClure Boat Club, Inc	MCCLURE LAKE BOAT CLUB TRAILER PARK	9885 BOAT CLUB, Snelling, CA 95369
McFarland City	McFarland WWTF	MELCHER & ELMO, Mcfarland, CA 93250
McKinleyville CSD	McKinleyville WWTP	675 Hiller Road, Mckinleyville, CA 95521
Mendocino City CSD	Mendocino City CSD	10500 KELLY, Mendocino, CA 95460
Mendocino Cnty WWD #2 Anchor Bay	Mendocino Cnty WWD#2-Anchor Bay	35501 Highway 1 UNIT #4, Gualala, CA 95445
Mendota City	Mendota WWTF	BASS, Mendota, CA 93640
Merced City	Merced WWTF	10260 GOVE Road, Merced, CA 95340
Merced Cnty Housing Authority	Merced & Los Banos Family Centers	MERCED & LOS BANOS, Merced County, CA
Millbrae City	MILLBRAE WWTP	400 East Millbrae Avenue, Millbrae, CA 94030
Miranda CSD	Miranda POTW	Avenue of the Giants, Miranda, CA 95553
Modesto City	Modesto Water Quality Control Facility (pri	1221 Sutter Avenue, Modesto, CA 95351
Mokelumne Hill SD	Mokelumne Hill WWTF	8970 Old Toll Road, Mokelumne Hill, CA 95245
Monarch Grove Reclamation H2O	MONARCH GROVE RECLAMATION	1945 Solano Street, Los Osos, CA 93402
Montague City	Montague STP	1030 13th Street, Montague, CA 96064
Montair Subdivision Homeowners Assoc.	Montair Subdivision, STP	Montague Road, Montague, CA 96064
Montecito Sanitary District	Montecito SD WWTP	1042 Monte Cristo Lane, Santa Barbara, CA 93108
Monterey Cnty Parks Dept	NORTHSHORE PLEYTO WWTP	2610 SAN ANTONIO, Bradley, CA 93426
Monterey Dunes Colony	MONTEREY DUNES COLONY WWTP	195 MONTEREY DUNES WY, Castroville, CA 95012
Morris J. Harwood	Harwood Products Branscomb Mill	14210 Branscomb Road, Branscomb, CA 95417
Morro Bay City	MORRO BAY TEMP EMERGENCY DESAL	176 ATASCADERO RD, Morro Bay, CA 93442
Mountain House CSD	Mountain House WWTP	17103 West Bethany Road, Mountain House, CA 95391

Mt Shasta City	Mount Shasta WWTP	2500 Grant Road, Mount Shasta, CA 96067
Murphys SD	Murphys WWTF	735 Six Mile Road, Murphys, CA 95247
Mustards Grill	Mustards Grill Wastewater System	7399 St Helena Highway, Yountville, CA 94558
NACO WEST/SNOWFLOWER, INC.	Naco West Waste Disposal	41776 Yuba Gap, Emigrant Gap, CA 95715
NAPA SANITATION DISTRICT	NAPA SD WWTP (Soscol Water Recycling F	1515 Soscol Ferry Road Road, Napa, CA 94558
NAPA VALLEY COUNTRY CLUB	NAPA VALLEY CNTRY CLB WW PONDS	3385 HAGEN, Napa, CA 94558
NEW AUBERRY WATER ASSOCIATION	New Auberry WWTF	44657 WILSON, Auberry, CA 93602
NIPOMO CSD	NIPOMO CSD BLACK LAKE - RECLAIMED WA	1526 WILLOW, Nipomo, CA 93444
NIPOMO CSD	Nipomo CSD Southland Treatment Facility	509 Southland Street, Nipomo, CA 93444
NOVATO DAYS INN (NOVATO MOTEL)	NOVATO DAYS INN (NOVATO MOTEL) - WA	8141 REDWOOD Boulevard, Novato, CA 94947
Napa Valley Marina	NAPA VALLEY MARINA SEWAGE PONDS	1200 MILTON, Napa, CA 94559
Nevada CSD No 1	Cascade Shores WWTP	14326 Gas Canyon Road, Nevada City, CA 95959
Nevada CSD No 1	Higgins Village WWTF	10019 Combie Road, Auburn, CA 95602
Nevada CSD No 1	Lake of the Pines WWTP	10903 Riata Way, Auburn, CA 95602
Nevada CSD No 1	Lake Wildwood WWTP	12622 Pleasant Valley Road, Penn Valley, CA 95946
Nevada CSD No 1	Penn Valley WWTP	12382 Spenceville, Penn Valley, CA 95946
Nevada CSD No 1	North San Juan WW Facility	End of Rush St, North San Juan, CA
Nevada City	Nevada City WWTP	650 Jordan, Nevada City, CA 95959
Nevada ID	Rollins Reservoir Rec Areas	Nevada (County), CA 95713
Nevada ID	Scotts Flat Reservoir Rec Area	23333 Scotts Flat, Nevada City, CA 95959
New Age Church of Being	Globe Hotel	101 Lincoln, Sierraville, CA 96126
New Don Pedro Recreation Agency	New Don Pedro WW Facilities	Moccasin Point, Jamestown, CA 95327
Newell CWD	Newell CWD STP	405 Fifth Avenue, Tulelake, CA 96134
Newman City	Newman City WWTF and Reclamation	2600 Hill Ferry Road, Newman, CA 95360
Nick's Cove and Cottages	Nick's Cove & Cottages	Highway 1, Tomales Bay, CA
North San Mateo County Sanitation District	NORTH SAN MATEO COUNTY SANITATION	153 Lake Merced Boulevard, Daly City, CA 94015
North of River SD #1	North of River WWTF	28970 7th Standard Road, Shafter, CA 93264
Northern California Conference of Seven Day Adventist	Leoni Meadows Retreat	6100 Leoni Road, Grizzley Flats, CA 95636
Novato Sanitary District	NOVATO AND IGNACIO WWTP	500 Davidson Street, Novato, CA 94945
OCAT, INC	TACO BELL - GOLDEN STATE BLVD	6735 GOLDEN STATE, Fresno, CA 93722
OLEMA R.V. RESORT	OLEMA RV RESORT-WASTEWATER SYSTEM	10155 HIGHWAY 1, Olema, CA 94950
Oakdale City	Oakdale WWTF	9700 Liberini, Oakdale, CA 95361
Oakwood Lake Water District	Oakwood Lake WWTP	874 East Woodward Avenue, Manteca, CA 95337
Oakwood Lake Water District/Beck Properties Inc	Oakwood Lake WWTP	874 East Woodward Avenue, Manteca, CA 95337
Occidental CSD	Occidental CSD	14445 Occidental Road, Occidental, CA 95465
Olivehurst PUD	Olivehurst WWTP	3908 Mary Avenue, Olivehurst, CA 95961
On The T Capital, LLC/Paradise With Purpose	Mayacamas Ranch	3975 Mountain Home Ranch Road, Calistoga, CA 94515
Orange Cove City	ORANGE COVE WWTF	PARLIER & MONSON, Orange Cove, CA 93646
Organizations Under Region 2 Watershed Permit	Region 2 Watershed Hg and PCB PermittesCA	
Orland City	Orland WWTP	First Street, Orland, CA
Oro Loma Sanitary District	ORO LOMA/CASTRO VALLEY SD WPCP	2600 GRANT Avenue, San Lorenzo, CA 94580
PENINSULA PACKAGING	RUSH CREEK OWTS	1030 North ANDERSON Road, Exeter, CA 93221
PEREIRA, PETE	DON PEDRO HOUSEBOATS/MINI MART	5021 LA GRANGE, La Grange, CA 95329
PETALUMA CITY	PETALUMA ELLIS CREEK WATER RECYCLING	3890 Cypress Drive Street, Petaluma, CA 94954
PLANADA CSD	Planada WWTF	8597 West TOEWS, Planada, CA 95365
PLOW AND TILL	FARMING D WWTF	24941 LASSEN, Five Points, CA 93624
POPLAR CSD	Poplar WWTF	PO BOX 3849, Poplar, CA 93257
PORT SONOMA MARINA	PORT SONOMA MARINA SEWAGE SYSTEM	270 SEARS POINT RD., Petaluma, CA 94952
Pacific Gas & Electric Company Auberry	HELMS HOUSING & SUPPORT FACILITY	33755 OLD MILL, Auberry, CA 93602
Pacific Gas & Electric Company Shaver Lake	HELMS HOUSING & SUPPORT FACILITY	33755 OLD MILL, Auberry, CA 93602
Pacific Gas & Electric Company Shaver Lake	PG&E HELMS PLANT	67250 HELMS CIRCLE, Shaver Lake, CA 93664
Pacifica City	CALERA CREEK WATER RECYCLING PLANT	Pacifica, CA
Pacificus Real Estate Group	Silvertip Resort WWTF	HWY 41, Fish Camp, CA
Pajaro Valley Water Management Agency	Pajaro Valley WMA and City of Watsonville	401 Panabaker Lane, Watsonville, CA 95077
Palo Alto City	PALO ALTO REGIONAL WQCP	2501 EMBARCADERO Way, Palo Alto, CA 94303
Parlier City	Parlier WWTF	BETHEL, Parlier, CA 93646
Paso Robles City	PASO ROBLES WWTP	3400 SULPHUR SPRINGS RD, Paso Robles, CA 93446
Patterson City	Patterson WWTF	14901 Poplar Avenue, Patterson, CA 95363
Peppermint Creek MHP	Peppermint Creek MHP WWTF	10155 PEPPERMINT, Jamestown, CA 95327
Pete Pereira Co., LLC	DON PEDRO HOUSEBOATS/MINI MART	5021 LA GRANGE, La Grange, CA 95329
Pilot Corporation	Pilot Travel Center 168 WWTF	30035 County Rd 8, Dunnigan, CA 95937
Pilot Travel Centers LLC	FLYING J TRAVEL PLAZA-KERN	17047 ZACHARY, Bakersfield, CA 93308
Pinecrest Permit Assoc & US Forest Service	Pinecrest WWTP	FOREST SERVICE RD 4N11, Pinecrest, CA 95364
Pinole City	City of PINOLE WWTP	FOOT OF TENNENT AVENUE, Pinole, CA 94564
Pismo Beach City	PISMO BEACH WWTP	550 FRADY LN, Pismo Beach, CA 93449
Pixley PUD	Pixley WWTF	ADJ TO HARMON FIELD, Pixley, CA 93256
Pla-Vada Community Association	Pla-Vada Community Assoc STP	Sewer Plant Rd at Conifer, Soda Springs, CA 95728
Placer Cnty Dept of Facility Services	Placer Cnty SMD No 1 WWTP	11755 Joeger Road, Auburn, CA 95602
Placer Cnty Dept of Facility Services	Placer Cnty SMD No 3	4928 Auburn Folsom Road, Loomis, CA 95650
Placer Cnty Dept of Facility Services	Placer Cnty SA No 28, ZONE No.6, Sheridan	E Street, Sheridan, CA 95486
Placer Union High School District	Foresthill High School	Auburn, CA

Placerville City	Hangtown Creek WRF	2300 Coolwater Creek Road, Placerville, CA 95667
Pleasant Rdg. Union Scho. Dist.	Pleasant Ridge Elementary School	22580 Kingston Rd, Grass Valley, CA 95949
Plumas Eureka CSD	Plumas Eureka Estates WWTF	200 Lundy Lane, Blairsden, CA 96103
Plymouth City	Plymouth WWTP	7784&7151 Old Sacramento Road, Plymouth, CA 95669
Point Arena City	Point Arena Wastewater Treatment Plant	Iverson Road Plant, Point Arena, CA 95468
Porterville City	Porterville WWTF	555 PROSPECT, Porterville, CA 93257
Portola City	Portola WWTP	120 Main Street, Portola, CA 96122
Princeton Water Works Dist	Princeton WWTP	Spencer, Princeton, CA
Protestant Episcopal Bishop of San Joaquin	DIOCESE OF SAN JOAQUIN, ECCO	43803 STATE HWY 41, Oakhurst, CA 93644
Quincy Community Services District	Leonhardt Ranch Reclamation	Ganser Airport Road, Quincy, CA 95971
Quincy Community Services District	Quincy WWTP & Collection System	900 Spanish Creek Road, Quincy, CA 95971
R-Ranch at the Lake	R-Ranch Campground WWTF	3 Mi NW Hwy 128 & Hwy 121, Napa County, CA
RANCHO COLINA MH ESTATES STP	RANCHO COLINA MH ESTATES STP	1045 ATASCADERO RD, Morro Bay, CA 93442
REGULAR BAPTIST CAMP INC	REGULAR BAPTIST CAMP	QUINCY-LAPORTE RD, La Porte, CA
REYNOLDS RESORTS-YOSEMITE SOUTH, LLC	Yosemite South Coarsegold Ranch	34094 Highway 41, Coarsegold, CA 93613
RHODIA INC.	Rhodia Martinez Facility	100 MOCOCO, Martinez, CA 94553
RHODIA, INC	Rhodia Martinez Facility	100 MOCOCO, Martinez, CA 94553
RICHGROVE CSD	Richgrove WWTF	ALONG SOUTHERN PACIFIC RR, Richgrove, CA 93261
RIVER ISLAND EAST HOA	River Island East WWTF	31989 RIVER ISLAND, Porterville, CA 93257
RIVERBEND MHP LLC	Sandy Point & River Bend MHPs	17604 EAST KINGS CANYON Road, Sanger, CA 93657
RODEO SANITARY DISTRICT	RODEO Sanitary District WWTP	800 SAN PABLO Avenue, Rodeo, CA 94572
RUSH CREEK MEADOW & DOUGLAS FAMILY TRUST	RUSH CREEK OWTS	1030 North ANDERSON Road, Exeter, CA 93221
Ralph Houannisian	Sequoia Dawn Farm Labor Center	35800 HWY 190, Springville, CA 93265
Rancho Cielo Youth Campus	Rancho Cielo Youth Campus	710 Old Stage Road, Salinas, CA 93912
Rancho Murieta CSD	Rancho Murieta CSD WWT & Rec	15160 Jackson, Rancho Murieta, CA 95683
Rawhide Investment Co Inc	Rawhide Mobile Home Park WWTF	8400 OLD MELONES, Jamestown, CA 95327
Red Bluff City	Red Bluff WW Reclamation Plant	700 Messer Drive, Red Bluff, CA 96080
Redding City	Clear Creek WWTP	2220 Metz Road, Anderson, CA 96007
Redding City	Stillwater WWTP Reclamation	6475 AIRPORT RD, Anderson, CA 96007
Redding City	Stillwater WWTF	6475 Airport Road, Anderson, CA 96007
Redway CSD	Redway POTW	153 Empire, Redway, CA 95568
Redwood Park CSD	Redwood Park STP	Redwood Park, CA 95548
Reedley City	Reedley WWTF	1701 West Huntsman, Reedley, CA 93654
Regents of the University of California - UC Davis	UC Davis, Bodega Marine Lab (WDR)	Westshore Road, Bodega Bay, CA 94923
Richardson Springs CSD	Richardson Springs CSD	15850 Richardson Springs Road, Richardson Springs, CA 959
Richmond City	RICHMOND WPCP	601 CANAL, Richmond, CA 94804
Richvale SD	Richvale STP	Eucalyptus Road, Richvale, CA 95974
Rio Alto WD	Lake California WWTP	22099 River View Drive, Cottonwood, CA 96022
Rio Dell City	Rio Dell City WWTF	475 Hilltop, Rio Dell, CA 95562
Rio Vista City	Rio Vista Beach WWTF	1000 Beach, Rio Vista, CA 94571
Rio Vista City	Northwest WWTF	3000 Airport Road, Rio Vista, CA 94571
Ripon City	Ripon Industrial & Domestic TP	1220 Vera, Ripon, CA 95366
Rite of Passage	Sierra Ridge WWTP	Fricot City Rd, Off Hwy 49, San Andreas, CA 95249
River City Recovery Center Inc	River City WWTF	12490 Alta Mesa, Galt, CA 95632
River Highlands CSD	Hammonton Gold Village WWTP	8204 Platinum Circle, Smartsville, CA 95977
River Pines PUD	River Pines WWTP	CA
Riverdale PUD	Riverdale WWTF	PO BOX 248, Riverdale, CA 93656
Riviera West Mutual Water Company	Riviera West WTP	8560 Soda Bay Road, Kelseyville, CA 95451
Roseville City	Dry Creek WWTP	1800 Booth Road, Roseville, CA 95747
Roseville City	Pleasant Grove WWTP	5051 Phillips Road, Roseville, CA 95747
SAN ARDO WATER DISTRICT	SAN ARDO STP	CATTLEMEN RD, San Ardo, CA 93450
SAN FRANCISCO AIRPORT COMMISSION	SF Arprt Mel Leong TP-Industrl	676 McDonnell Road, San Francisco, CA 94128
SAN FRANCISCO AIRPORT COMMISSION	SF ARPRT MEL LEONG TP-SANITARY WASTE	676 McDonnell Road, San Francisco, CA 94128
SAN FRANCISCO, CITY & CO, PUBLIC UTILITIES COMMIS	SF - OCEANSIDE WPCP	3500 Great Highway, San Francisco, CA 94132
SAN FRANCISCO, CITY & CO, PUBLIC UTILITIES COMMIS	SF-SE WPCP, N-Point & Bayside	750 PHELPS, San Francisco, CA 94124
SAN LEANDRO CITY	SAN LEANDRO WPCP	3000 DAVIS Street, San Leandro, CA 94577
SAN LORENZO VALLEY USD	SAN LORENZO VALLEY HS	7015 HWY 9, Felton, CA 95018
SAN LORENZO VALLEY WD	Bear Creek Estates WWF	BEAR CREEK RD, Boulder Creek, CA 95006
SAN LUIS OBISPO CSA #07	OAK SHORES LAKE NACIMIENTO	SOUTH END OF RIDGE RD, Paso Robles, CA 93446
SAN LUIS RV RESORT	Los Banos West I-5 KOA	28485 Gonzaga, Santa Nella, CA 95322
SAN MIGUEL CSD	SAN MIGUEL SD WWTP	NORTH EXTENSION OF N ST, San Miguel, CA 93451
SAN MIGUELITO MUTUAL WATER CO	San Miguelito Wild Cherry Canyon	WILD CHERRY CANYON, Avila Beach, CA 93424
SAN SIMEON CSD	SAN SIMEON WWTP	9245 BALBOA, San Simeon, CA 93452
SANTA BARBARA CITY PWD	EL ESTERO RECLAMATION FACILITY	402 EAST MASON ST, Santa Barbara, CA 93101
SANTA BARBARA CITY PWD	EL ESTERO WWTP NPDES	520 East Yanonali Street, Santa Barbara, CA 93103
SANTA CLARA, County of	MARIPOSA LODGE-Wastewtr System	9500 MALECH, San Jose, CA
SEENO DUCK CLUB	SEENO DUCK CLUB Wastewatr Pond	JACKSNIPE RD., Suisun Marsh, CA
SELMA-KINGSBURG-FOWLER CSD	SKF CSD WWTF	11301 CONEJO, Kingsburg, CA 93631
SEQ LAKE CONF OF YMCA/VIS YMCA	YMCA CAMP TULEQUOIA	Miramonte, CA 93641
SEWER AUTHORITY MID-COASTSIDE	SAM WWTP (Sewer Authority Mid-Coasts)	11000 North Cabrillo Highway, Half Moon Bay, CA 94019
SEWERAGE AGENCY OF SOUTHERN MARIN	SASM WWTP	450 Sycamore Avenue, Mill Valley, CA

SHERWOOD MHP	Sherwood MHP WWTF	339 FRANKWOOD, Sanger, CA 93657
SIERRA JOINT UNION HIGH SC	Sierra High School WWTF	33326 LODGE, Tollhouse, CA 93677
SIERRA SHADOWS MHP	Sierra Shadows WWTF	1269 LINDMORE, Lindsay, CA 93247
SIERRA SUMMIT, INC	Sierra Summit Ski Area WWTF	HWY 168, Huntington Lake, CA 93629
SIERRA UNIFIED SCHOOL DISTRICT	Foothill Middle School WWTF	AUBERRY, Prather, CA
SINOR, WILLIAM & WENDY	Yosemite South Coarsegold Ranch	34094 Highway 41, Coarsegold, CA 93613
SMITH, MYRON	QUAIL VALLEY REC PARK	PO BOX 33, Calif Hot Springs, CA 93207
SNELLING CSD	Snelling WWTF	Merced County, CA
SOUTH BAYSIDE SYSTEM AUTHORITY	SBSA WWTP	1400 Radio Road, Redwood City, CA 94065
SOUTH COUNTY REG WW AUTHORITY	SCRWA RECLAIMING WW FACILITY	LUCHESSA AVE, Gilroy, CA 95020
SOUTH COUNTY REG WW AUTHORITY	SCRWA WWTP	900 SOUTHSIDE DR, Gilroy, CA 95020
SOUTH SAN LUIS OBISPO CO SD	South San Luis Obispo SD WWTP	1600 Aloha Place, Oceano, CA 93445
SPEEDWAY SONOMA LLC	SPEEDWAY SONOMA Sewage Ponds	HIGHWAYS 37 & 121, Sonoma, CA 95476
SPIRIT ROCK MEDITATION CENTER	SPIRIT ROCK Mdtm Cntr WW Systm	5000 SIR FRANCIS DRAKE Boulevard, Woodacre, CA 94973
ST FRANCIS YACHT CLUB	Tinsley Island WWTF	San Joaquin County, CA
ST. HELENA CITY	ST. HELENA CITY WWTP	1 THOMANN Lane, St. Helena, CA 94574
ST. HELENA HOSP & HEALTH CTR	ST HELENA HOSPITAL WWTP	650 SANITARIUM, Deer Park, CA 94576
STINEHART, RICHARD	WILDWOOD MHP	8701 HWY 41, #70, Fresno, CA 93720
STONYBROOK CORPORATION	Stonybrook WWTF	Keene, CA 93531
STRASBAUGH INC	Strasbaugh Recycled Wastewater Waiver	825 Buckley Road, San Luis Obispo, CA 93401
STRATHMORE PUD	Strathmore WWTF	CR HWY 65 & AVE 196, Strathmore, CA 93267
SUMMERLAND SD	SUMMERLAND WWTP	2435 Wallace Avenue, Summerland, CA 93067
SUNNYVALE CITY	SUNNYVALE WPCP	1444 BORREGAS Avenue, Sunnyvale, CA 94088
SUNOL VALLEY GOLF & RECREA CO	SUNOL VALLEY GOLF COURSE WWTP	ANDRADE RD & I 680, Sunol, CA 94586
SYSCO Food Services of Sacramento	SYSCO Food Services of Sacramento	7062 Pacific Avenue, Pleasant Grove, CA 95688
Sacramento City	Sac City Combined WW Collection/TRT Sys	1395 35th Avenue, Sacramento, CA 95822
Sacramento City	EA Fairbairn WTP	7501 College Town Drive, Sacramento, CA 95826
Sacramento City	Sacramento River WTP	1 Water Street, Sacramento, CA 95814
Sacramento Cnty Airport System	Sacramento INTL Airport WWTP	6900 Airport Boulevard, Sacramento, CA 95837
Sacramento Cnty DPW-Elk Grove	Boys Ranch WWTF	Scott, Sloughhouse, CA 95683
Sacramento MUD	Rancho Seco Nuclear Generating Station W	14440 Twin Cities Road, Herald, CA 95638
Sacramento MUD	Rancho Seco Recreational Area WWTF	14440 Twin Cities Road, Herald, CA 95638
Sacramento Regional CSD	Sacramento Regional WWTP	8521 Laguna Station Road, Elk Grove, CA 95758
Saddle Creek Golf Course LP	Copper Cove WWRf	5130 Kiva Place, Copperopolis, CA 95228
Salida Sanitary District	Salida WWTP	Salida, CA
Salinas City	SALINAS INDUSTRIAL WWTP	DAVIS RD AT RIVER CROSSING, Salinas, CA 93901
Samoa Pacific LLC	Samoa Town Site	3 North Bay View Road, Samoa, CA 95564
San Andreas SD	San Andreas WWTP	675 Gold Oak Road, San Andreas, CA 95249
San Francisco City	LOG CABIN RANCH Wastwtr System	500 Log Cabin Ranch Road, La Honda, CA 94020
San Francisco City & County	New Don Pedro WW Facilities	Moccasin Point, Jamestown, CA 95327
San Francisco City & County	O'Shaughnessy WWTP	Moccasin, CA 95347
San Francisco International Airport	SF Arprt Mel Leong TP-Industrl	676 McDonnell Road, San Francisco, CA 94128
San Francisco International Airport	SF ARPRT MEL LEONG TP-SANITARY WASTE	676 McDonnell Road, San Francisco, CA 94128
San Jerardo Inc.	SAN JERARDO WWTP	1401 OLD STAGE RD, Salinas, CA 93908
San Joaquin City	San Joaquin WWTF	PO BOX 758, San Joaquin, CA 93660
San Joaquin Cnty	CSA 15 - STP	Waterloo & Hwy 99, Stockton, CA
San Joaquin Cnty	Linne Estates WWTF	7701 Bates, San Joaquin, CA
San Joaquin Cnty	Apricot Acres WWTF, CSA 44, Zone E	San Joaquin County, CA
San Joaquin Cnty Housing Authority	Migrant Housing, Harney Ln	14320 Harney Lane, Lodi, CA 95240
San Joaquin Cnty Housing Authority	Thornton Farm Labor Camp	26188 Manor, Thornton, CA 95686
San Jose City	San Jose City Family Camp	HWY 120, Groveland, CA 95321
San Jose City	SAN JOSE/SANTA CLARA WPCP	700 LOS ESTEROS Road, San Jose, CA 95134
San Lucas County Water District	SAN LUCAS WWTF	HIGHWAY 198 & FREEMAN FLAT RD., San Lucas, CA 93954
San Luis Obispo City	SAN LUIS OBISPO WWTP	35 Prado Road, San Luis Obispo, CA 93401
San Luis Obispo City	SAN LUIS OBISPO WATER RECLAMATION F	35 PRADO, San Luis Obispo, CA 94524
San Luis Water District	FOX HILLS WWTF	SEC 36, T10S, R9E, MDB&M, Los Banos, CA
San Luis Water District	San Luis Hills WWTF	GONZANGA RD & SAN LUIS DR, Santa Nella, CA
San Mateo City	SAN MATEO WWTP	2050 DETROIT Drive, San Mateo, CA 94404
San Mateo County	GLENWOOD BOYS RANCH WW System	400 Log Cabin Ranch Road, La Honda, CA 94020
San Mateo County	SAN MATEO CO HONOR CAMP WWTP	La Honda, CA 94020
San Mateo County Department of Parks	SAN MATEO MEMORIAL PARK WWTP	9500 PESCADERO ROAD, Loma Mar, CA 94021
Sanger City	Sanger WWTF	333 NORTH, Sanger, CA 93657
Santa Barbara Cnty Parks Dept	JALAMA BEACH COUNTY PARK WWTP	STAR RTE, Lompoc, CA 93436
Santa Cruz City	SANTA CRUZ WWTP	null
Santa Maria City	SANTA MARIA WWTP	2065 East Main Street, Santa Maria, CA 93454
Santa Nella CWD	Santa Nella WWTF	Merced County, CA
Santa Rosa City Dept of Public Works	Santa Rosa Subregional Water Reclamation	4300 Llano Road, Santa Rosa, CA 95407
Sausalito-Marín City San Dist	SAUSALITO MARIN CITY STP	1 Fort Baker, Sausalito, CA 94965
Scotts Valley City	Scotts Valley WWTP	700 Lundy Lane, Scotts Valley, CA 95066
Scotts Valley City	SCOTTS VALLEY WWTF PRODUCER	700 LUNDY LN, Scotts Valley, CA 95066
Sewerage Commission Oroville Region	Oroville WWTP	2880 South 5th Avenue, Oroville, CA 95965

Shasta CSA #17	Cottonwood WWTP	3425 Live Oak, Cottonwood, CA 96022
Shasta CSA 8	Palo Cedro WWTF	Charolais Way, Palo Cedro, CA 96073
Shasta Lake City	Shasta Lake WWTF	3700 Tibbits Road, Shasta Lake, CA 96019
Sierra Cnty Service Area 5 Zone 5A	980 West Sierra Brooks	Sierra Valley, Sierra County, CA
Sierra Health Foundation	Grizzly Creek Ranch WWTF	Grizzly RD & HWY 70, Portola, CA 96122
Sierra Moon HOA	Sierra Moon HA WWTF	Chico, CA
Sierra Moon LLC	Sierra Moon HA WWTF	Chico, CA
Singh, Lexander	Lebec Holiday Inn Express	Wainright Court, Lebec, CA 93243
Smith, Andy	Golden Hills MH & RV Park	10625 PINEY CREEK Road, Coulterville, CA 95311
Solano & Colusa Counties C.Y.A	Fouts Springs Youth Facility	Fouts Springs, Stonyford, CA 95979
Soledad City	Soledad Sewage Treatment Plant	248 MAIN, Soledad, CA 93960
Solvang City	Solvang WWTP	WEST OF ALISAL RD, Solvang, CA 93463
Sommerville I-5 Partnership	I-5 & Jayne Avenue Facility	I-5 & JAYNE AVE, Fresno County, CA
Sonoma Cnty Water Agency (SCWA) R1	SCWA Airport WRF (Airport-Larkfield-Wikiu	Skylane Boulevard, Santa Rosa, CA 95403
Sonoma Cnty Water Agency (SCWA) R1	Occidental CSD	14445 Occidental Road, Occidental, CA 95465
Sonoma Cnty Water Agency (SCWA) R1	SCWA Oceanic Properties Sea Ranch Centra	Highway 1 at Whitesurf Rd, The Sea Ranch, CA 95445
Sonoma Cnty Water Agency (SCWA) R1	SCWA Graton CSD	Ross, Graton, CA 95444
Sonoma Cnty Water Agency (SCWA) R1	SCWA Geyserville CSD	Geyserville, Geyserville, CA 95441
Sonoma Cnty Water Agency (SCWA) R1	SCWA Russian River CSD	18400 Neely Road, Guerneville, CA 95446
Sonoma Cnty Water Agency (SCWA) R1	SONOMA VALLEY COUNTY SD WWTP	22675 8 th Street, Sonoma, CA 95476
Sonoma Valley County Sanitation District	SONOMA VALLEY COUNTY SD WWTP	22675 8 th Street, Sonoma, CA 95476
Sonora Cascade Properties I, LP	Cascade MHP WWTF	18330 Wards Ferry Road, Sonora, CA 95370
South San Francisco City	South San Francisco-San Bruno WQCP	195 BELLE AIR Road, South San Francisco, CA 94080
South Sutter Water District	Camp Far West Res South Side	9300 McCourtney, Lincoln, CA 95692
South Tahoe PUD	STPUD WASTEWATER TRTMENT PLANT	1275 MEADOW CREST DR, South Lake Tahoe, CA 96150
Southern California Edison- Rosemead	BIG CREEK POWERHOUSE NO 1 WWTF	Big Creek, CA 93605
Southern Estates LLC	Sandy Point & River Bend MHPs	17604 EAST KINGS CANYON Road, Sanger, CA 93657
Spanish Flat Water District	Spanish Flat WWT & Disposal Facility	4340 Spanish Flat Loop Road, Napa, CA 94558
Spanish Flat Water District/Monticello Public Cemetery	Spanish Flat WWT & Disposal Facility	4340 Spanish Flat Loop Road, Napa, CA 94558
Springville PUD	Springville WWTF	3514 TULE RIVER, Springville, CA 93265
Stallion Springs CMSD	Stallion Springs WWTF	28500 Stallion Springs, Tehachapi, CA 93561
Stanislaus Cnty Dept of Parks & Rec	Modesto Reservoir WWTP	18143 Reservoir, Waterford, CA
Stanislaus Cnty Dept of Parks & Rec	Woodward Reserior Reg Park	14528 26 Mile, Oakdale, CA
Stanislaus Cnty Office of Education	Foothill Horizons School	21925 LYONS BALD MOUNTAIN Road, Sonora, CA 95370
Stephen J Schuster	Pheasant Landing III HA WWTP	Garner Road, Chico, CA 95973
Stephen J Schuster	Sierra Moon HA WWTF	Chico, CA
Stockton City	Silver Lake Family Camp	Hwy 88, Amador County, CA
Stockton City	Stockton Regional WW Control Facility	2500 Navy Drive, Stockton, CA 95206
Stoco Mutual Water and Sewer Company	Stoco WWTF	Kern County, CA
Stratford PUD	Stratford WWTF	P.O. BOX 85, Stratford, CA 93266
Sugar Pine HOA	Sugar Pine OWTS	47557 ROAD 630, Oakhurst, CA 93644
Super Store Industries	Super Store Industries Stockton	Stockton, CA
Susanville Consol SD	SUSANVILLE CSD	Susanville, CA
Sutter Cnty DPW	Rio Ramaza WW Disposal Ponds	Sutter County, CA
Sutter Cnty DPW	Robbins WWTF	Riggins, Robbins, CA
Sutter Creek City	Sutter Creek WWTP	18 Main, Sutter Creek, CA 95685
TEJON GRAPEVINE	TEJON HEADQUARTERS WWTF	R-5, 33 S OF BAKERSFIELD, Kern County, CA
TEJON RANCH COMPANY	Tejon Ranch - Grapevine	GRAPEVINE INTERCHANGE ON I-5, Kern County, CA
TEMPLETON CSD	MEADOWBROOK WWF	P.O. BOX 780, Templeton, CA 93465
TERRA BELLA SEWER MD	Terra Bella WWTF	Terra Bella, CA 93270
TIMELESS INVESTMENT DBA E-Z TRIP	E-Z GOLDEN STATE TRUCK STOP	6725 GOLDEN STATE, Fresno, CA 93711
TIPTON CSD	Tipton WWTF	1 M N OF POPLAR AV, W OF HY 99, Tipton, CA 93272
TRANQUILITY PUD	Tranquility WWTF	Fresno County, CA
TULARE CO BLD SERV & PRKS DEPT	Sequoia Field WWTF	36000 RD 112, Visalia, CA 93291
TWIN CREEKS HOMEOWNERS ASSOCIATION	SOLANO TWIN CREEKS WW SYSTEM	39 TWIN CREEKS Drive, Suisun City, CA 94585
Taft City	Taft WWTF	AIRPORT, Taft, CA 93268
Taft City	Taft Federal Prison WWTF	1510 CADET, Taft, CA 93268
Tahoe Truckee Sanitation Agency	TAHOE TRUCKEE SANITATION AGEN	13720 JOERGER DR, Truckee, CA 96161
Tehachapi City	Tehachapi WWTF	750 ENTERPRISE WAY, Tehachapi, CA 93561
Tehama Co SD #1	Mineral WWTP	37735 Hwy 36E, Mineral, CA 96063
Tejon Castac Water District	Tejon Industrial Complex West WWTF	I-5 AT WHEELER RIDGE, Lebec, CA 93243
Tejon Castac Water District	Tejon Industrial Complex East WWTF	Near Wheeler Ridge road and 1st Street, Lebec, CA 93243
Tejon Ranchcorp	Tejon Industrial Complex West WWTF	I-5 AT WHEELER RIDGE, Lebec, CA 93243
Tejon Ranchcorp	Tejon Industrial Complex East WWTF	Near Wheeler Ridge road and 1st Street, Lebec, CA 93243
Tennant CSD	Tennant CSD ST/LF	13515 Tennant, Macdoel, CA 96058
The City of San Juan Bautista	SAN JUAN BAUTISTA WWTP	NORTH END OF THIRD ST, San Juan Bautista, CA 95054
The Ranch Sewer Maint Dist	Clay Station 1200 Res Dev	Clay Station Rd, East of Tavernor, Sacramento, CA
The Villas At Butte Creek HA	The Villas at Butte Creek WWTP	549 Mission Santa Fe Circle, Chico, CA 95926
Thousand Trails, Inc Naco West	Yosemite Lakes Campground	31191 HARDIN FLAT Road, Groveland, CA 95321
Tomales Village CSD	TOMALES VILLAGE WWTP	IRVIN ROAD, Tomales, CA 94948
Tower Park Marina & Village	Tower Park Marina/Village WWTF	14900 Hwy 12, Lodi, CA 95242

Town of Discovery Bay CSD	Discovery Bay WWTP	Ship Channel Rd, North of Highway 4 and West of Old River, 3900 Holly Drive, Tracy, CA 95376
Tracy City	Tracy WWTP	5800 WHEELER RIDGE, Arvin, CA 93203
Travel Centers of America	Truckstops Corp of America	8511 SOUTHSIDE RD, Tres Pinos, CA 95075
Tres Pinos WD	TRES PINOS WWTP	8511 SOUTHSIDE RD, Tres Pinos, CA 95075
Trinity Cnty Waterworks District	Trinity Cnty Waterworks District #1 Hayfork	T31N, R11W, MDB&M, Hayfork, CA 96041
Tulare City	Tulare WWTF	1875 South West Street, Tulare, CA 93274
Tulare Cnty Office of Education	SCICON WWTF	39250 Bear Creek Road, Springville, CA 93265
Tulare Cnty Resource Mgmt Agency	DELFT COLONY WWTF	S26 T165 R23E, MDB&M, Delft Colony, CA
Tulare Cnty Resource Mgmt Agency	Tooleville WWTF	Tooleville, CA
Tulare Cnty Resource Mgmt Agency	Traver WWTF	S15T17SR32E, MDB&M, Traver, CA
Tulelake City	Tulelake City WWTP	Tulelake, CA 96134
Tuolumne City SD	Tuolumne STP	18050 BOX FACTORY, Tuolumne, CA 95379
Tuolumne Utilities District	MI-WUK VILLAGE WW SYSTEM	2 Green, Sonora, CA 95370
Tuolumne Utilities District	Sonora Regional WWTP	1400 South Gate Drive, Sonora, CA 95379
Tuolumne Utilities District	TWAIN HARTE WWTP	Twain Harte, CA
Tuolumne Utilities District	Sonora Regional WWTF	1400 SOUTHGATE, Sonora, CA 95370
Turlock City	Turlock WWTP	901 South Walnut Road, Turlock, CA 95380
Turlock ID	New Don Pedro WW Facilities	Moccasin Point, Jamestown, CA 95327
U.A. Local 38 Trust Fund	Konocti	8727 Soda Bay, Kelseyville, CA 95451
UC Davis	UC Davis Main WWTP	1140 Old Davis Road Avenue, Davis, CA 95616
UC Half Moon Bay	ELKUS YOUTH RANCH WW System	1500 PURISIMA CREEK, Half Moon Bay, CA 94019
UNION SANITARY DISTRICT	Raymond A. Boege Alvarado WWTP (Union	5072 Benson Road, Union City, CA 94587
US Air Force Mather AFB	Domestic WWTF (SAC CO SD 1)	10503 Armstrong, Mather, CA 95655
US Army Corps of Engineers Lake Kaweah	LAKE KAWEAH/TERMINUS DAM	34443 Sierra, Lemon Cove, CA 93244
US Army Corps of Engineers Porterville	Success Reservoir Campground	Success Lake, Porterville, CA 93258
US Army Corps of Engineers Raymond	HENSLEY LAKE	25207 RD 407/PO BOX 85, Raymond, CA 93653
US Army Corps of Engineers Sacramento	EASTMAN LAKE ADMIN AREA	32175 Road 29, Raymond, CA 93653
US Army Corps of Engineers Sacramento	EASTMAN LAKE CHOWCHILLA REC	32175 ROAD 29, Raymond, CA 93653
US Army Corps of Engineers Sacramento	EASTMAN LAKE CORDONIZ REC	32175 ROAD 29, Raymond, CA 93653
US Army Corps of Engineers Smartville	Englebright Lake WWTF	12896 Englebright Dam, Smartville, CA 95977
US Army Corps of Engineers Valley Springs	New Hogan Lake WWTP	2713 Hogan Dam, Valley Springs, CA 95252
US Army Garrison Fort Hunter Liggett	FT. HUNTER LIGGETT WWTP	JOLON ROAD, King City, CA 93930
US Army Sierra Army Depot	SIERRA ARMY DEPOT SEW TRT PLN	SIERRA ARMY DEPOT, Herlong, CA
US Coast Guard TRACEN	USDOT Coast Guard TRACEN - Tomales	599 Tomales Road, Petaluma, CA 94952
US DEPT OF VETERANS AFFAIRS (PAHCS)	V.A. MED CENTER, LIVERMORE-WWTP	4951 ARROYO, Livermore, CA 94550
US Department of Interior	Glory Hole Recreation Area	Whittle Rd & Hwy 49, Angels Camp, CA 95222
US Dept of Defense, Defense Logistics Agency	DDJC, Sharpe - WWTP, Stormwater	Roth, Lathrop, CA
US Dept of Defense, Defense Logistics Agency	DDJC, Tracy - WWTP, Stormwater	25600 Chrisman, Tracy, CA 95296
US Marine Corps Coleville	USMC-MWTC WWTC	PO BOX 5001, Bridgeport, CA 93517
US Navy Naval Air Station Lemoore	LEMOORE NAS WWTF	HWY 198, Lemoore, CA 93246
US Navy Naval Air Station Lemoore	Naval Radio Transmitting Fac	7200 Radio Station, Dixon, CA 95620
US Navy Treasure Island	TREASURE ISLAND WWTP/DOD	1220 Avenue M, San Francisco, CA 94130
USA PETROLEUM CORP	Station #3088, Dunnigan	29770 County Rd #8, Dunnigan, CA 95937
USDA Forest Service Six Rivers National Forest Eureka	USFS Orleans Ranger Station STP	Highway 96, Orleans, CA 95556
USDI Bureau of Land Management Bakersfield	Maricopa Wastewater Disposal Facility	SECT 7,T11N,R23W,SBM, Maricopa, CA
USDI Bureau of Reclamation Napa	Admin Center & Oak Shores Area	CA
USDI Bureau of Reclamation Sacramento	Gianelli (San Luis) Pump-Generate Plant W	31770 HWY 152, Santa Nella, CA 95322
USDI Bureau of Reclamation Sacramento	Tuttletown Recreation Area	6850 Studhorse Flat, Sonora, CA 95370
USDI National Park Service Devils Postpile	USDI NPD Devils Postpile Facilities	351 Pacu Lane, Bishop, CA 93514
USDI National Park Service Sequoia & Kings Canyon	Ash Mountain WWTF	ASH MOUNTAIN, Tulare (County), CA
USDI National Park Service Sequoia & Kings Canyon	Upper Sherman Tree OWTS	CA
USDI National Park Service Sequoia & Kings Canyon	Grant Grove WWTF	Three Rivers, CA 93271
USDI National Park Service Sequoia & Kings Canyon	Clover Creek WWTF	LODGEPOLE AREA, Tulare (County), CA
USDI National Park Service Sequoia & Kings Canyon	Cedar Grove WWTF	Three Rivers, CA 93271
USDI National Park Service Sequoia & Kings Canyon	Buckeye WWTF	BUCKEYE RESIDENTIAL AREA, Tulare (County), CA
USDI National Park Service Yosemite	BADGER PASS WWTF	BADGER, Yosemite Natl Park, CA 95389
USDI National Park Service Yosemite	WAWONA WWTF	PO BOX 2025, WAWONA STATION, Yosemite Natl Park, CA 9
USDI National Park Service Yosemite	YOSEMITE INSTITUTE CRANE FLAT	HWY 120 E OF CRANE FLAT, Yosemite Natl Park, CA 95389
USDI National Park Service Yosemite	Glacier Point WWTF	Glacier Point, Yosemite National Park, CA 95389
USDI National Park Service Yosemite	El Portal WWTF	5083 FORESTA Road BLDG 750, El Portal, CA 95318
Ukiah City	Ukiah City WWTP	300 Treatment Plant Road, Ukiah, CA 95482
United Auburn Indian Community	Thunder Valley Casino WWTP	1200 Athens Avenue, Lincoln, CA 95648
VALLEJO SAN AND FLOOD CONT DIS	VALLEJO SFCD WWTP	450 RYDER STREET, Vallejo, CA 94590
Vacaville City	Easterly WWTP	6040 Vaca Station Road, Elmira, CA 95625
Vacaville City	Gibson Canyon Creek WWTP	7050 Leasure Town Road, Vacaville, CA 95688
Valley Springs SD	Valley Springs SD WWTF	Hwy 12, E OF JNCT W/Hwy 26, Valley Springs, CA 95252
Vintners Inn	Vintners Inn	4350 Barnes Road, Santa Rosa, CA 95403
Visalia City	VISALIA WWTF	7579 AVE 288, Visalia, CA 93277
WEST COUNTY WASTEWATER DISTRICT	WEST COUNTY WW DISTRICT WPCP	2377 GARDEN TRACT, Richmond, CA 94806
WINE COUNTRY INN	CWMS WWTP (CULINARY INST OF AMERIC	2812 MAIN Street, St. Helena, CA 94574
WISH I AH CARE CENTER	WISH I AH CARE CENTER WWTF	35680 WISH I AH, Auberry, CA 93602

WOODVILLE PUD	Woodville WWTF	12 MI WEST OF PORTERVILLE, Woodville, CA 93257
WOODWARD BLUFFS, LLC	Woodward Bluffs MHP WWTF	9360 BLACKSTONE, Fresno, CA 93720
Walker Ranch CSD	Bailey Creek WWTF	Walker Road, Lake Almanor, CA 96137
Wallace Community Service Dist	Wallace Wastewater Treatment Facility	Wallace, CA 95254
Wasco City	Wasco WWTF	746 8th Street, Wasco, CA 93280
Water Dynamics	Sequoia Dawn Farm Labor Center	35800 HWY 190, Springville, CA 93265
Waterford City	Waterford WWTP	335 South Western Avenue, Waterford, CA
Watsonville City	WATSONVILLE WWTP	401 Panabaker Lane, Watsonville, CA 95077
Weaverville Sanitary District	Weaverville SD WWTP	630 Mountain View Street, Weaverville, CA 96093
Weed Dept of Public Works	Weed Shastina WWTP	Highway 97, Weed, CA 96094
Weed Dept of Public Works	Weed WWTP	Highway 97, Weed, CA 96094
Weimar Institute	Weimar Institute WWTP	20601 Paoli, Weimar, CA 95736
Weott CSD	Weott WWTP	School Rd and Newton Rd, Weott, CA 95571
West County Agency	RICHMOND WPCP	601 CANAL, Richmond, CA 94804
West County Agency	WEST COUNTY WW DISTRICT WPCP	2377 GARDEN TRACT, Richmond, CA 94806
Westley Community Serv. Dist.	Westley Comm Sewage Trt Fac	Westley, CA
Westport CWD	Westport CWD	Westport, Westport, CA 95488
Westwood CSD	Westwood STP	First & Fir Street, Westwood, CA 96137
Wheatland City	City of Wheatland WWTP	Malone, Wheatland, CA 95692
Whitehawk Ranch Mutual Water Company	Whitehawk Ranch WWTP	100 Miners Passage, Clio, CA 96106
Wild Wings Co Service Area	Wild Wings Water Recycling Facility	State Hwy 16 & County Rd 94B, Woodland, CA 95695
Williams City	Williams WWTP	700 B Street, Williams, CA 95987
Willits City	Willits City WWTP	300 North Lenore Street, Willits, CA 95490
Willows City	Willows Wastewater Treatment Plant	1600 South Tehama, Willows, CA 95988
Windsor Water District	Windsor Town WWTP	8400 Windsor Road, Windsor, CA 95492
Winters City	Winters WWTF	501 County Rd 32A, Winters, CA
Woodbridge Sanitary District	Woodbridge SD-Sewage Treatment	19720 Benedict, Woodbridge, CA 95258
Woodlake City	WOODLAKE WWTF	811 South Valencia Boulevard, Woodlake, CA 93286
Woodland City	Woodland Water Pollution Control Facility	42929 County Road 24, Woodland, CA 95776
YOSEMITE LAKES PARK, INC	Yosemite Lakes Clubhouse Facility	30250 YOSEMITE SPRINGS, Coarsegold, CA 93614
YOSEMITE MOTELS GP	CEDAR LODGE WWTF	9966 HWY 140, El Portal, CA
YOSEMITE/MARIPOSA KOA	Yosemite-Mariposa KOA WWTF	6323 HWY 140, Midpines, CA 95345
YOUNG LIFE CAMPAIGN	Woodleaf Camp STP	11359 La Porte, Challenge, CA 95925
Yolo Cnty Housing Authority	Davis Migrant Center WWTF	Rd 36 & Rd 105, Davis, CA 95616
Yolo Cnty Housing Authority	Dixon Migrant Center WWTF	7290 Radio Station, Dixon, CA 95620
Yosemite Vista Estates	Yosemite Vista Estates	22625 FERRETTI, Groveland, CA 95321
Yountville, Town of	YOUNTVILLE / CA VETS HOME WWTP	7501 SOLANO Avenue, Yountville, CA 94599
Yreka City	Yreka City WWTP	856 North Main Street, Yreka, CA 96897
Yuba City	Yuba City WTP	701 Northgate, Yuba City, CA 95991
Yuba City	Yuba City WWTF	302 Burns Drive, Yuba City, CA 95991
Yuba Cnty	Hammonton Gold Village WWTP	8204 Platinum Circle, Smartsville, CA 95977
Yuba Cnty Motorplex LLC	Yuba Cnty Motorplex WWTF	2793 Forty Mile, Marysville, CA 95901

APPENDIX C GRID SYNCHRONIZATION, PI CONTROL AND THE DQ TRANSFORMATION

The utilization of inverters for the interconnection of distributed generation to the grid requires application of controls systems capable of regulating the active and reactive output currents, ensuring high power quality levels and achieving relative immunity to grid perturbations. Power converters are being increasingly utilized in distributed generation applications for the interconnection to the grid be it a PV array or other primary energy source. These converters are typically one or three phase voltage source inverters, depending on the size of the source, and connected to the grid via a filter which in principle acts as a low-pass impedance attenuating the high frequency switching harmonics of the inverter [141].

Proper integration of medium or large PV systems in the grid may require additional functionality from the inverter, such as reactive power control. Furthermore, the increase of average PV system size may lead to new strategies like eliminating the DC-DC converter that is usually placed between the PV array and the inverter, and moving the MPPT to the inverter, resulting in increased simplicity, overall efficiency and cost reduction. Reference [142] discusses fuzzy MPPT control of an inverter, eliminating the need for the DC-DC converter.

Current control is an important issue in power electronic circuits, particularly in dc to ac inverters where the objective is to produce a sinusoidal ac output whose magnitude and frequency can both be controlled. This Appendix discusses how the current control of three-phase pulse width modulated voltage source inverter (PWM-VSI) has been implemented in the rotating d,q reference frame.

Three major classes of regulators have been developed over the last few decades: hysteresis regulators, linear PI regulators and predictive dead-beat regulators [115]. Although high performance control strategies have been proposed, they still exhibit coupling problems (not allowing the independent control of the active and reactive power). The synchronous frame controller (dq reference frame) used in ac machines has also become the standard solution for current control of PWM rectifiers. Current control of PWM-VSI has been implemented in the rotating d,q reference frame because the synchronous frame controller can eliminate steady state error and has fast transient response by decoupling control. The synchronous frame controller requires transforming the measured stationary frame ac current to rotating frame dc components, and transforming the result of control back to the stationary frame for implementation [115].

The DQ transformation is a transformation of coordinates from the three-phase stationary coordinate system to the dq rotating coordinate system. This transformation is made in two steps:

1. A transformation from the three-phase stationary coordinate system to the two-phase, so called α, β stationary coordinate system developed by E. Clarke [115].
 $(a, b, c) \Rightarrow (\alpha, \beta)$ (Clarke transformation) The α and β axes are orthogonal as shown in the Figure C-1a below.

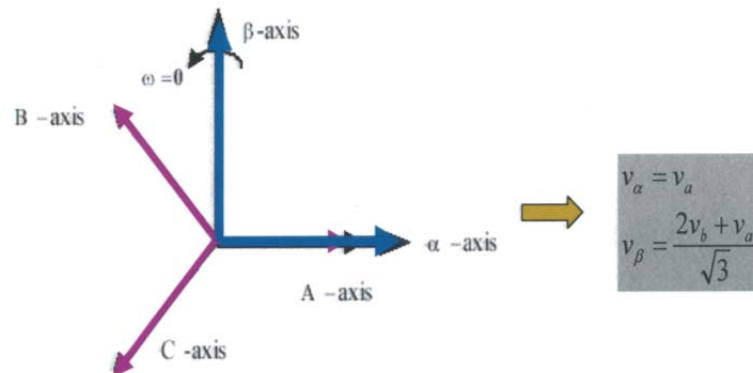


Figure C-1a Clarke's Transformation

2. A transformation from the α, β stationary coordinate system to the dq rotating coordinate system. In the late 1920s, R.H Park introduced a revolutionary approach to electric machine analysis. Park's transformation is the well-known three-phase to two-phase transformation in machine analysis. While it has the unique property of eliminating all time varying inductances from the voltage equations of three-phase ac machines due to the rotor spinning it can also be applied to current control PWM-VSI.

$(\alpha, \beta) \Rightarrow (d, q)$ (Park transformation) Park's Transform is usually split into Clarke's Transform and one rotation; and Park converts balanced three phase quantities into balanced two phase orthogonal quantities. Reference Figure C-1b

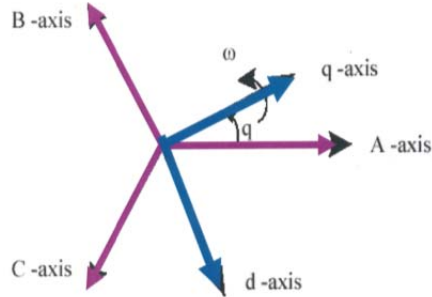


Figure C-1b Park's Transformation

$$\begin{array}{c}
 \boxed{abc} \longrightarrow \boxed{\alpha\beta} \longrightarrow \boxed{dq} \\
 f_a + f_b + f_c = 0 \\
 \begin{bmatrix} f_\alpha \\ f_\beta \end{bmatrix} = \frac{2}{3} \begin{bmatrix} 1 & -\frac{1}{2} & -\frac{1}{2} \\ 0 & \frac{\sqrt{3}}{2} & -\frac{\sqrt{3}}{2} \end{bmatrix} \times \begin{bmatrix} f_a \\ f_b \\ f_c \end{bmatrix} \quad \begin{bmatrix} f_d \\ f_q \end{bmatrix} = \begin{bmatrix} \cos(\phi) & \sin(\phi) \\ -\sin(\phi) & \cos(\phi) \end{bmatrix} \times \begin{bmatrix} f_\alpha \\ f_\beta \end{bmatrix} \\
 \begin{bmatrix} f_d \\ f_q \end{bmatrix} = \frac{2}{3} \begin{bmatrix} \cos(\phi) & \cos(\phi - \gamma) & \cos(\phi + \gamma) \\ -\sin(\phi) & -\sin(\phi - \gamma) & -\sin(\phi + \gamma) \end{bmatrix} \times \begin{bmatrix} f_a \\ f_b \\ f_c \end{bmatrix}
 \end{array}$$

The power circuit of the three-phase VSI is shown in Figures C-2a and C-2b. The mathematical model will be developed from the circuits [115].

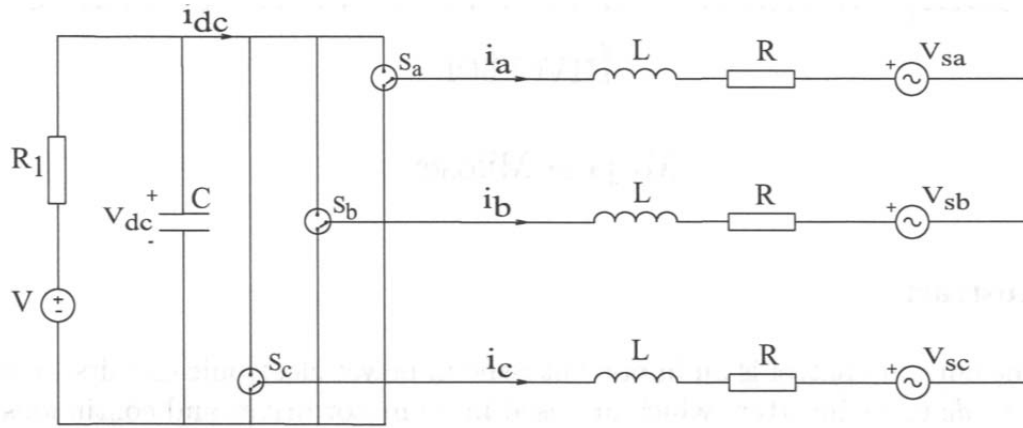


Figure C-2a VSI Power Topology

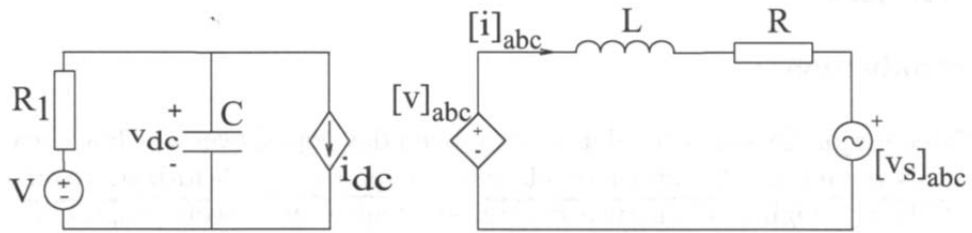


Figure C-2b Equivalent Circuit for the VSI

$$C \frac{dv_{dc}}{dt} + i_{dc} = \frac{V - v_{dc}}{R_1} \quad (C.1)$$

$$L \frac{d[i]_{abc}}{dt} + Ri = \Delta[v]_{abc} ; \Delta[v]_{abc} = [v]_{abc} - [v_s]_{abc} \quad (C.2)$$

$$i_a + i_b + i_c = 0 \quad (C.3)$$

Applying the Park transformation 3ϕ (abc) to rotating frame (dq):

$$\begin{bmatrix} x_d \\ x_q \end{bmatrix} = \frac{2}{3} \begin{bmatrix} \cos\omega_1 t & \cos(\omega_1 t - 120^\circ) & \cos(\omega_1 t + 120^\circ) \\ -\sin\omega_1 t & -\sin(\omega_1 t - 120^\circ) & -\sin(\omega_1 t + 120^\circ) \end{bmatrix} \times \begin{bmatrix} x_a \\ x_b \\ x_c \end{bmatrix} \quad (\text{C.4})$$

to the current $[i]_{abc}$ yields:

$$i_d = \frac{2}{3} [i_a \cos\omega_1 t + i_b \cos(\omega_1 t - 120^\circ) + i_c \cos(\omega_1 t + 120^\circ)] \quad (\text{C.5})$$

$$i_q = -\frac{2}{3} [i_a \sin\omega_1 t + i_b \sin(\omega_1 t - 120^\circ) + i_c \sin(\omega_1 t + 120^\circ)] \quad (\text{C.6})$$

And similarly to the voltage $\Delta[v]_{abc}$

$$\Delta v_d = \frac{2}{3} [\Delta v_a \cos\omega_1 t + \Delta v_b \cos(\omega_1 t - 120^\circ) + \Delta v_c \cos(\omega_1 t + 120^\circ)] \quad (\text{C.7})$$

$$\Delta v_q = -\frac{2}{3} [\Delta v_a \sin\omega_1 t + \Delta v_b \sin(\omega_1 t - 120^\circ) + \Delta v_c \sin(\omega_1 t + 120^\circ)] \quad (\text{C.8})$$

Differentiating equation (C.5) yields:

$$\begin{aligned} \frac{di_d}{dt} &= \frac{2}{3} \left[\frac{di_a}{dt} \cos\omega_1 t + \frac{di_b}{dt} \cos(\omega_1 t - 120^\circ) + \frac{di_c}{dt} \cos(\omega_1 t + 120^\circ) \right] - \\ &\quad - \frac{2}{3} \omega_1 [i_a \sin\omega_1 t + i_b \sin(\omega_1 t - 120^\circ) + i_c \sin(\omega_1 t + 120^\circ)] \quad (\text{C.9}) \end{aligned}$$

From equation (C.2)

$$\begin{aligned} \frac{di_a}{dt} &= \frac{1}{L} \Delta v_a - \frac{R}{L} i_a \\ \frac{di_b}{dt} &= \frac{1}{L} \Delta v_b - \frac{R}{L} i_b \end{aligned} \quad (\text{C.10})$$

$$\frac{di_c}{dt} = \frac{1}{L} \Delta v_c - \frac{R}{L} i_c$$

Using equations (C.5), (C.6), (C.7) and (C.10); equation (C.9) can be rewritten as:

$$\frac{di_d}{dt} = \omega_1 i_q - \frac{R}{L} i_d + \frac{1}{L} \Delta v_d \quad (\text{C.11})$$

Similarly, if we apply the derivative to equation (C.6)

$$\frac{di_q}{dt} = -\omega_1 i_d - \frac{R}{L} i_q + \frac{1}{L} \Delta v_q \quad (\text{C.12})$$

Equations (C.11) and (C.12) transformed in the Laplace domain:

$$(sL + R)I_d = \Delta V_d + \omega_1 L I_q \quad (C.13)$$

$$(sL + R)I_q = \Delta V_q + \omega_1 L I_d \quad (C.14)$$

Multiplying equation (C.14) by the complex number j and adding the result to equation (C.13) yields

$$(sL + R)(I_d + jI_q) = \Delta V_d + j\Delta V_q + \omega_1 L(I_q - jI_d) \quad (C.15)$$

which can be rewritten as: $(sL + R + j\omega_1 L) \vec{I} = \Delta \vec{V}$ where $\vec{I} = I_d + jI_q$ and $\Delta \vec{V} = \Delta V_d + j\Delta V_q$; therefore the transfer function $G(s)$ is

$$G(s) = \frac{\vec{I}}{\Delta \vec{V}} = \frac{1}{sL + R + j\omega_1 L} \quad (C.16)$$

Equation (C.16) shows cross-coupling between the d and q components (because of the $j\omega_1 L$ component) which is shown in Figure C-3. Decoupling can be accomplished by feed-forward and feedback methods for current control of the VSI in the rotating d,q frame as shown in Figures C-4 and C-5 respectively.

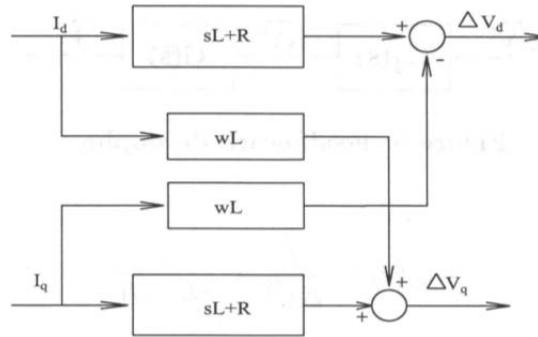


Figure C-3 Cross-coupling of the d & q components

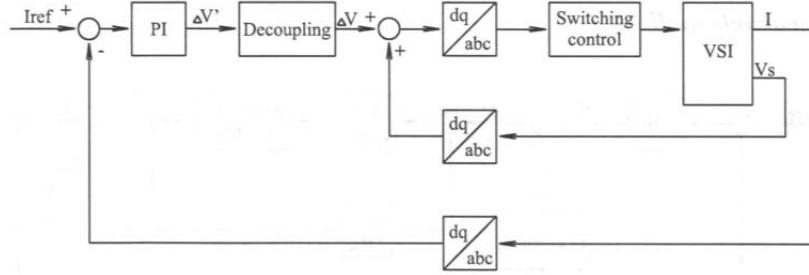


Figure C-4a Current control of VSI feed-forward decoupling method

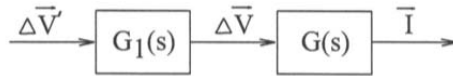


Figure C-4b Feed-forward decoupling block

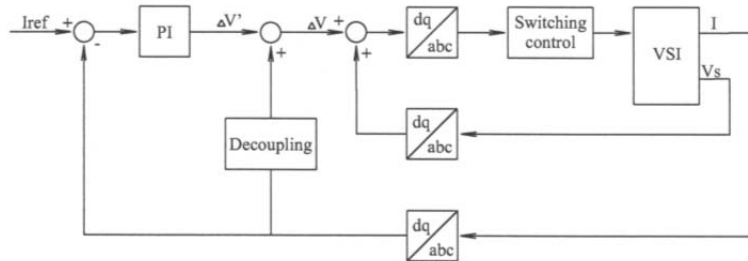


Figure C-5a Current Control of VSI Feedback decoupling method

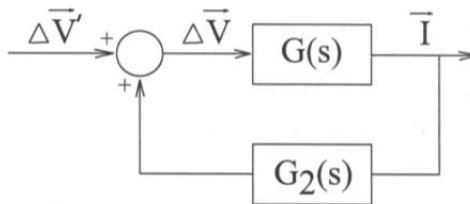


Figure C-5b Feedback decoupling block

APPENDIX D PWM TECHNIQUES

Multilevel voltage-fed inverters (MLI) with space vector pulse width modulation (SVM) have established their importance in high power high performance industrial drive applications [137,138]. There are basically three PWM schemes for controlling multilevel inverters: 1- carrier based sinusoidal PWM (SPWM) 2- space vector PWM (SVM) and 3- selective harmonics elimination PWM (SHE-PWM) [132]. The two most popular control strategies for multilevel inverter topologies are Carrier and Space Vector modulation [138]. In SPWM, a sinusoidal reference voltage waveform is compared with a triangular carrier waveform to generate gate signals for the switches of the inverter. The SVM strategy has been used in three-level inverters. The SVM and SHE-PWM methods are fundamental frequency switching methods and perform one or two commutations of the power semiconductors during one cycle of the output voltages to generate a staircase waveform [136].

The most common MLI topologies can be classified into three types: 1- diode clamped 2- flying capacitor and 3- cascade H bridge. The recent applications of these devices include: motor drives, active rectifiers, filters, **interface to renewable energy sources**, flexible AC transmission systems (FACTS) and static compensators. Among the three types of multilevel inverters, the cascade inverter has the least components for a given number of levels [136].

Carrier based modulation techniques control each phase leg of the inverter separately and allow the line to line voltage to be developed implicitly. In contrast SVM identifies each switching state of an inverter as a point in complex (α, β) space (Clarke) as discussed in Appendix C. The reference phasor rotating in the (α, β) plane at the fundamental frequency is sampled within each switching period, and the nearest three inverter switched states are selected with duty cycles calculated to achieve the same voltage second average as the sampled reference phasor. The roots of vectorial representation of three-phase systems are presented in the research contributions of Park [134]. Park's Transform is usually split into Clarke's transform plus one rotation as discussed in Appendix C.

To help better understand space vector modulation consider the three-leg voltage source inverter (VSI) shown in Figure D-1 [133].

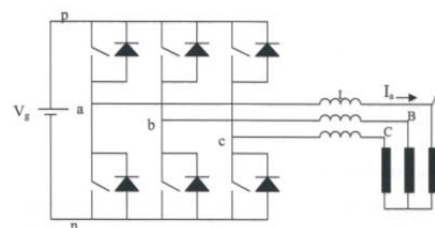


Figure D-1 Topology three-leg voltage source inverter

Because the input lines must never be shorted and the output current must always be continuous, a voltage source inverter can assume only eight topologies (**V1-V8**). Topology **V1**(pnn) is shown in Figure D-2a with line voltages V_{ab} , V_{bc} and V_{ca} given by:

$$\begin{aligned} V_{ab} &= V_g \\ V_{bc} &= 0 \\ V_{ca} &= -V_g \end{aligned} \tag{D.1}$$

and Figure E-2b shows the zero output voltage topologies **V7**(ppp) and **V8**(nnn).

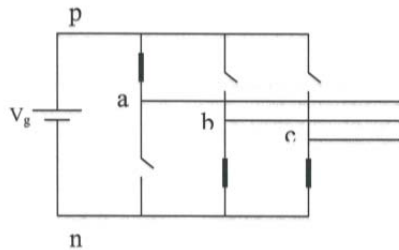


Figure D-2(a) Topology **V1**(pnn) of voltage source inverter

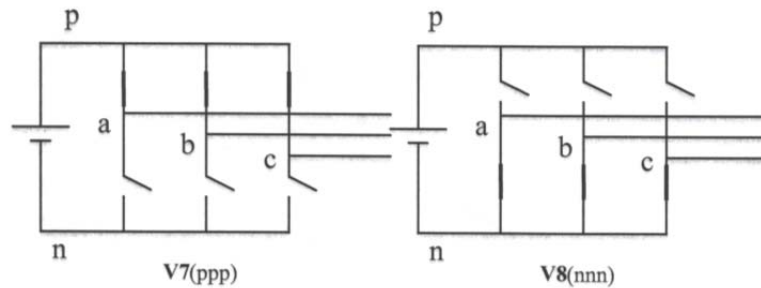


Figure D-2b Zero output voltage topologies

Space vector modulation (SVM) for three-leg VSI can be represented in the (α, β) plane shown in Figure D-3 for the zero voltage vectors [133].

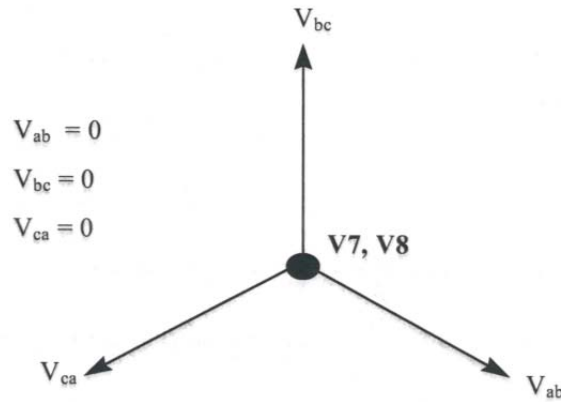


Figure D-3 zero voltage vectors in the (α, β) plane

The desired three phase voltages at the output of the inverter could be represented by an equivalent vector \mathbf{V} rotating in the counter clock wise direction as shown in Figure D-4a. The magnitude of the vector is related to the magnitude of the output voltage shown in Figure D-4b and the time this vector takes to complete one revolution is the same as the fundamental time period of the output voltage.

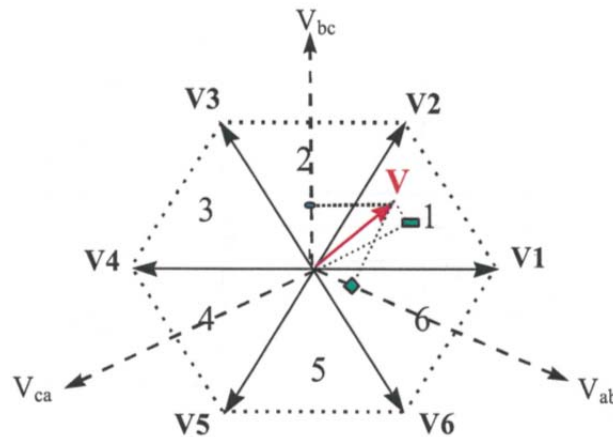


Figure D-4a Output voltage vector in the (α, β) plane

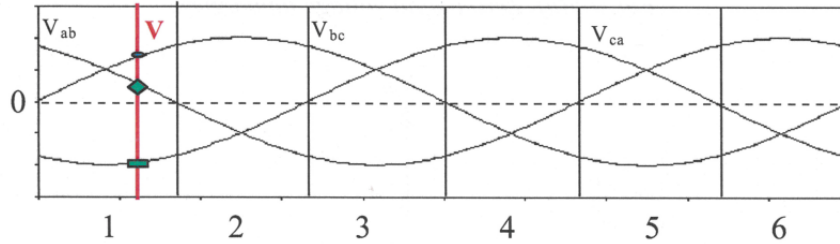


Figure D-4b Output line voltages in the time domain

The line-line output voltage vector \mathbf{V} shown in E-4b and in expanded view in Figure D-5 can be synthesized by the pulse-width-modulation (PWM) of the two adjacent switching state vectors (SSV) $\mathbf{V}_1(\text{pnn})$ and $\mathbf{V}_2(\text{ppn})$, the duty cycle of each d_1 and d_2 respectively, and the zero vector ($\mathbf{V}_7(\text{nnn})/\mathbf{V}_8(\text{ppp})$) of duty cycle d_0 [133]:

$$d_1 \mathbf{V}_1 + d_2 \mathbf{V}_2 = \mathbf{V} = m \mathbf{V}_g e^{j\theta} \quad (\text{D.2})$$

$$d_1 + d_2 + d_0 = 1 \quad (\text{D.3})$$

Where, $0 \leq m \leq 0.866$, is the modulation index. This would correspond to a maximum line-to-line voltage of $1.0 \mathbf{V}_g$

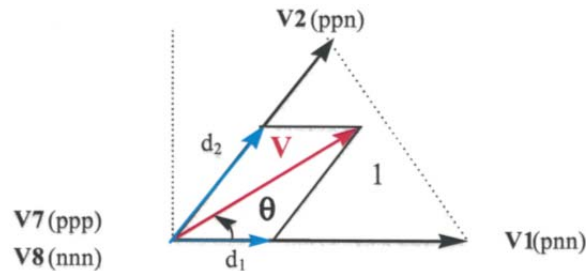


Figure D-5 Synthesis of required output voltage in sector 1

All SVM schemes and most of the other PWM algorithms use (2.2) and (2.4) for the output voltage synthesis. The modulation algorithms that use non-adjacent SSV's have been shown to produce higher THD and/or switching losses and are not analyzed here, although some of them can be very simple to implement and can provide faster transient response. The duty cycles d_1 , d_2 , and d_0 are uniquely determined from Figure D-5 and (2.2) and (2.3). The only difference between PWM schemes that use adjacent

vectors is the choice of the zero vectors and the sequence in which the vectors are applied within the switching cycle. The degrees of freedom for a given modulation algorithm include: 1- the choice of the zero vector V_7 or V_8 or both 2- sequencing of the vectors 3- splitting of the duty cycles of the vectors without introducing additional commutations.

Figure D-6 shows the SVM algorithm for symmetric sequence. This scheme has been shown to have the lowest THD (Total harmonic distortion) [133] because of the symmetry in the switching waveforms.

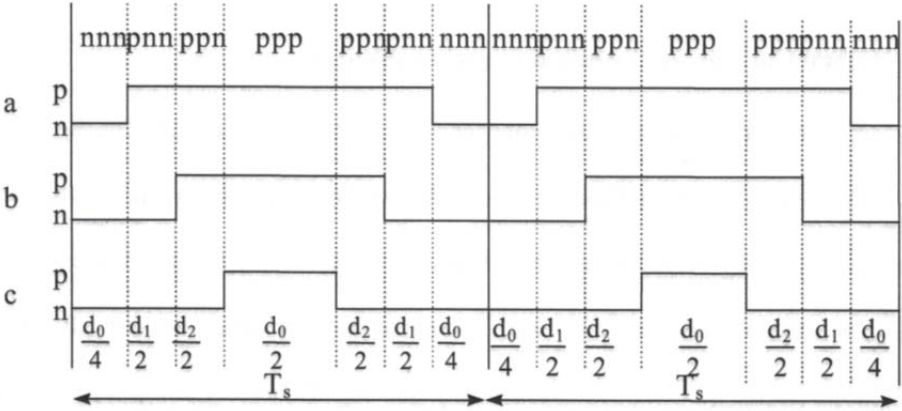


Figure D-6 Phase gating signals for SVM2 Symmetric Sequence

Let's examine a 3-level space vector modulation (SVM). SVM is more complex and challenging than carrier based (sine PWM) techniques, but there are some potential advantages [114, 135, 139]. Multilevel pulse width modulation (PWM) inverters have been developed to overcome shortcoming in solid state switching device ratings. The two multilevel PWM methods most discussed are carrier based PWM and space vector PWM. While the multilevel PWM techniques developed thus far have been extensions of two-level PWM methods, the multiple levels in a diode-clamped inverter (an example discussed below) offer extra degrees of freedom, and greater possibilities in terms of device utilization, state redundancies, and effective switching frequency.

Figure D-7 shows the space vector modulation for a 3-level voltage sourced neutral point clamped inverter with portioned dc-link by diode clamps [135]. With each switching schema each phase voltage can have three different voltage levels: the P state the phase has voltage level E; the O state has the zero voltage on a phase; and the N state has voltage –

E on a phase. Since each phase voltage has three levels, the line-to-line voltages has 5 different voltage levels, namely +2E, +E, 0, -E, -2E. The whole space is divided into 6 sections similar to that shown in Figure D-4a above, but each sector is divided into 4 regions for 3-level operation. Note that each position in the d,q space is represented by a voltage state for phases a, b, and c. For example Sector 1, Region II is enclosed with three space vectors 100(V₁), 210(V₇), and 221(V₂) meaning ONN, PON and PPO. By applying (D.2) where the duty cycle is the defined time interval T_a, T_b, T_c, a reference space vector using the three vectors can be obtained.

$$V_{ref}T_s = V_1T_a + V_7T_b + V_2T_c, \tag{D.4}$$

where T_s is the switching period.

Using the fixed space vectors and reference vector can be formed at any instant, thus for every period T_s the direct and quadrature components of the reference vector can be calculated as well as which sector and region the reference vector lies. As can be seen in the figure, there are 27 different switching states for the inverter.

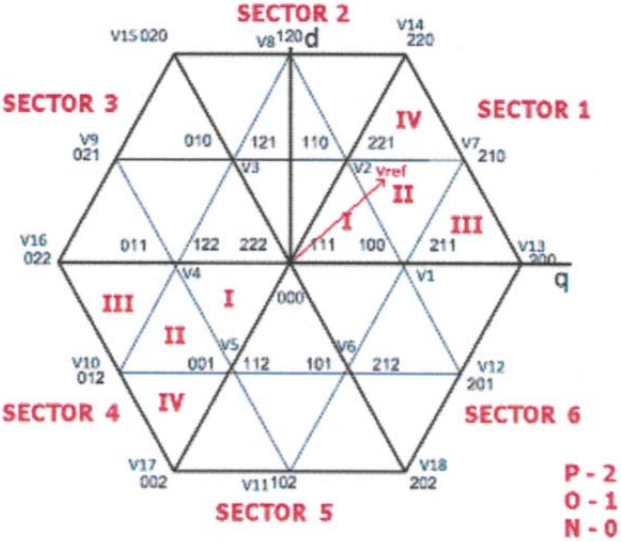


Figure D-7 Space Vector Modulation Divisions and Positions

Equation (D.5) shows the calculations used for the dwell times of Regions 1-4) for the three phase NPC circuit shown in Figure D-8 [135].

REGION I

$$\begin{aligned}T_a &= T_s \left[2m_a \sin \left(\frac{\pi}{3} - \phi \right) \right] \\T_b &= T_s \left[1 - 2m_a \sin \left(\frac{\pi}{3} + \phi \right) \right] \\T_c &= T_s [\sin(\phi)]\end{aligned}\tag{D.5}$$

REGION II

$$\begin{aligned}T_a &= T_s [1 - 2m_a \sin(\phi)] \\T_b &= T_s \left[2m_a \sin \left(\frac{\pi}{3} + \phi \right) - 1 \right] \\T_c &= T_s \left[1 - 2m_a \sin \left(\frac{\pi}{3} - \phi \right) \right]\end{aligned}$$

REGION III

$$\begin{aligned}T_a &= T_s \left[2 - 2m_a \sin \left(\frac{\pi}{3} + \phi \right) \right] \\T_b &= T_s [2m_a \sin(\phi)] \\T_c &= T_s \left[2m_a \sin \left(\frac{\pi}{3} - \phi \right) - 1 \right]\end{aligned}$$

REGION IV

$$\begin{aligned}T_a &= T_s [2m_a \sin(\phi) - 1] \\T_b &= T_s \left[2m_a \sin \left(\frac{\pi}{3} - \phi \right) \right] \\T_c &= T_s \left[2 - 2m_a \sin \left(\frac{\pi}{3} + \phi \right) \right]\end{aligned}$$

Where m_a , the modulation index ($0 \leq m_a \leq 1$) used for creating the reference with different magnitudes is given by:

$$m_a = \sqrt{3} V_{ref} / V_d ; \text{ where } V_d \text{ is the DC link voltage [135]}\tag{E.6}$$

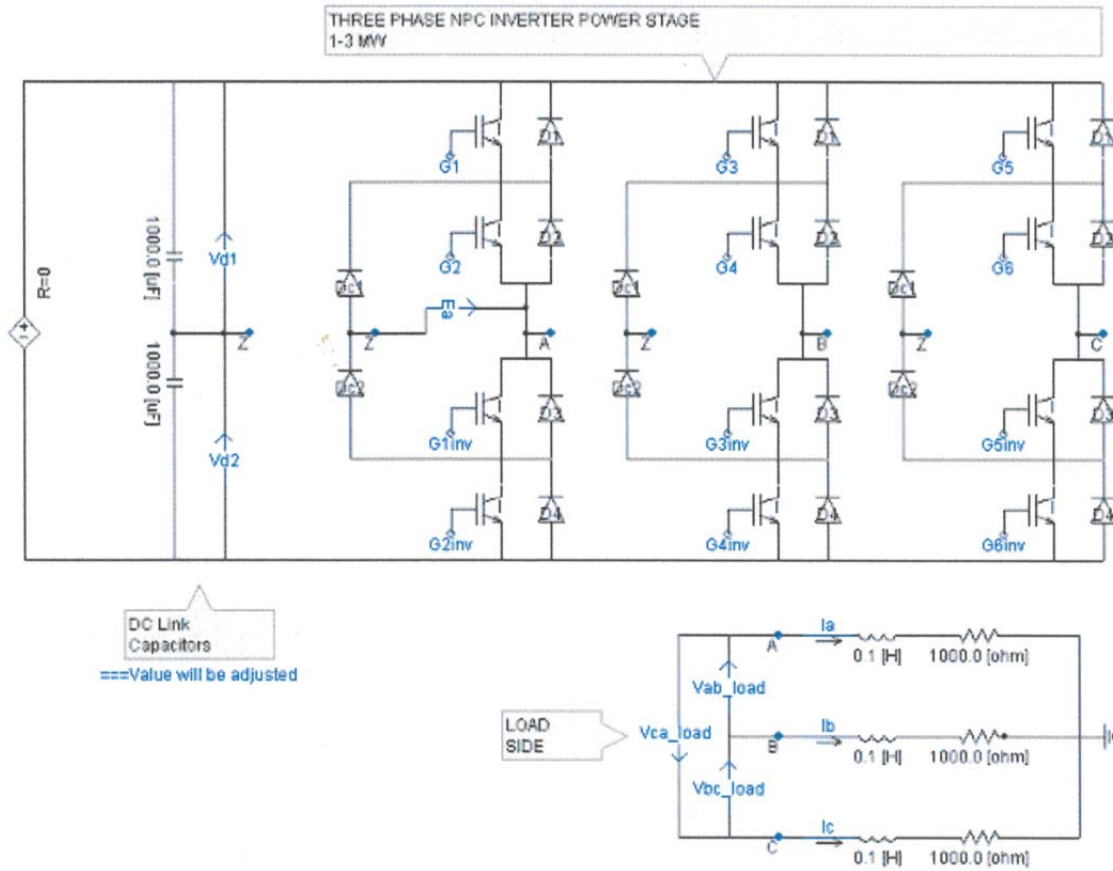


Figure D-8 3 phase NPC Circuit

APPENDIX E SOLAR STORMS AND EFFECT ON THE GRID

Mankind is still learning about the nature of energy generation in the sun. It is generally accepted that a hydrogen-to helium thermonuclear reaction is the source of the sun's energy, yet it is unclear precisely what role the turbulent flows in the sun play, and how solar prominences and sunspots are created [3]. It is interesting that the same radiation that is converted to electricity and connected to electrical transmission and distribution systems can also destroy these grid system components and cause power outages due to severe solar storms [4][5].

The photos below in Figure 1.1 show permanent damage to the Salem New Jersey Nuclear Plant Generation Step Up Transformer caused by the 1989 solar geomagnetic storm (GMD).

According to scientists, solar coronal holes and coronal mass injections (CME) are the two categories of solar activity that drive solar disturbances on earth. Geomagnetic induced currents (GICs) that interact with the power system appear to be produced when large CME occur and are directed at earth perturbing the earth's geomagnetic field, inducing voltage potential at the earth's surface. Current is induced on transmission lines through voltage induction on the loop formed by grounded transmission lines and earth. On average, there are 200 days during the 11-year solar cycle with strong to severe geomagnetic storms and approximately four days of extreme conditions [159].

The two main risks resulting from the introduction of GICs to the bulk power system are damage typically associated with transformers and loss of reactive power support, which could lead to voltage instability and power system collapse [6].

This is an interesting solar energy topic that is receiving increasing attention by the U.S. Congress, Federal Energy Regulatory Commission (FERC) and the National Electrical Regulatory Corporation (NERC). On May 16, 2013 in Docket RM12-22, FERC issued Order No. 779. The EOP-010-1 (Geomagnetic Disturbance Operations) initial draft standard is in development to meet the directives of the FERC Order No. 779 [23].

The photos below in Figure E.1 show permanent damage to the Salem New Jersey Nuclear Plant Generation Step Up Transformer caused by the 1989 solar geomagnetic storm (GMD).



Figure E.1 Salem N.J. Nuclear Plant GSU Transformer Damage

The Salem No. 1 Nuclear Plant Generator Step-Up (GSU) transformer is comprised of three single-phase transformers and is rated at 360 MVA, 500 kV Grounded &-24kV Delta. Effects observed during the storm included the following:

- 50 MVAR (14% of nameplate rating) increase in MVAR demand.
- Unacceptable levels of dissolved combustible gases in oil.
- High noise levels.

After the units were removed from service a week later, internal inspection of all three phases revealed the following:

- Charred winding series connections between two parallel low voltage windings.
- Degree of burning varied for different series connections
- Phases A and C had burnt connections, but phase B was clean.

A more detailed description of the circulating GIC currents and design methods for mitigation can be found in “Calculation Techniques and Results of GIC Currents as Applied to Two Large Power Transformers” [153, 154].

